

COMPUTED NMR SHIELDING VALUES OF UNSATURATED FIVE-MEMBERED-
HETEROCYCLIC RING COMPOUNDS AND THEIR BENZO-ANALOGS AS A
MEASURE OF AROMATICITY

Eddie LaReece Pittman

A Thesis Submitted to the
University of North Carolina Wilmington in Partial Fulfillment
of the Requirements for the Degree of
Master of Science

Department of Chemistry and Biochemistry

University of North Carolina Wilmington

2008

Approved by

Advisory Committee

Dr. James H. Reeves

Dr. Pamela J. Seaton

Dr. Paulo F. Almeida

Dr. Ned H. Martin
Chair

Accepted by

Dean, Graduate School

TABLE OF CONTENTS

ABSTRACT	iv
ACKNOWLEDGEMENTS	v
LIST OF TABLES	viii
LIST OF FIGURES	ix
1. INTRODUCTION	1
2. OBJECTIVE	8
3. EXPERIMENTAL METHODS.....	11
A. Computational Methods.....	11
B. Data Treatment.....	14
4. RESULTS	15
A. Unsaturated Five-Membered Heterocyclic Ring Compounds.....	15
B. Correlation with other Methods	40
C. Other Methods Correlated with each other	44
D. Benzo-Fused Unsaturated-Five-Membered Heterocyclic Ring Compounds	50
E. Correlation with other Methods	69
F. Correlations with other Methods; Probe over Heterocyclic Ring	70
G. Other Methods Correlated with each other; Probe over Heterocyclic Ring	73
H. Correlations with other Methods; Probe over Benzene side.....	77
I. Other Methods Correlated with each other; Probe over Benzene side.....	81
J. Correlations with other Methods; Probe over Center bond.....	85

K. Other Methods Correlated with each other; Probe over Center bond.....	89
L. Summary Tables of most important Data related to this Study	93
5. DISCUSSION.....	99
A. Unsaturated Five-Membered Heterocyclic Ring Compounds.....	99
6. CONCLUSIONS.....	104
REFERENCES	105

ABSTRACT

The gauge independent atomic orbital (GIAO) Hartree-Fock (HF) technique with a 6-31 G(d, p) basis set was used to calculate the isotropic NMR shielding values of a diatomic hydrogen probe above a set of unsaturated 5-membered heterocyclic aromatic compounds and their benzo- analogs. It has been shown that this technique produced results indicating substantial shielding of the probe over the center of aromatic rings. The current study was conducted to determine if the computed shielding of a diatomic H₂ probe is related quantitatively to the extent of aromaticity. Aromaticity is a chemical property in which a conjugated ring of unsaturated bonds, lone pairs of electrons or empty orbitals exhibits a stabilization due to conjugation alone. Aromaticity is both a qualitative and quantitative concept. The qualitative aspect, which is the method for identifying a molecule or species as either aromatic, non-aromatic or anti-aromatic, is soundly understood, but the quantitative aspect of aromaticity is less well defined. There are several established methods for measuring aromaticity quantitatively but they are only loosely correlated. This study's method ($\Delta\sigma$) for calculations done over the five-membered rings correlated well with Cyransky's published data of ASE, Λ , NICS(0), NICS(1) and HOMA calculations to yield correlation coefficients of 0.64, 0.49, 0.66, 0.88 and 0.69, respectively. This study's method ($\Delta\sigma$) with calculations done over the heterocyclic ring portion of the benzo-analogs yielded a correlation coefficient of 0.67 when matched with Bird's published ASE data.

ACKNOWLEDGEMENTS

I would initially like to show appreciation to Dr. Ned Martin for accepting me into his research agenda and doing everything professionally possible in order to assure that I would be at this point with my MS studies. Dr. Martin has not only provided me with the guidance I needed while pursuing my MS degree, he also has consistently given me professional advice that I anticipate on using for my PhD studies as well. This advice relates to my need to enhance my social skills involving being professional during crucial times when dealing with people. That is something that can't be learned in a textbook, it takes practice, persistence and most importantly, the proper mindset. Dr. Martin was always there for me at crucial times during my tenure here at UNCW and he did it not so much as a favor for me, he did it more so for the potential enhancement of the Chemistry profession. Martin recognized that I, Eddie LaReece Pittman, had the potential to make a significant contribution to the Chemistry profession, thus, he was there to set me back on track when it looked as if I was deviating. He was willing to tolerate personal baggage that I may have brought to the plate and focus on Eddie LaReece Pittman's ability to hit the homerun. Most people are not willing to do that. An individual can study anyone and find something wrong with one, so individuals should learn how help people maximize their potential to achieve constructive goals.

I also would like to show appreciation to Drs. Almeida, Seaton and Reeves who make up the rest of my research committee. Each of these individuals significantly helped me in some manner while I was pursuing my MS degree at UNCW. I took a class under each of these professionals and if I had to do it all over again, I would take the same classes. I have always been Analytical inclined, so I had no problem appreciating

Dr. Seaton's NMR class, but I can't say that for either Biochemistry or Physical Chemistry. However, Drs. Almeida and Reeves made BCH and PCHEM so interesting to me that towards the end of each of those classes, I had developed an appreciation for them. Furthermore, all of these individuals were also willing to provide me with countless numbers of letters of recommendations when I was trying to get admitted into a decent PhD program over the past 10 months. I really appreciate those letters because I would not have had the chance to pursue my PhD without those letters.

An extra thanks goes out to Dr. Reeves for going a step further and acting as an assistant advisor/mentor to me. Dr. Reeves basically wanted me to be in position to move forward and make a significant contribution to the Chemistry profession some day. He recognized that I, Eddie LaReece Pittman, had a vision to do constructive things within the Chemistry profession so he was willing to professionally guide me.

A special thanks goes out to the UNCW Graduate Coordinator, Dr. Robert Kieber, for assisting me before and after I initially started at UNCW. Dr. Kieber assisted me with making the right decision to pursue my MS studies at UNCW after bouncing around from program to program in an effort to find the perfect fit. An appreciation also goes out to his wife, Mrs. Cecilia Kieber, for her extraordinary professional guidance to me when I was working as a teacher's assistant. Thus, both Dr. Kieber and his wife played a fundamental role with my establishing myself in UNCW's Chemistry MS program, so I am proud to assert that their efforts as well were worth it and very much appreciated.

I would also like to show appreciation to UNCW's Chemistry department as a whole. The program offered me opportunities and benefits that I did not find anywhere else. I knock myself for not starting at UNCW 4 years ago as opposed to just last year. However, I am happy to assert that it was an experience that I would cherish and I hope that I could leave a permanent positive impression with this program that no one can ever take away.

LIST OF TABLES

Table	Page
1. Summary of measures of aromaticity [16(a-k)].....	7
2. Cartesian coordinates of 1H-benzotriazole.....	12
3. XY Coordinates of (0,0) with proximal hydrogen at 2.5Å above plane of structure.....	13
4. XY Coordinates of (1,0) with proximal hydrogen at 2.5Å above plane of structure.....	13
5. This study's $\Delta\sigma$ values calculated at 2.5Å above the geometric center of five-membered rings along with published results [16] corresponding to the same rings.....	39
6. This study's maximum isotropic shielding increment values (ppm) at 2.5 Å joined with this study's NICS(0), NICS(1) and NICS(2.5) values calculated over the heterocyclic side of benzo-analogs. All compared with published results from Bird's (ASE) [12] for five of the same structures.....	69
7. This study's maximum isotropic shielding increment values (ppm) at 2.5 Å joined with this study's NICS(0), NICS(1) and NICS(2.5) values calculated over the benzene side of benzo-analogs. All compared with published results from Bird's (ASE) [12] for five of the same structures.....	77
8. This study's maximum isotropic shielding increment values (ppm) at 2.5 Å joined with this study's NICS(0), NICS(1) and NICS(2.5) values calculated over the center bond of benzo-analogs. All compared with published results from Bird's (ASE) [12] for five of the same structures.....	85
9. Summary of shielding increments ($\Delta\sigma$) of five-membered rings and their benzo-analogs.....	93
10. Correlation (R^2) values involving this study's $\Delta\sigma_{\max}$ and other published results [16] relating to the five-membered rings.....	97
11. Summary of correlation (R^2) values involving this study's $\Delta\sigma_{\max}$, NICS(0), NICS(1); NICS(2.5) over the heterocyclic side (top), benzene side (middle) and center bond (bottom of the benzo-analogs along with other published results [12] relating to the same benzo-analogs.....	98

LIST OF FIGURES

Figure	Page
1. Illustration of what causes proton shielding/deshielding [34, p.18].....	2
2. Aromatic stabilization energy (ASE) sample calculation for benzene [11].....	4
3. Chemical shielding vs. chemical shift representation.....	9
4. Orientation of 1H-benzotriazole in the XY plane of Cartesian space.....	12
5. NMR shielding increment surfaces (in ppm) at the 2.5, 3.0 & 4.0 Å levels for pyrrole 1	16
6. Unsaturated five-membered heterocyclic compounds (five-membered rings).....	17
7. Benzo-fused unsaturated five-membered heterocyclic compounds (benzo-analogs) and miscellaneous fused-ring heterocyclic compounds.....	18
8. NMR shielding increment surfaces (in ppm) at the 2.5 Å level for five-membered rings: pyrrole 1 , 1H-pyrazole 2 and 1H-imidazole 3	22
9. NMR shielding increment surfaces (in ppm) at the 2.5 Å level for five-membered rings: 1,2,3-triazole 13 , 1,2,4-triazole 14 and 1H-tetrazole 15	23
10. NMR shielding increment surfaces (in ppm) at the 2.5 Å level for five-membered rings: furan 4 , isoxazole 5 and oxazole 6	24
11. NMR shielding increment surfaces (in ppm) at the 2.5 Å level for five-membered rings: phosphole (lp side) 7 , phosphole (P-H side) 7 and isophosphazole (P-H side) 8	25
12. NMR shielding increment surfaces (in ppm) at the 2.5 Å level for five-membered rings: isophosphazole (lp side) 8 , phosphazole (P-H side) 9 and phosphazole (lp side) 9	26
13. NMR shielding increment surfaces (in ppm) at the 2.5 Å level for five-membered rings: thiophene 10 , isothiazole 11 and thiazole 12	27
14. NMR shielding increment surfaces (in ppm) at the 2.5 Å level for five-membered rings: pyrrole 1 , furan 4 and phosphole (lp side) 7	28
15. NMR shielding increment surfaces (in ppm) at the 2.5 Å level for five-membered rings: phosphole (P-H side) 7 and thiophene 10	29

16. Models of a series of phosphorus containing five-membered rings showing the P-H group out of the plane of the rest of the atoms.....	31
17. NMR shielding increment surfaces (in ppm) at the 2.5 Å level for parent five-membered structure derivatives with nitrogen in α position: 1H-pyrazole 2 , isoxazole 5 and isophosphazole (P-H side) 8	33
18. NMR shielding increment surfaces (in ppm) at the 2.5 Å level for parent five-membered structure derivatives with nitrogen in α position: isophosphazole (lp side) 8 and isothiazole 11	34
19. NMR shielding increment surfaces (in ppm) at the 2.5 Å level for parent five-membered structure derivatives with nitrogen in β position: 1H-imidazole 3 , oxazole 6 and phosphazole (P-H side) 9	36
20. NMR shielding increment surfaces (in ppm) at the 2.5 Å level for parent five-membered structure derivatives with nitrogen in β position: phosphazole (lp side) 9 and thiazole 12	37
21. This study's NMR maximum shielding increments ($\Delta\sigma_{\max}$) correlated with (A) Cyraňsky et al's ASE and (B) Magnetic Susceptibility measurements for the five-membered rings.....	41
22. This study's NMR maximum shielding increments ($\Delta\sigma_{\max}$) correlated with (A) Cyraňsky et al's NICS(0) and (B) NICS(1) measurements for the five-membered rings.....	42
23. This study's NMR maximum shielding increments ($\Delta\sigma_{\max}$) correlated with Cyraňsky et al's HOMA measurements for the five-membered rings.....	43
24. Correlations of Cyraňsky et al's ASE with their magnetic susceptibility (A) and their ASE with their HOMA (B) for the five-membered rings.....	45
25. Correlations of (A) Cyraňsky et al's ASE with their NICS(1) and (B) their ASE with their HOMA for the five-membered rings.....	46
26. Correlations of Cyraňsky et al's magnetic susceptibility with their NICS(0) (A) and their magnetic susceptibility with their NICS(1) (B) for the five-membered rings.....	47
27. Correlations of Cyraňsky et al's magnetic susceptibility with their HOMA (A) and their NICS(0) with their HOMA (B) for the five-membered rings.....	48

28. Correlations of Cyraňsky et al's NICS(1) with their HOMA (A) and their NICS(0) vs. NICS(1) for the five-membered rings.....	49
29. NMR shielding increment surfaces (in ppm) at the 2.5 Å level for benzo-analogs: indole 1b , indazole 2b and benzimidazole 3b	52
30. NMR shielding increment surfaces (in ppm) at the 2.5 Å level for benzo-analogs: 1H-benzotriazole 13c , benzofuran 4b and 1,2-benzisoxazole 5b	53
31. NMR shielding increment surfaces (in ppm) at the 2.5 Å level for benzo-analogs: 1,3-benzoxazole 6b , benz[b]phosphole 7b and 1,2-benzisophosphazole 8b	54
32. NMR shielding increment surfaces (in ppm) at the 2.5 Å level for benzo-analogs: 1,3-benzphosphazole 9b , benzo[b]thiophene 10b and 1,2-benzisothiazole 11b	55
33. NMR shielding increment surfaces (in ppm) at the 2.5 Å level for benzo-analogs: 1,2-benzothiazole 12b , purine 17 and carbazole 18	56
34. NMR shielding increment surfaces (in ppm) at the 2.5 Å level for benzo-analogs: isoindole 1c , isobenzofuran 4c and benzo[c]thiophene 10c	57
35. NMR shielding increment surfaces (in ppm) at the 2.5 Å level for benzo-analogs: indazoline 19 and cycl[3,2,2]azine 20	58
36. NMR shielding increment surfaces (in ppm) at the 2.5 Å level for benzo-analogs of parent five-membered rings: indole 1b , benzofuran 4b and benz[b]phosphole 7b	59
37. NMR shielding increment surfaces (in ppm) at the 2.5 Å level for the benzo-analog of parent five-membered ring: benzo[b]thiophene 10b	60
38. NMR shielding increment surfaces (in ppm) at the 2.5 Å level for benzo-analogs of parent five-membered structure derivatives with nitrogen in α position: indazole 2b , 1,2-benzisoxazole 5b and 1,2-benzisophosphazole 8b	62
39. NMR shielding increment surfaces (in ppm) at the 2.5 Å level for benzo-analog of parent five-membered structure derivative with nitrogen in α position: 1,2- benzisothiazole 11b	63
40. NMR shielding increment surfaces (in ppm) at the 2.5 Å level for the benzo-analog of the parent five-membered structure derivative with nitrogen in β position: benzimidazole 3b , 1,3-benzoxazole 6b and 1,3-benzphosphazole 9b	65

41. NMR shielding increment surfaces (in ppm) at the 2.5 Å level for benzo-analog of parent five-membered structure derivative with nitrogen in β position: 1,2-benzothiazole 12b	66
42. NMR shielding increment surfaces (in ppm) at the 2.5, 3.0 & 4.0 Å levels for indole 1b	68
43. This study's NMR maximum shielding increments ($\Delta\sigma_{\max}$) over the heterocyclic side correlated with ASE [12] (A) and this study's NICS(0) (B) measurements for the benzo-analogs.....	71
44. This study's NMR maximum shielding increments ($\Delta\sigma_{\max}$) over the heterocyclic side correlated with this study's NICS(1) (A) and this study's NICS(2.5) (B) for the benzo-analogs.....	72
45. ASE [12] correlated with both this study's NICS(0) over the heterocyclic side (A) and NICS(1) over the heterocyclic side (B), both for the benzo-analogs.....	74
46. This study's NICS(2.5) over the heterocyclic side correlated with ASE [12] (A) and this study's NICS(0) and NICS(1) both over the heterocyclic side correlated with each other (B) for the benzo-analogs.....	75
47. This study's NICS(0) and NICS(2.5), both over the heterocyclic side, correlated with each other (A) and this study's NICS(1) and NICS(2.5), both over the heterocyclic side, with each other (B) for the benzo-analogs.....	76
48. This study's NMR maximum shielding increments ($\Delta\sigma_{\max}$) over benzene correlated with both ASE [12] (A) and this study's NICS(0) over benzene (B) for the benzo-analogs.....	79
49. This study's NMR maximum shielding increments ($\Delta\sigma_{\max}$) over benzene correlated with both this study's NICS(1) over benzene (A) and this study's NICS(2.5) over benzene (B) for the benzo-analogs.....	80
50. ASE [12] correlated with both this study's NICS(0) over benzene side of benzo- analogs (A) and NICS(1) over benzene side of benzo-analogs(B).....	82
51. This study's NICS(2.5) over benzene side of benzo-analogs correlated with ASE [12] (A). This study's NICS(0) and NICS(1) both over benzene side of benzo-analogs correlated with each other (B).....	83

52. This study's NICS(0) and NICS(2.5), both over benzene side of benzo-analogs, correlated with each other (A). This study's NICS(1) and NICS(2.5), both over benzene side of benzo-analogs, correlated with each other (B).....	84
53. This study's NMR maximum shielding increments ($\Delta\sigma_{\max}$) over the center bond correlated with both ASE [12] (A) and this study's NICS(0) over the center bond (B) for the benzo-analogs.....	87
54. This study's NMR maximum shielding increments ($\Delta\sigma_{\max}$) over the center bond correlated with both this study's NICS(1) over the center bond (A) and this study's NICS(2.5) over the center bond (B) for the benzo-analogs.....	88
55. ASE [12] correlated with this study's NICS(0) (A) and NICS(1) (B) both over the center bond of the benzo-analogs.....	90
56. This study's NICS(2.5) over the center bond of benzo-analogs correlated with ASE [12] (A). This study's NICS(0) and NICS(1) both over the center bond of benzo-analogs correlated with each other (B).....	91
57. This study's NICS(0) and NICS(2.5), both over the center bond of benzo-analogs, correlated with each other (A). This study's NICS(1) and NICS(2.5), both over the center bond of benzo-analogs, correlated with each other (B).....	92

1. INTRODUCTION

Consistent and reliable ways to measure the extent of aromaticity can be appreciated within the petroleum, pharmaceutical, cosmetic and food industries. Aromatic compounds are prevalent in these industries because these compounds are stable and resist chemical degradation. Thus, research geared towards implementing a new method in measuring aromaticity while helping to provide better correlations between different methods, is worth appreciating as well.

Cyclic compounds are routinely categorized as either aromatic, non-aromatic or anti-aromatic [1,2,3,4,5,6,7,8,9,10,11]. Aromaticity is a widely known phenomenon, but poorly understood in the world of chemistry. Aromaticity may be considered in either a qualitative or quantitative manner [2, 12, 13]. The qualitative aspect of aromaticity is well understood, but the quantitative aspect is controversial and not universally defined. Since the concept of aromaticity was introduced by Kekulé 143 years ago [14], many different methods have been described to determine whether a substance is antiaromatic, aromatic or to what extent aromatic [2,3,15,16,17,8,9,18, 19,20,21,22,23,24,25,26,27,10,28,11]. Some are experimental and some are theoretical. Loose correlations have been determined among the four most widely used measures of aromaticity [16,10]. They are 1) the harmonic oscillator model of aromaticity (HOMA), a measure of the similarity of ring CC bond lengths, 2) aromatic stabilization energy (ASE), 3) exaltation of magnetic susceptibility (Λ) and 4) nucleus independent chemical shift (NICS), a measure of the diamagnetic field (for aromatic compounds) produced by the ring current induced by the strong applied magnetic field. Each of these methods will be discussed below.

Our goal is to help bring about better consistency with the quantitative aspect through the use of shielding increments ($\Delta\sigma$) [2] and the methodological details are discussed later within the experimental section. However, the chemistry behind our approach relates to the magnitude of NMR shielding a proton will experience while being in proximity to and above the plane of an aromatic system. This proton shielding [29,30,31] is a result of the applied magnetic field of the aromatic system.

In the presence of a strong magnetic field (Figure 1, B_0), pi electrons of an aromatic ring are induced to circulate [32,33,3,10]. The circulation of electrons generates an induced magnetic field (B_i) which opposes the applied field above and below the center of the aromatic ring, but is aligned with the magnetic field in the vicinity of the protons attached to the aromatic ring. This causes protons on the aromatic ring to experience NMR deshielding [33].

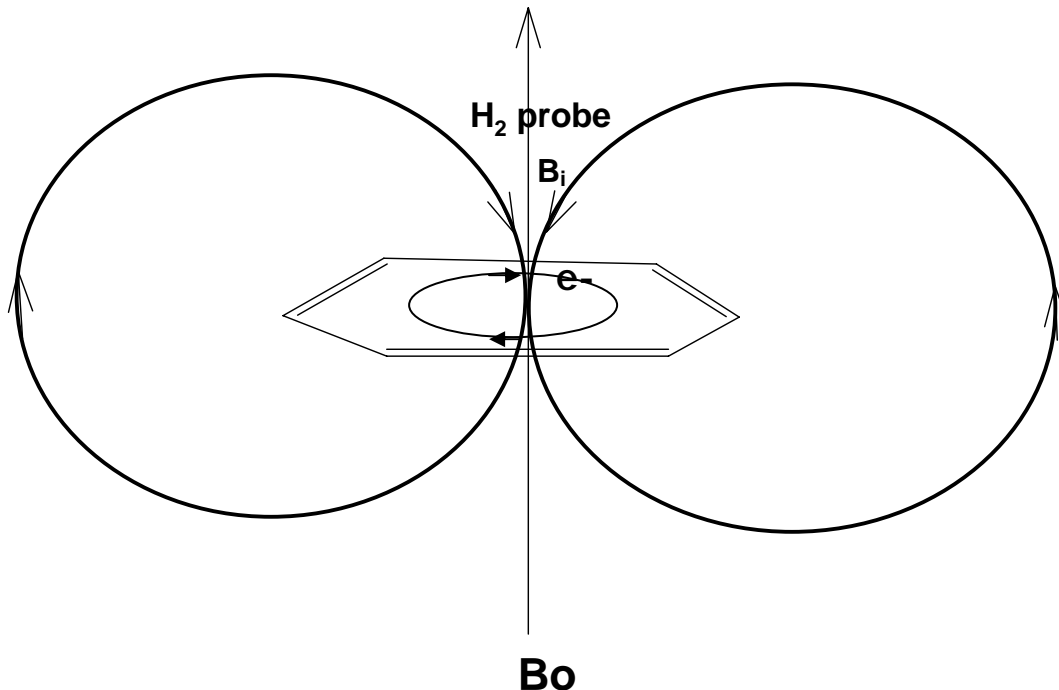


Figure 1: Illustration of what causes proton shielding/deshielding [34, p.18]

Established Methods of Measuring Aromaticity

1) The harmonic oscillator model of aromaticity (HOMA) is the most widely used geometric measure of the aromatic character of a π -electron system [35,10,36,3,34,37]. It is defined as the normalized sum of squared deviations of bond lengths from the optimal value. The optimal value is assumed to be realized for a fully aromatic system, such as benzene, in which all bond lengths are identical [34,37]. The direct determination of bond lengths, which can be done experimentally *via* gas-phase electron diffraction(ED) [8], or computationally using high level quantum calculations provides valuable information on the extent of electron delocalization in molecules. Thus, singlet states of antiaromatic compounds have localized pi electrons and generally have alternating single and double bonds which differ greatly, i.e. over 0.2 Å, in length, in contrast to the bonds of aromatic compounds, which are more nearly equal in length.

A HOMA value can be obtained using the following equation [9]:

$$\text{HOMA} = (1 - 257.7/n) \Sigma(d_{\text{opt}} - d_i)^2$$

where n = # of bonds taken into summation

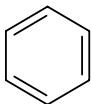
257.7 is the normalization value

d_{opt} is the optimized bond length

d_i is the experimental or computed bond length

Sample Calculation:

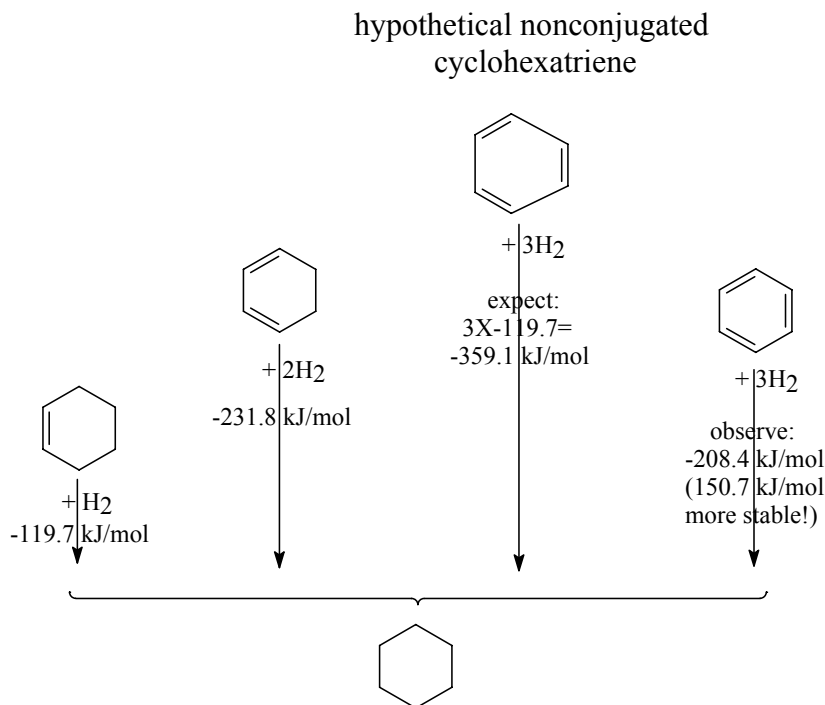
(Benzene)



$$\text{HOMA} = 1 - (257.7/6)\Sigma(d_{\text{opt}} - d_i)^2$$

$$= 1 - (257.7/6)\Sigma(1.395\text{Å} - 1.395\text{Å})^2 = 1 - (257.7/6)* (0) = 1 - 0 = 1.00$$

2) The aromatic stabilization energy (ASE) is the most commonly used measure of aromaticity [20,3,16,19,38,39,40,41]. It is based on assessments of energies of aromatic or antiaromatic systems relative to reference systems, such as olefins or conjugated polyenes. This analysis usually involves measuring (or theoretically computing) the heat of combustion, the heat of hydrogenation, or the heat of formation and using these values to calculate the aromatic stabilization energy (also called the resonance energy). ASE depends dramatically on the kind of reaction involved and the level of theory applied, therefore, it is important to use accurate energetic data (from high quality quantum chemical computational methods) and a well-chosen reference [1,27,38,39,40,41].



$$\begin{aligned}
 \text{ASE} &= -208.4 \text{ kJ/mol} - (-359.1 \text{ kJ/mol}) \\
 &= 150.7 \text{ kJ/mol} \\
 &= 150.7 \text{ kJ/mol} * (\text{kcal}/4.19 \text{ kJ}) = 36.0 \text{ kcal/mol}
 \end{aligned}$$

Figure 2: Sample Calculation (Benzene)[11]

3) Exaltation of magnetic susceptibility (Λ) is defined as the difference between the computed magnetic susceptibility (X_m) for a compound and the value estimated for the hypothetical system without cyclic electron delocalization (X'_m) [23,42,43,44,12].

$$\Lambda = X_m - X'_m$$

where X_m denotes bulk magnetic susceptibility of the compound and X'_m denotes the susceptibility estimated from an increment system for structure components (isomers without cyclic delocalization). The magnetic susceptibility exaltation of benzene is calculated below (note that the calculation of the hypothetical cyclohexatriene may be found in the Appendix of Simon [45]):

Sample Calculation:

$$\Lambda_{\text{benzene}} = \chi_{\text{av benzene}} - \chi'_{\text{av cyclohexatriene}} = -52.89 - (-37.79) = -15.1 \text{ ppm cgs [45]}$$


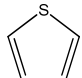
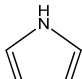
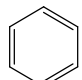
This value of -15.1 for benzene is confirmed as valid in comparison with experimental value of -13.7 ppm obtained by Dauben [46]. It is an expected standard for aromatic compounds to yield negative exaltation values while antiaromatic produce positive values.

cgs = metric units based upon cm, gram or second

av = average susceptibility tensor value for sum of isotropic parts

4) The nucleus-independent chemical shift (NICS) is a relatively new criterion of aromaticity based on the absolute magnetic shielding computed at the geometrical center of the ring (NICS(0)) or 1 Å above the ring center (NICS(1)) [25,47,48,2]. The NICS(1) provides an additional assessment of the ring current effects in a simple quick calculation. NICS has been used extensively for the identification of aromatic properties of molecules, ions, intermediates and transition states since its introduction in 1996. The NICS method involves the use of *Gaussian 03* [49]. A model of the molecule is structurally optimized at the B3LYP/6-311G* level of theory. The NICS value is the negative of the computed isotropic chemical shielding of a ghost atom (Bq; a point in space), at the center of the molecule (NICS or NICS(0)) or at a point 1 Å above the center (NICS(1)), calculated using the GIAO (gauge-independent atomic orbital) method, a subroutine in *Gaussian 03*[49]. Table 1 presents the values reported for each of the methods for a series of organic compounds.

Table 1:
Summary of measures of aromaticity [16]

Molecule	NICS (ppm)	NICS(1) (ppm)	HOMA	ASE (kcal/mol)	Δ (ppmcgs)	structure
Furan	-12.3	-9.40	0.78	14.8	-2.90	
Thiophene	-13.8	-10.8	0.89	18.6	-7.00	
Pyrrole	-14.9	-10.6	0.90	20.6	-6.50	
Benzene	-17.2	-12.9	1.00	36.0	-15.1	

cgs = metric units based upon cm, gram or second

2. OBJECTIVE

Martin et al. [7] showed that NMR shielding calculations using a diatomic H₂ probe above the plane of the ring was a simple method to qualitatively distinguish between aromatics and antiaromatic hydrocarbons. The NICS calculation method was not completely reliable at that task, however, in that the cyclopropenyl anion analysis yielded a value with the wrong sign. Even though its absolute value was one of the smallest, there were values for other structures which were smaller but had the correct sign indicating a significant flaw with this method. By using the NICS(2.5) technique, one should obtain negative values for aromatic systems and positive values for antiaromatic systems. Thus, cyclopropenyl anion which is known to be antiaromatic should have yielded a positive value using the NICS(2.5) method but its NICS(2.5) was negative. This NICS(2.5) method is similar to the diatomic H₂ probe method used in this study and only differs in that NICS(2.5) uses a relative point in space and our method uses a diatomic H₂ probe for measuring through-space NMR shielding effects. In previous studies using the diatomic H₂ probe method, Martin et al. were able to successfully distinguish all systems tested as being either aromatic or antiaromatic. In this research we are investigating the use of through space NMR shielding computations via diatomic H₂ as a means for predicting the extent of aromaticity. This will be demonstrated by determining if our results correlate with results of already established methods for measuring the degree of aromaticity.

Chemical shielding has the same magnitude and units (ppm) as the chemical shift. We will use quantum mechanical computations that compute isotropic chemical shielding values. Shielding increment ($\Delta\sigma$) values may be calculated by subtracting the shielding value (26.772 ppm) of a proton of H₂ by itself from the measured shielding value of the

proton at 2.5Å from the center of the molecule in question. Fig. 3 illustrates these differences.

Chemical Shielding vs. Chemical Shift

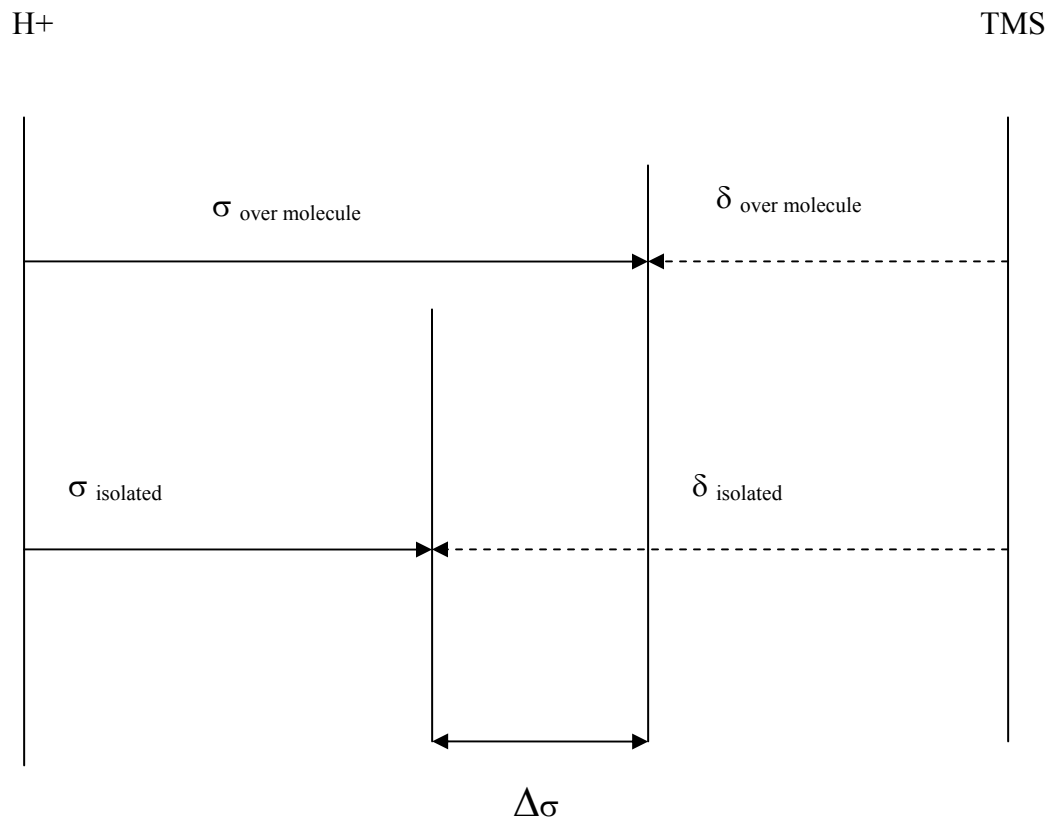


Figure 3. Chemical shielding vs. chemical shifting representation

$$\Delta\sigma = \sigma_{\text{H2 over benzene}} - \sigma_{\text{H2 isolated}} = +\Delta\sigma \text{ for aromatic systems}$$

It is well known that aromatic rings have NMR shielding effects on protons above them and anti-aromatic rings have deshielding effects on protons above them. Therefore, aromatic systems yield positive $\Delta\sigma$ values and antiaromatic systems yield negative $\Delta\sigma$ values.

3. EXPERIMENTAL METHODS

A. Computational Methods

Computer models of a set of five-membered ring heterocyclic aromatic compounds and their benzo-derivatives were constructed in order to calculate shielding increment ($\Delta\sigma$) values at 2.5, 3.0, and 4.0 Angstroms above the plane of the molecule. Models of each structure were created using the *Titan* [50] software program. Building these models was a simple process that involved joining the specific atoms required to make a particular molecule with the appropriate type of bond. After the crude model of each molecule was constructed, it was submitted to a molecular mechanics geometry optimization calculation using the Merck molecular force field (38, 30) within *Titan*. The MMFF optimized structure was then subjected to a geometry optimization calculation in *Titan* using the Hartree-Fock ab initio method and the 6-31G(d,p) basis set. The resulting equilibrium structure was then saved as a .pdb file.

The program *orient.jar* (a Java script written by UNCW Computer Science faculty Dr. Clayton Ferner and his students) [51] was then used to orient each molecule in Cartesian space. The five-membered heterocyclic structures were positioned with the molecule centered at the origin in the XY plane. The benzo-heterocyclic structures (benzo-analogs) were positioned in the XY plane with the bond between the five-membered ring and benzene ring on the Y-axis with the bond midpoint at the origin (Figure 4). After achieving these orientations, the Cartesian coordinates were written (by *orient.jar*) in a file format similar to the input file format needed in the subsequent calculation. The Cartesian coordinates of 1H-benzotriazole are shown in Table 2.

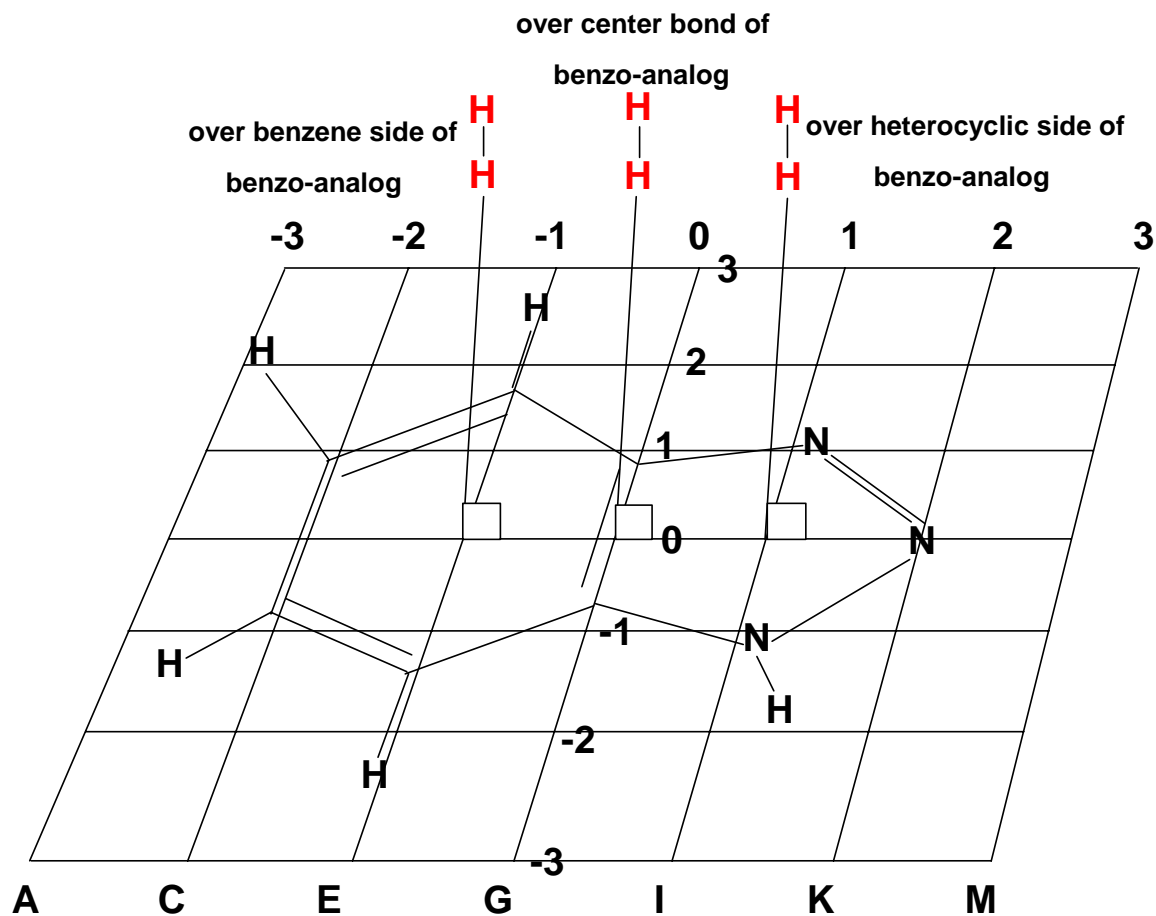


Figure 4. Orientation of 1H-benzotriazole in the XY plane of Cartesian space

Table 2.

Cartesian coordinates of 1H-benzotriazole

N	1.320677	-0.998537	0.000000
N	2.056199	0.113531	0.000000
N	1.308071	1.117883	0.000000
C	0.000000	0.691747	0.000000
H	1.775405	-1.879691	0.000000
C	0.000000	-0.691747	0.000000
C	-1.197743	1.413973	0.000000
C	-1.183394	-1.440664	0.000000
C	-2.361894	0.693582	0.000000
H	-1.191479	2.488525	0.000000
H	-3.308868	1.203439	0.000000
C	-2.349069	-0.720581	0.000000
H	-1.181662	-2.515002	0.000000
H	-3.288383	-1.244889	0.000000

A diatomic hydrogen (H_2) probe was placed along the Z-axis at various distances (2.5, 3.0, or 4.0Å) above the plane of the molecule by inserting the following two lines into the input file just above the Cartesian coordinates of the aromatic molecule. As seen, this example (Table 3) applies to the proximal hydrogen of the probe being 2.5Å above the plane, thus for 3.0Å, a 3.0 would be in place of 2.5 and 3.7326 would be beneath it. Likewise, for 4.0Å, 4.0 would be in the top line and 4.7326 in the next line.

Table 3. XY Coordinates of (0,0) with proximal hydrogen at 2.5Å above plane of at structure.

H	0.000	0.000	2.5000
H	0.000	0.000	3.2326

The *Gaussian 03* [49] program was used to perform NMR shielding calculations at the Hartree-Fock level using the 6-31G(d,p) basis set and the keyword NMR. The diatomic hydrogen probe was moved in 1Å increments in the X and Y directions in separate input files over a 3Å by 3Å grid in each quadrant of the XY plane. The following lines show the H_2 in a different grid position:

Table 4. XY Coordinates of (1,0) with proximal hydrogen at 2.5Å above plane of at structure.

H	1.000	0.000	2.5000
H	1.000	0.000	3.2326

Shielding increment ($\Delta\sigma$) values at each grid coordinate were obtained by subtracting the isotropic shielding value of one of the hydrogens of the H₂ probe alone (26.77 ppm) from the isotropic shielding value acquired from the proximal hydrogen of the H₂ probe at that point relative to the modeled structures. The process was repeated with the H₂ probe at proximal hydrogen distances of 2.5, 3.0 and 4.0 Å from the particular molecule being studied.

B. Data Treatment

TableCurve 3D [52] was used to create 3-D NMR shielding increment surfaces ($\Delta\sigma$ versus X & Y). These 3-D graphs serve as visualizations of the magnitudes and localities of shielding and deshielding regions over the structures being studied. The maximum shielding increment ($\Delta\sigma_{\max}$) values calculated, which corresponded with the probe at 2.5 Å above the center (coordinates 0, 0) of each five-member ring heterocycle, were graphed in *MS Excel* [53] against four different methods for measuring aromaticity collected by Cyranski [16]. Linear correlation coefficients were obtained for the best fit line. The $\Delta\sigma$ values of the benzo-analogs were obtained at 2.5 Å above the midpoint of the benzene ring portion of the benzo-analog, the midpoint of the five member ring portion of the benzo-analog, and the midpoint of the bond separating the benzene ring from the five member ring (Fig. 4). These three $\Delta\sigma$ values as exemplified in Figure 4 were calculated independently from each other then graphed in *MS Excel* against published quantitative measures of aromaticity, Bird's ASE data [12], to obtain linear correlation coefficients.

4. RESULTS

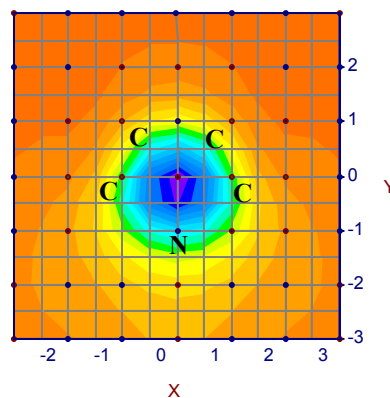
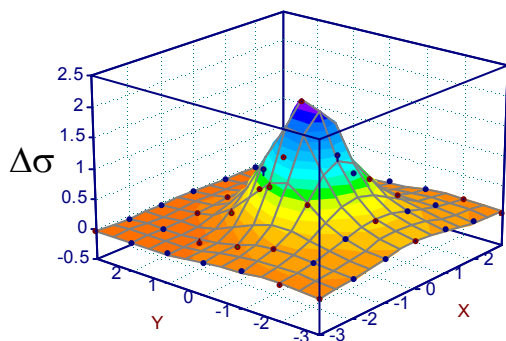
A. Unsaturated Five-Membered Heterocyclic Ring Compounds

NMR shielding computations were done over the entire surface on each of the unsaturated five-membered heterocyclic ring compounds (five-membered rings) listed in Fig. 6. Similar computations were done on the benzo-fused unsaturated five-membered heterocyclic ring compounds (benzo-analogs) listed in Fig. 7. The results of these calculations were used to make 3D NMR shielding surface graphs at the 2.5, 3.0 and 4.0 Å levels. The graphs at the 2.5 Å level as seen in Figs. 8-12 and Figs. 29-35 were studied extensively. The analysis was done to compare the shielding surfaces along with the structural makeup of different but similar structures.

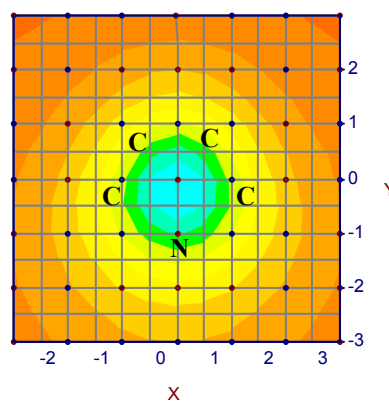
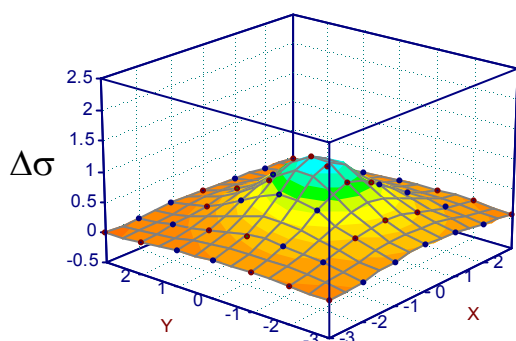
Graphs at the 2.5 Å level were chosen over results from the 3.0 Å and 4.0 Å levels for detailed analysis because the closer the proximal hydrogen of the diatomic probe is to the plane of the structure, the greater the shielding it experiences. Also, the shapes of the shielding surfaces have more distinctive features when the proximal hydrogen of the diatomic probe is closer to the structure causing the shielding, as seen in Figs. 5 (five-membered rings) and 42 (benzo-analogs).

Selected 2.5 Å maximum shielding increment values were compared graphically with results from established methods for measuring aromaticity for the same structures. This was done in order to find correlations between the shielding increments produced from this research with results of established methods of measuring aromaticity. Good correlations would validate the technique tested in this research as being a credible method for measuring the extent of aromaticity.

pyrrole 1 (2.5Å)



pyrrole 1 (3.0Å)



pyrrole 1 (4.0Å)

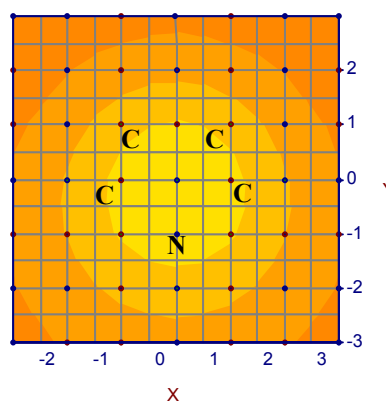
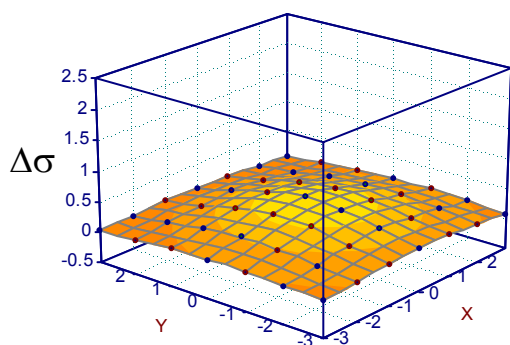


Fig.5. NMR shielding increment surfaces (in ppm) at the 2.5, 3.0 & 4.0 Å levels for pyrrole 1.

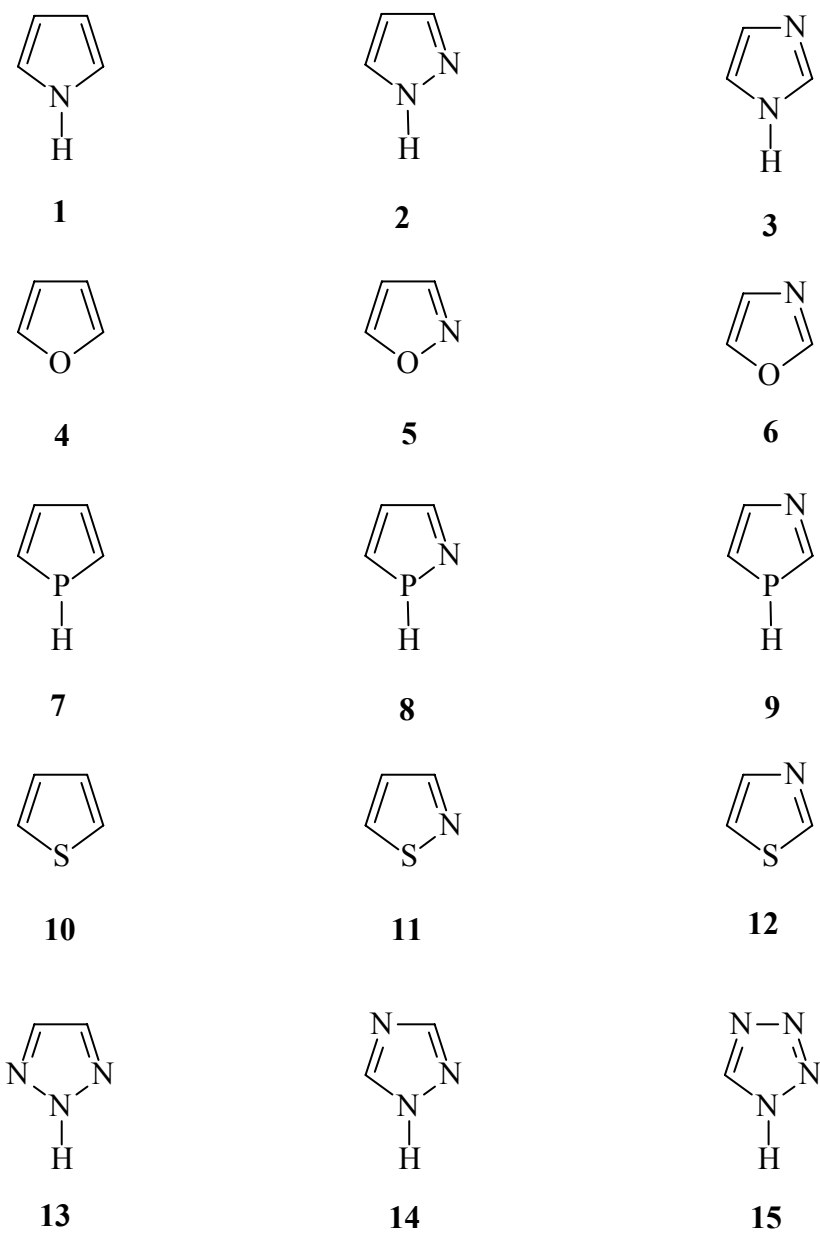


Fig. 6. Unsaturated five-membered heterocyclic compounds (five-membered rings).

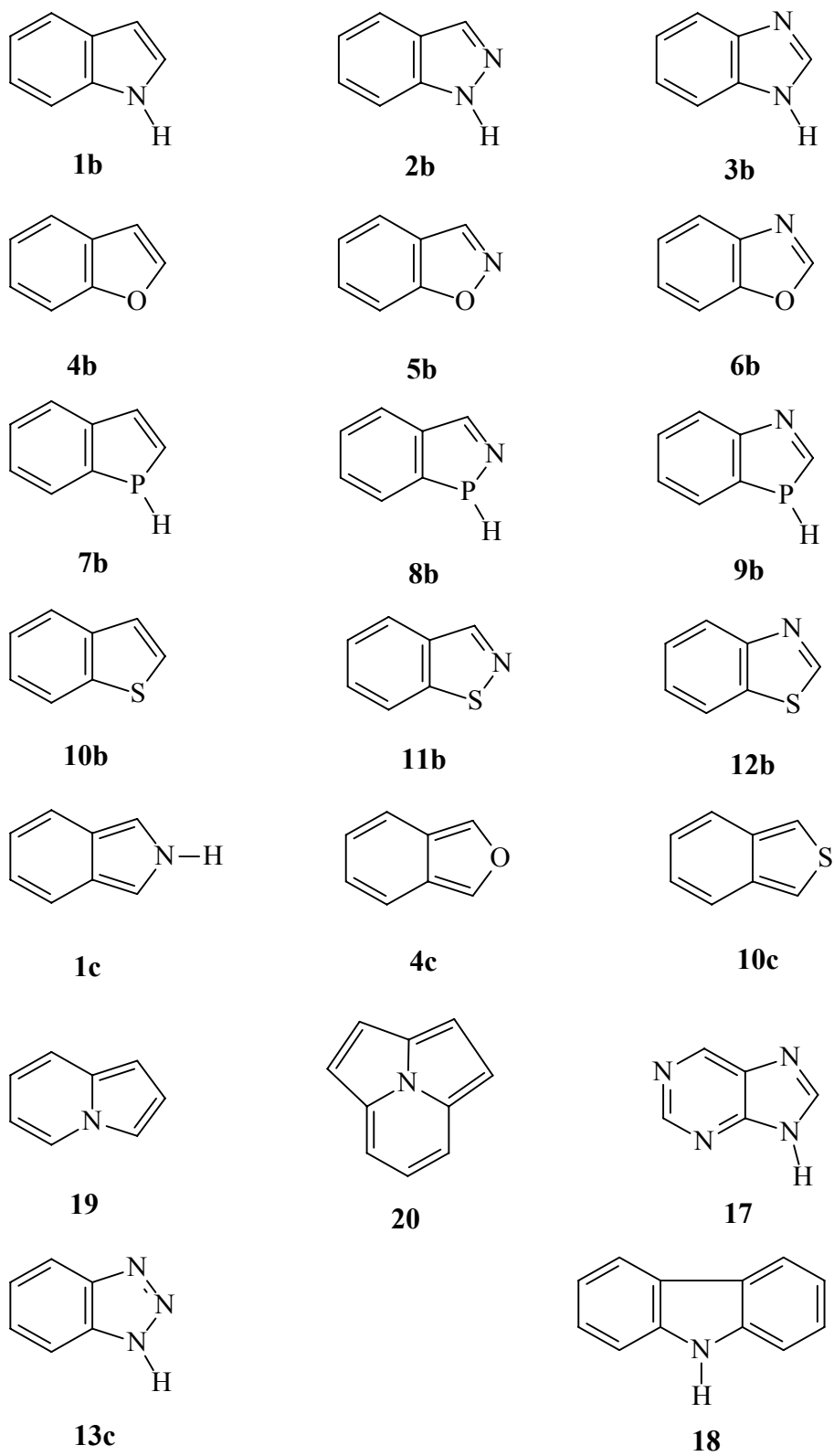


Fig. 7. Benzo-fused unsaturated five-membered heterocyclic compounds (benzo-analogs) and miscellaneous fused-ring heterocyclic compounds.

Figs. 8-12 are the shielding maps corresponding to $\Delta\sigma$ values calculated at 2.5 Å over the five-membered rings. As can be seen in Fig. 6, the structures of these five-membered rings follow a pattern. The first structure in each of the first four rows are the four parent structures (1st column except 1,2,3-triazole **13**), characterized by the atom at the bottom of the ring: (N) pyrrole **1**, (O) furan **4**, (P) phosphole **7**; (S) thiophene **10**. Additional structures within each row have a nitrogen atom either adjacent (α) to the bottom heteroatom or one atom removed (β) from the bottom heteroatom which makes them analogs of the parent. The last row of structures in Fig. 6 contains derivatives of pyrrole having more than one additional nitrogen atom.

Shielding maps of the four parent structures are gathered in Fig. 14. The shielding surface of pyrrole **1** has a smooth steep mound of shielding with the maximum near the ring center. The shielding surface outside the ring atoms appears to be smooth and level with a shielding increment near zero. Amongst all four parent five-membered rings furan **4** seems to be the most similar to pyrrole **1**. However, the shielding surface near (0, -3), beyond where the nitrogen is for pyrrole and beyond where the oxygen is for furan, reflects slight deshielding ($\Delta\sigma < 0$) for furan which is not observed in the shielding map of pyrrole. The difference may lie in the fact that oxygen is slightly more electron rich. It is apparent that thiophene **10** has a larger maximum shielding value than phosphole **7**. Significant deshielding effects ($\Delta\sigma < 0$) are also observed near (0, -2). The phosphorus atom in phosphole and the sulfur atom in thiophene are significantly larger in size than nitrogen and oxygen. Phosphorus and sulfur are also rich in electrons; two of which are identified as either lone pair of electrons or lp on each atom (phosphorus and sulfur). The phosphorus atom of phosphole is bonded to a hydrogen atom which projects

above or below the plane of the rest of the atoms. Shielding maps of both sides are shown in Figures 14 and 15. Their differences will be discussed later. The major feature in both maps is a region of deshielding over the hydrogen (or lone pair of electrons) attached to phosphorus, in addition to the mound of shielding over the ring. Thiophene **10** also displays deshielding in the comparable region.

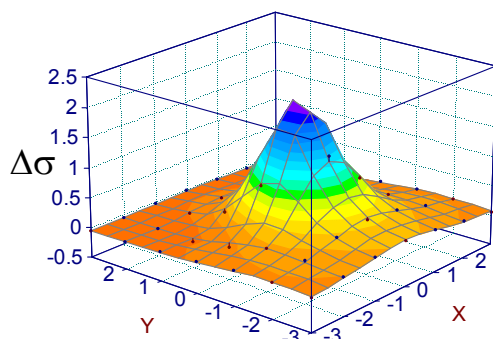
The shielding maps of pyrrole **1** and its derivatives containing a second nitrogen atom (1H-pyrazole **2** and 1H-imidazole **3**) are shown in Fig. 8. The position of the additional nitrogen leads to slightly different shielding increment surfaces. The maximum $\Delta\sigma$ value corresponds to the very distinct sharp peak in pyrrole **1** (Fig. 8). The shielding mound of 1H-pyrazole **2** (Fig. 8) is fuller than that of pyrrole **1**. The structural difference between pyrrole **1** and 1H-pyrazole **2** is that the latter has an additional nitrogen α to the bottom heteroatom. Furthermore, the centermost shading within the top view of 1H-pyrazole is greater in area than the centermost shading corresponding to pyrrole. The shielding map of 1H-imidazole **3**, which has the additional nitrogen β to the bottom heteroatom, shows a narrower mound close to the center of the shielding mound. A major difference between the shielding map of 1H-pyrazole **2** and pyrrole **1** is a region of deshielding beyond the additional nitrogen in the former. A similar, but more pronounced trend is seen in 1H-imidazole **3**.

Furan **4** (Fig. 10) and its nitrogen-containing derivatives isoxazole **5** and oxazole **6** displayed the same sort of trend seen with pyrrole **1** and its nitrogen-containing derivatives. This is evident with a region of deshielding in beyond the nitrogen in each case.

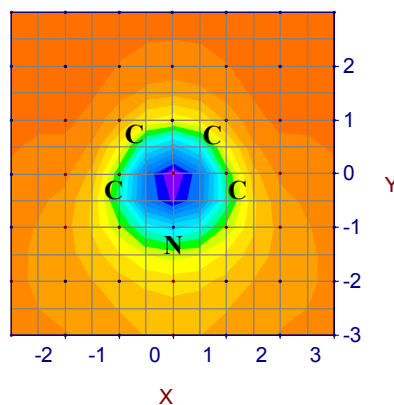
Phosphole **7** and its nitrogen-containing derivatives isophosphazole **8** and phosphazole **9** also displayed slight deshielding trends beyond the position of the nitrogen (Figs. 11 and 12). This established trend as seen with the previously discussed five-membered rings is barely noticeable here though because of the major deshielding regions in proximity to the phosphorus heteroatom of these five-membered rings. Thus, the shielding surfaces of phosphole **7** and its derivatives exhibit no significant differences qualitatively.

Thiophene **10** and its nitrogen-containing derivatives (Fig. 13) also showed significant deshielding regions in proximity to its heteroatom, sulfur, similar to, though not to the same extent, as what was observed with phosphole **7** and its nitrogen-containing derivatives. Qualitatively though, these derivatives displayed trends similar to what was observed earlier with pyrrole **1** and its nitrogen-containing derivatives. There are significant regions of deshielding beyond the position of nitrogen.

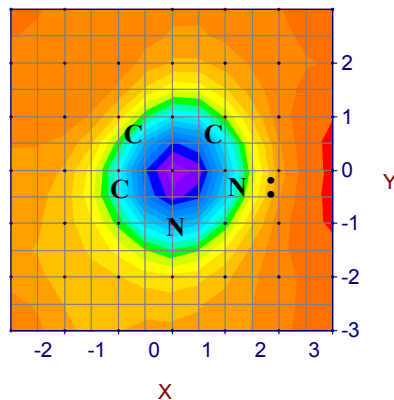
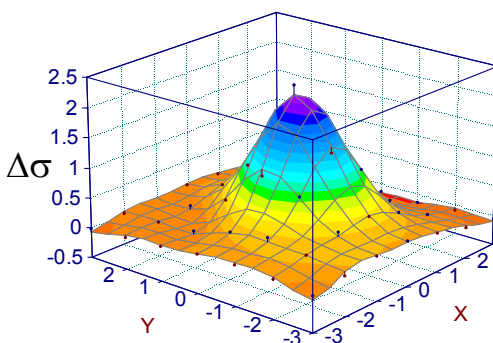
Side View
pyrrole 1



Top View



1H-pyrazole 2



1H-imidazole 3

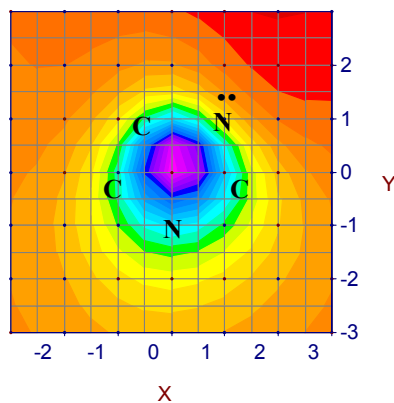
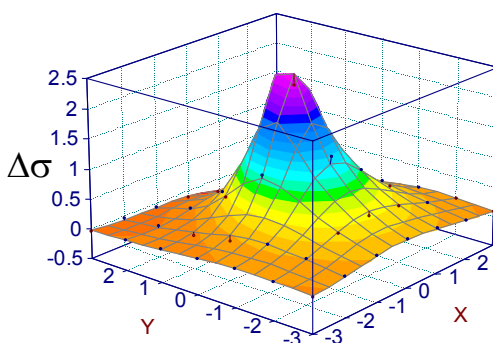
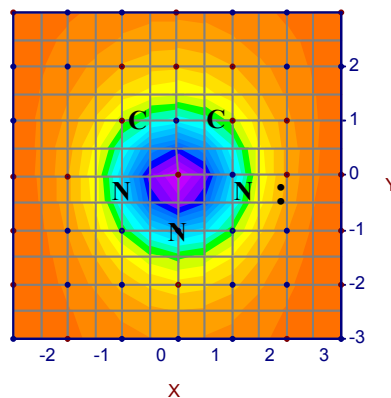
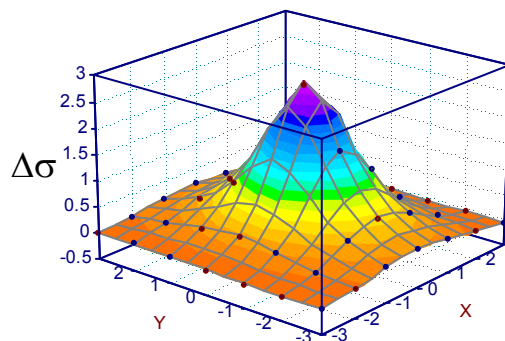
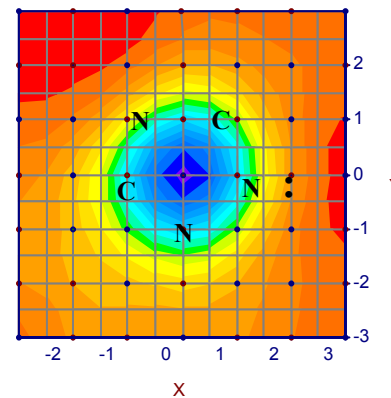
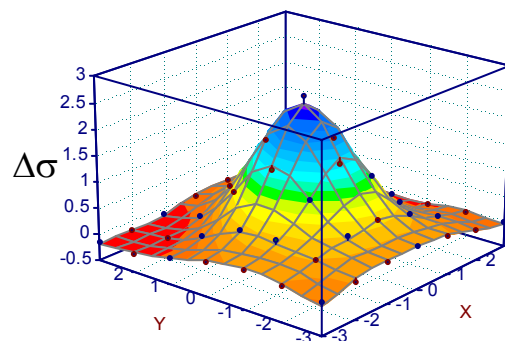


Fig. 8. NMR shielding increment surfaces (in ppm) at the 2.5 Å level for five-membered rings: pyrrole 1, 1H-pyrazole 2 and 1H-imidazole 3.

1,2,3-triazole **13**



1,2,4-triazole **14**



1H-tetrazole **15**

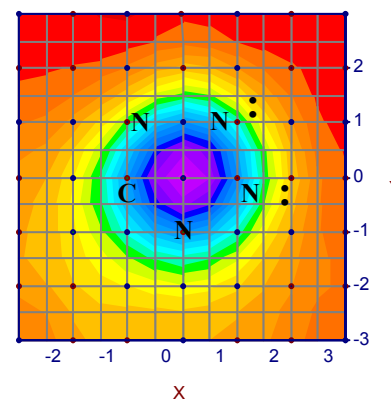
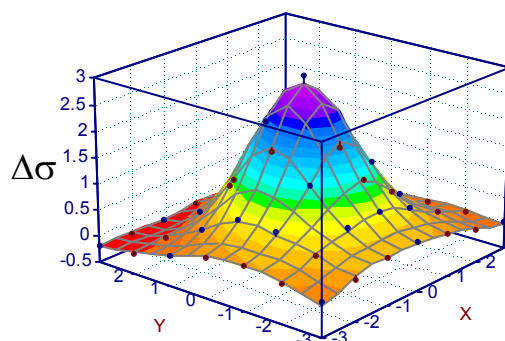
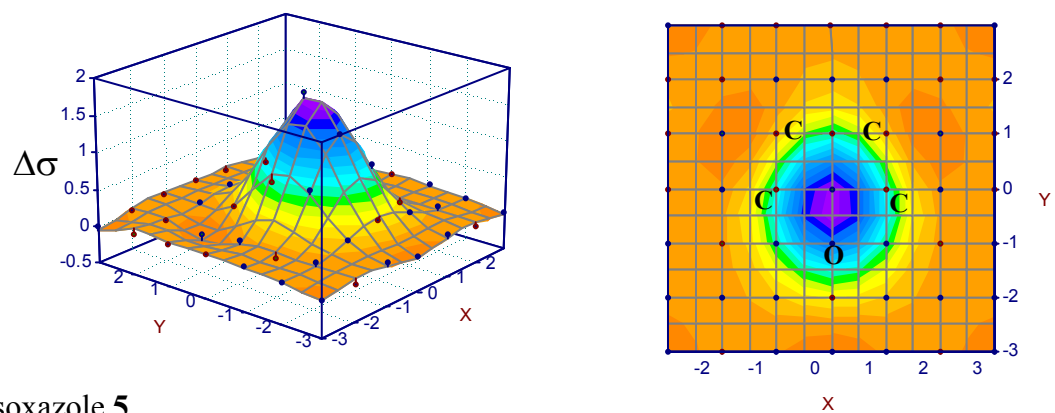
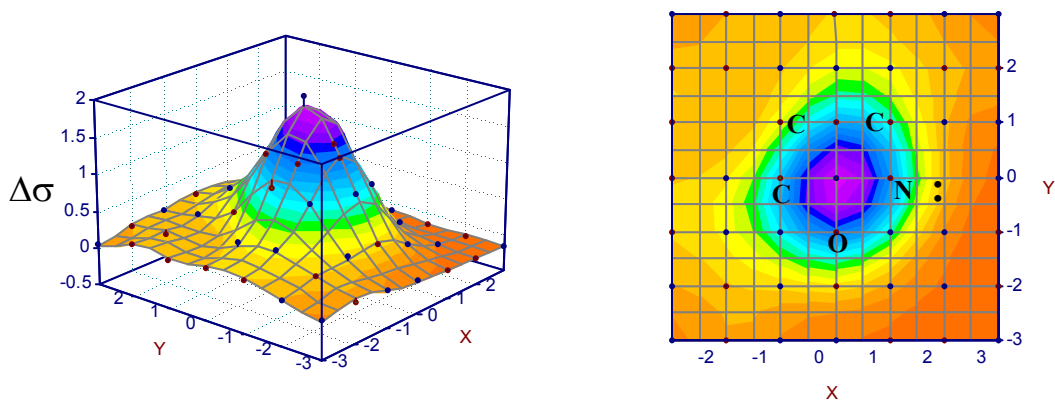


Fig. 9. NMR shielding increment surfaces (in ppm) at the 2.5 Å level for five-membered rings: 1,2,3-triazole **13**, 1,2,4-triazole **14** and 1H-tetrazole **15**.

furan **4**



isoxazole **5**



oxazole **6**

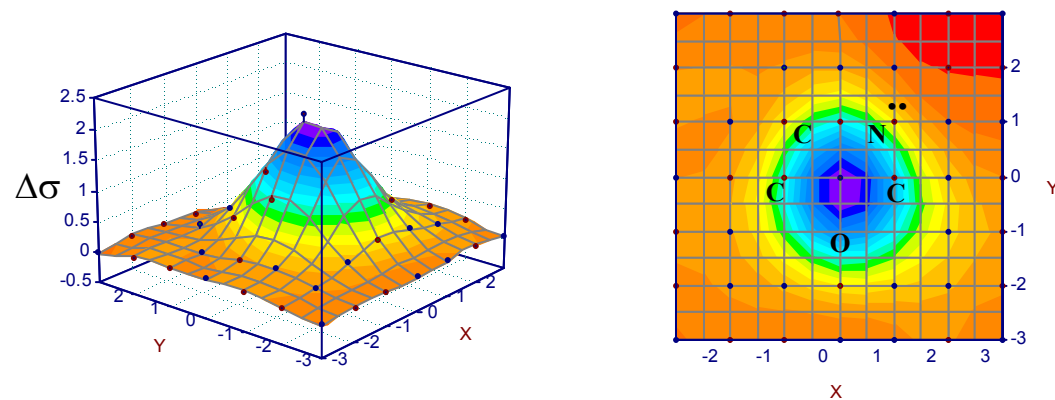
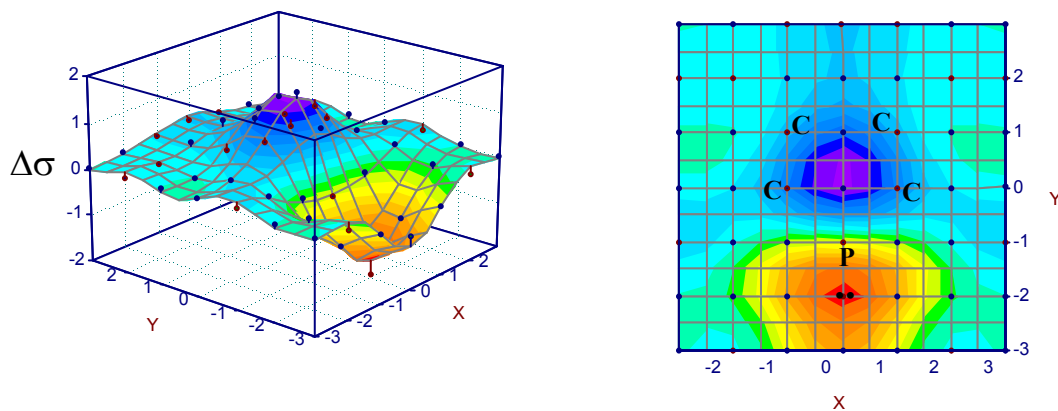
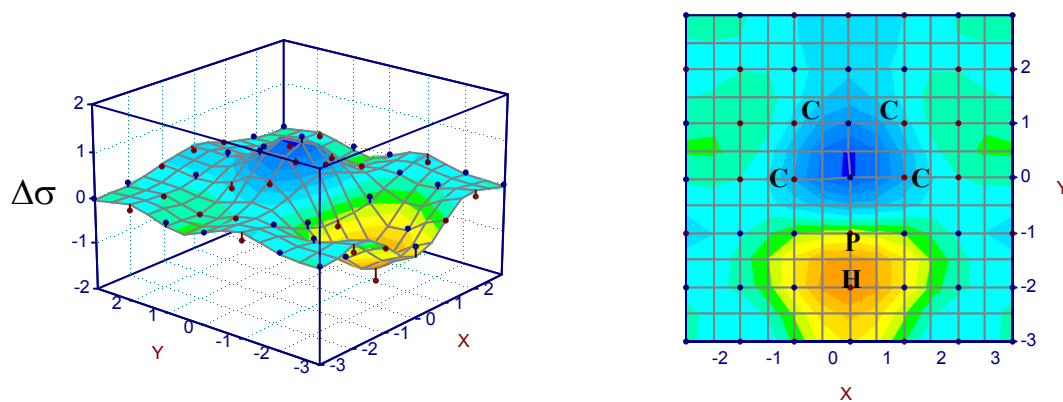


Fig. 10. NMR shielding increment surfaces (in ppm) at the 2.5 Å level for five-membered rings: furan **4**, isoxazole **5** and oxazole **6**.

phosphole (lp side) 7



phosphole (P-H side) 7



isophosphazole (P-H side) 8

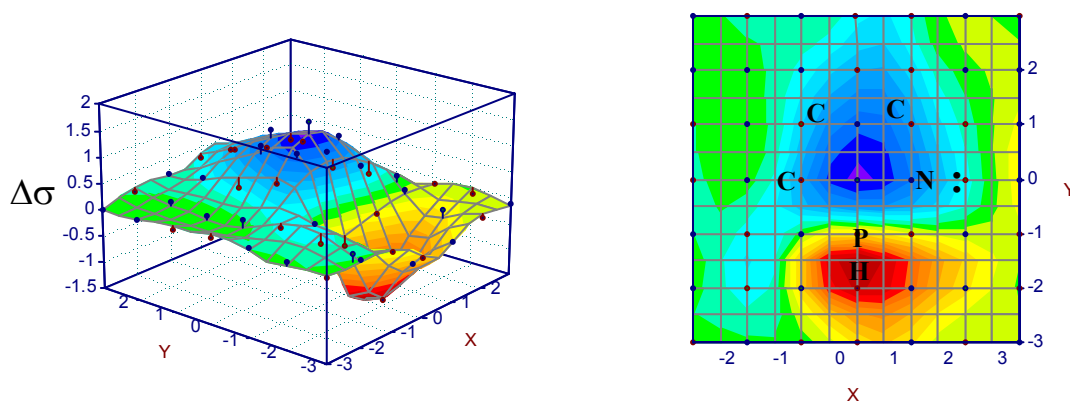
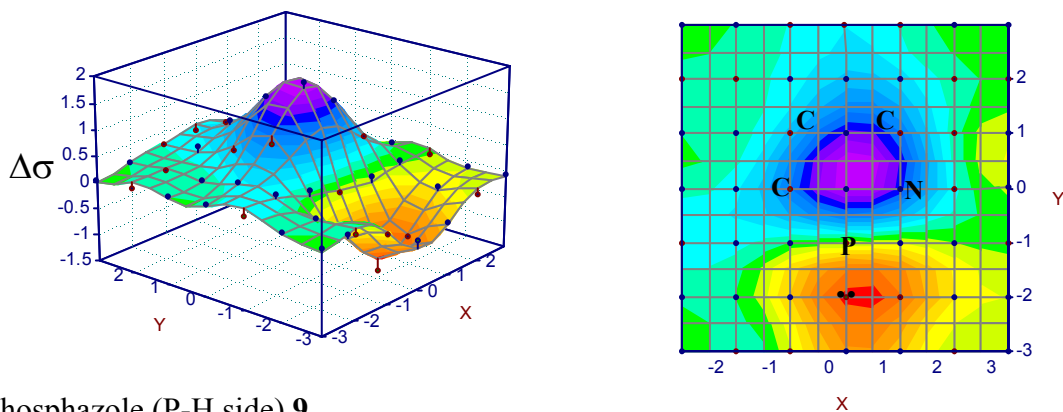
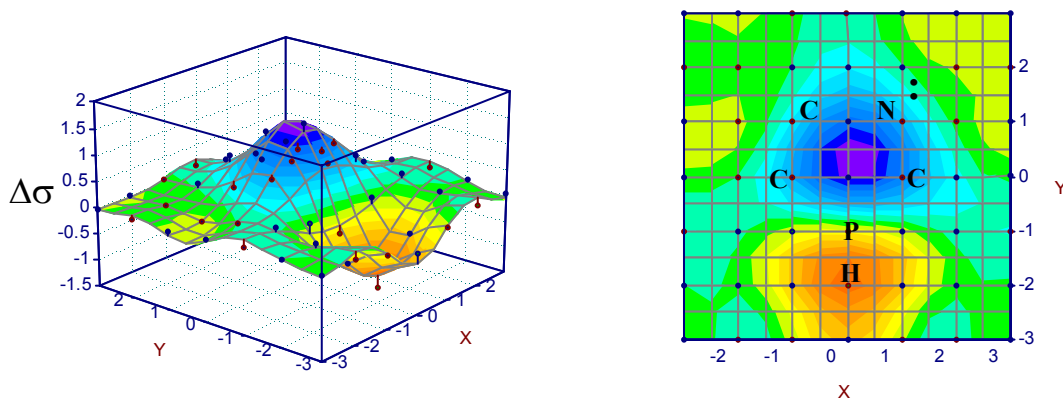


Fig. 11. NMR shielding increment surfaces (in ppm) at the 2.5 Å level for five-membered rings: phosphole (lp side) 7, phosphole (P-H side) 7 and isophosphazole (P-H side) 8.

isophosphazole (lp side) **8**



phosphazole (P-H side) **9**



phosphazole (lp side) **9**

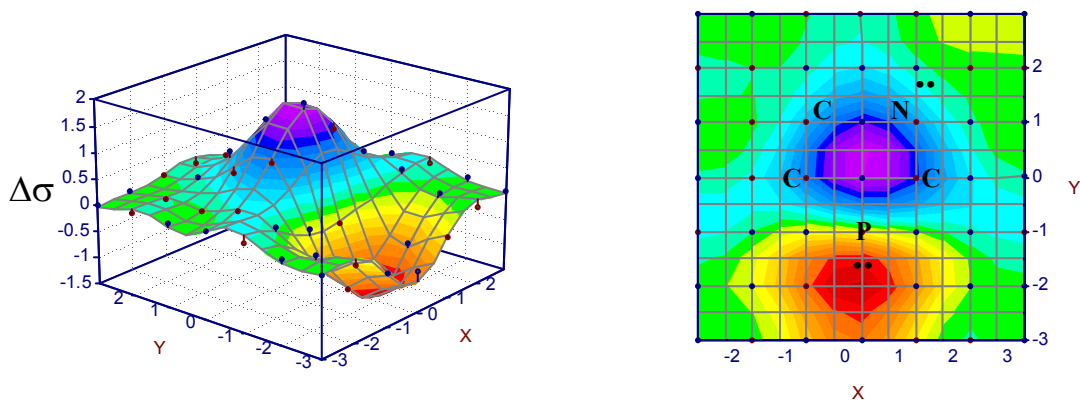
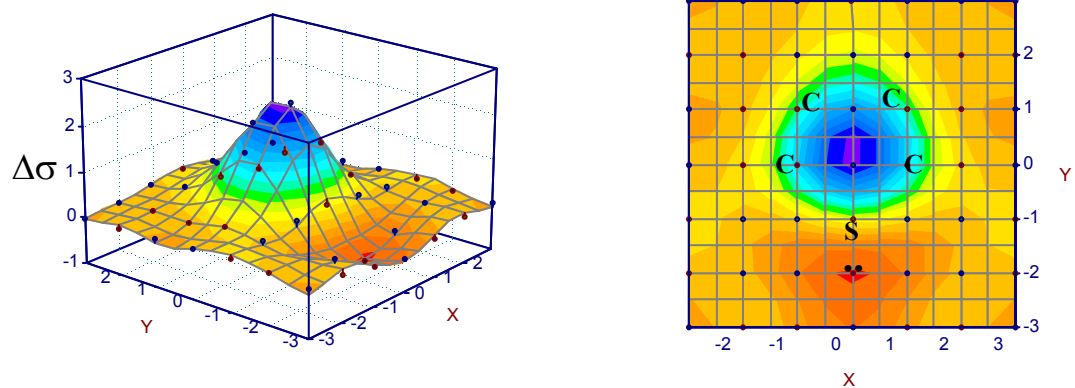
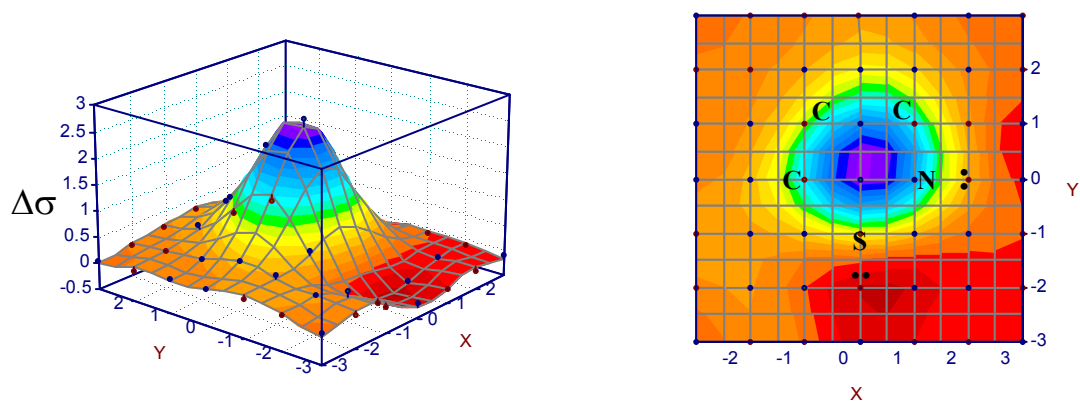


Fig. 12. NMR shielding increment surfaces (in ppm) at the 2.5 Å level for five-membered rings: isophosphazole (lp side) **8**, phosphazole (P-H side) **9** and phosphazole (lp side) **9**.

thiophene **10**



isothiazole **11**



thiazole **12**

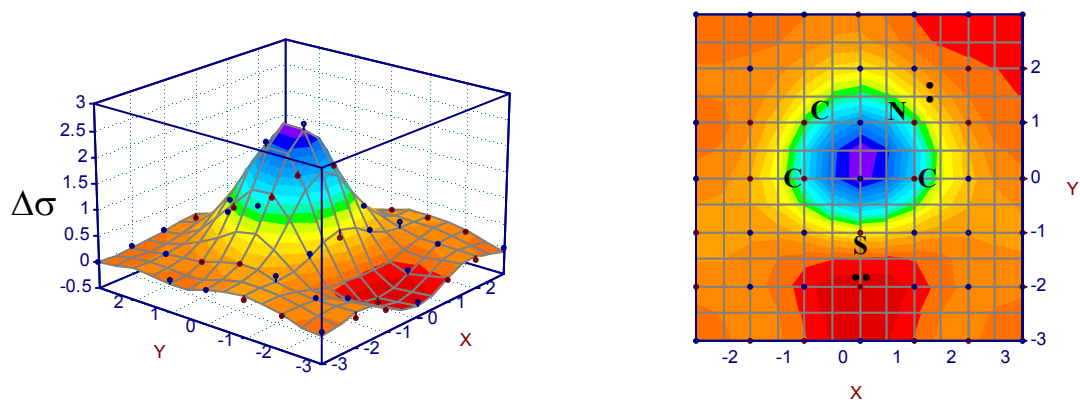
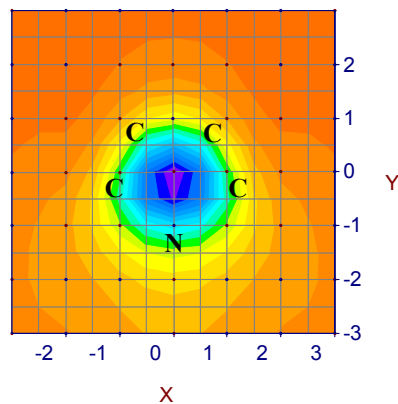
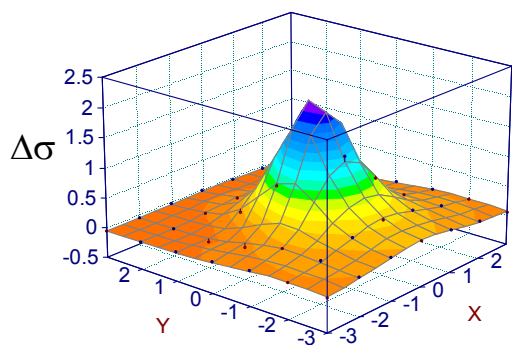
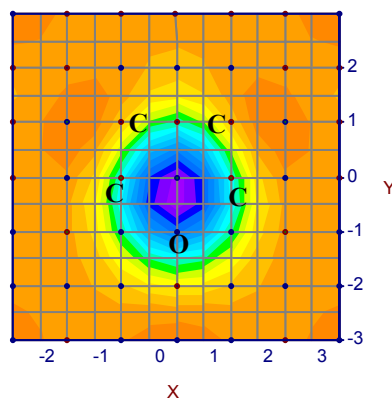
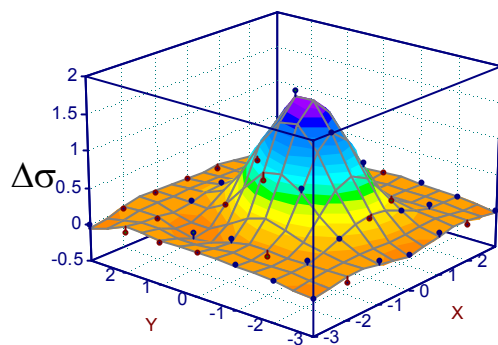


Fig. 13. NMR shielding increment surfaces (in ppm) at the 2.5 Å level for five-membered rings: thiophene **10**, isothiazole **11** and thiazole **12**.

pyrrole 1



furan 4



phosphole (lp side) 7

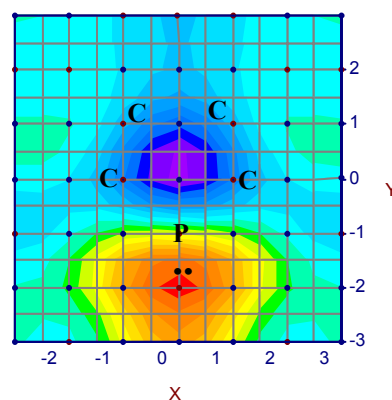
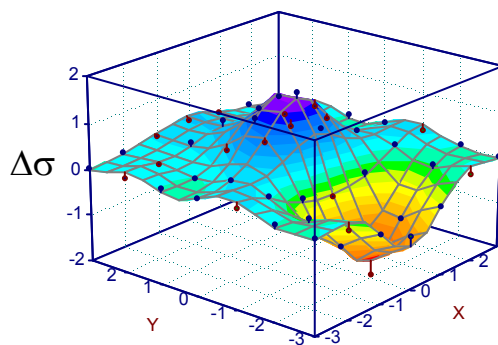
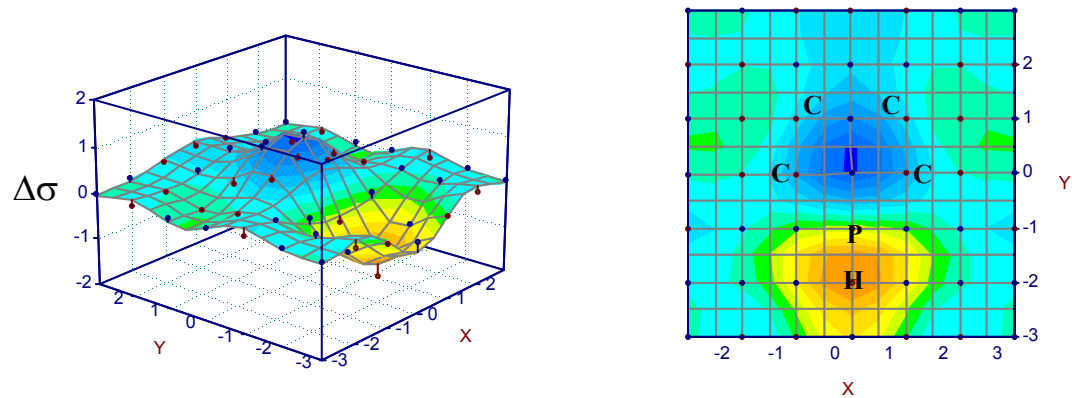


Fig. 14. NMR shielding increment surfaces (in ppm) at the 2.5 Å level for five-membered rings: pyrrole 1, furan 4 and phosphole (lp side) 7.

phosphole (P-H side) **7**



thiophene **10**

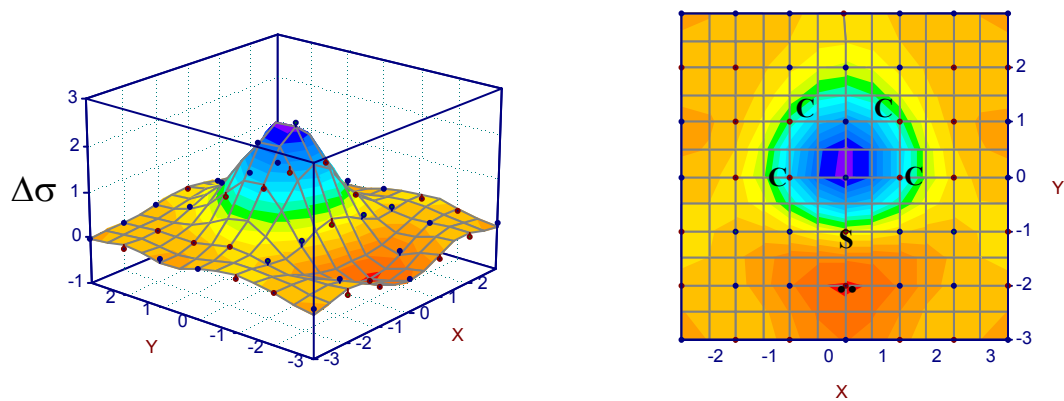


Fig. 15. NMR shielding increment surfaces (in ppm) at the 2.5 Å level for five-membered rings: phosphole (P-H side) **7** and thiophene **10**.

As seen below, phosphorus has a pyramidal shape in all of the structures listed in Fig. 16 which is the result of phosphorus having unequal bonds (two joining ring atoms and one with hydrogen) and a lone pair of electrons. This pyramidal shape in phosphole causes the hydrogen bonded to phosphorus (P-H) to extend out of the plane of the rest of the structure as seen in Fig. 16 (a and b). Phosphole **7** (Fig. 16, a and b) and isophosphazole **8** (Fig. 16, c and d) are situated with the P-H extending toward the front. However, phosphazole **9** (Fig. 16, e and f) is situated with P-H extending from the plane of the structure toward the back. When the P-H is on the back side, the lone pair of electrons (lp) on phosphorus is extending toward the front, and vice-versa. Qualitatively, the diatomic hydrogen probe calculations on either the P-H or lp side generates similar effects, but the quantitative results may be different. Therefore, two sets of $\Delta\sigma$ calculations were done on phosphole, isophosphazole and phosphazole, one with the diatomic hydrogen probe on the P-H side and the other with the probe on the lp side. These results will be discussed later quantitatively.

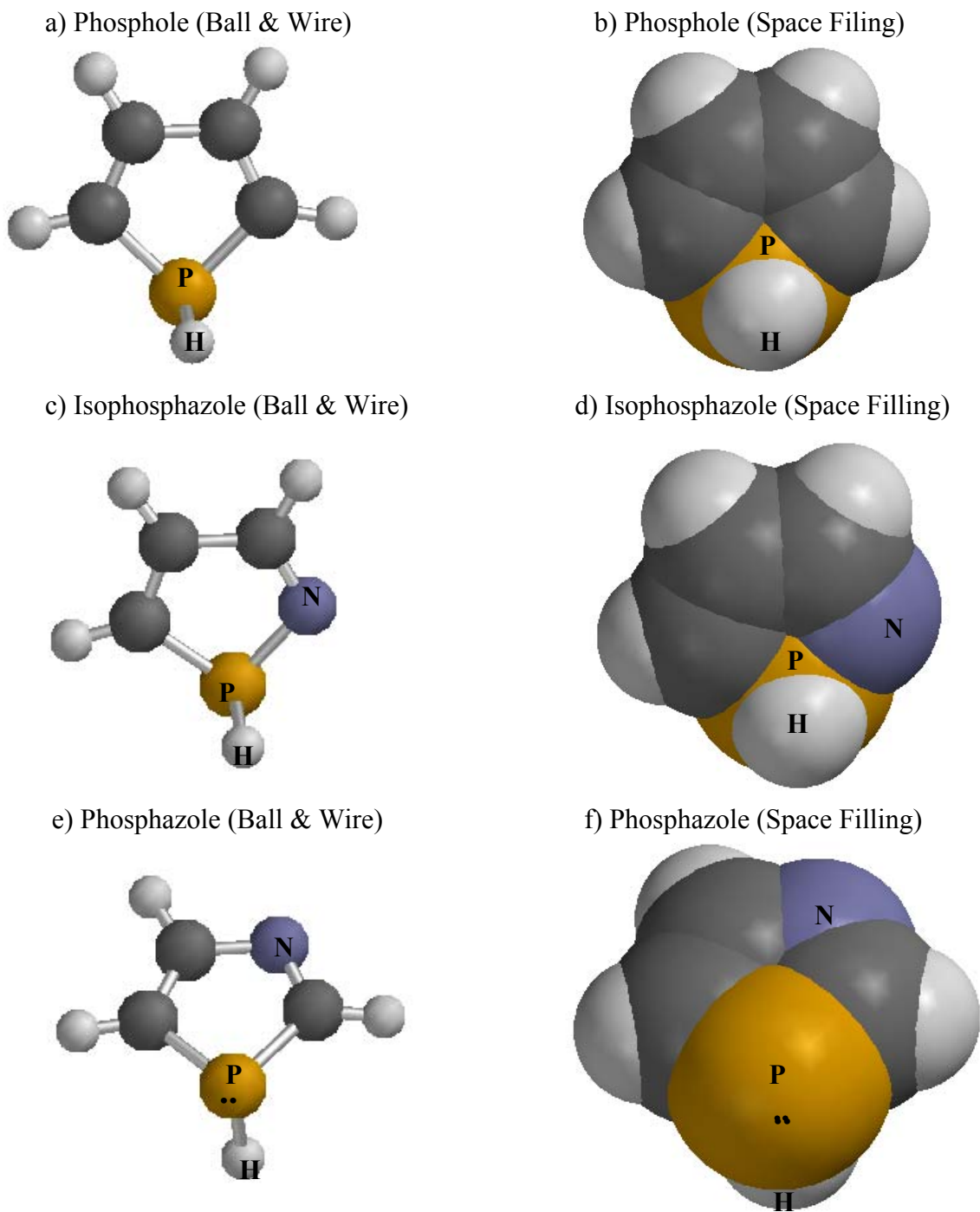
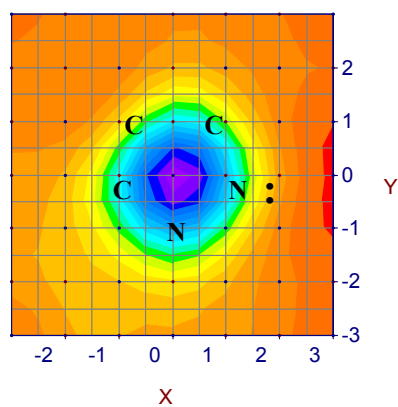
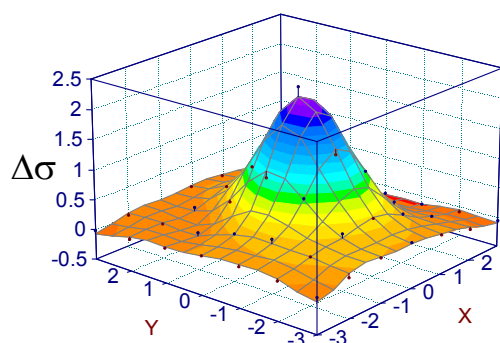


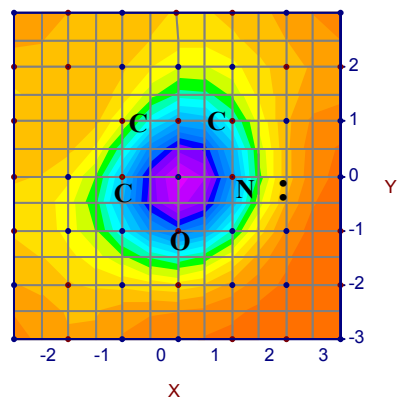
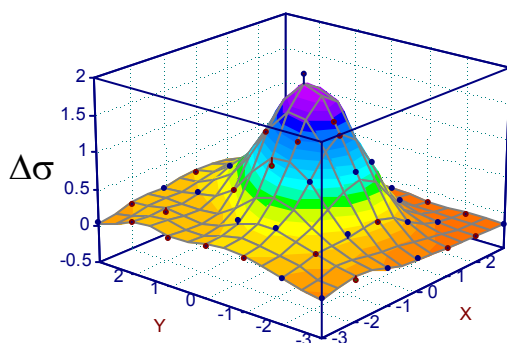
Fig. 16. Models of a series of phosphorus containing five-membered rings showing the P-H group out of the plane of the rest of the atoms.

Figures 17 and 18 display derivatives of the parent five-membered rings with nitrogen in the α position. These structures all have a common region of slight deshielding in the lower right portion of their shielding maps which is in an area beyond the nitrogen in the α position. This deshielding is caused by nitrogen's lone pair of electrons which are in the same plane of the structure, projecting out from nitrogen. 1H-Pyrazole **2** and isoxazole **5** do not exhibit as much deshielding as isophosphazole **8** and isothiazole **11**. Isoxazole **5** displays slightly more deshielding in proximity to the bottom heteroatom, in comparison to 1H-pyrazole **2**. This is consistent with the greater electron density expected on oxygen because it is more electronegative than nitrogen. Qualitatively, isophosphazole **8** appears to have the flattest looking shielding mound while the rest look similar to one another. Even though isothiazole **11**, 1H-pyrazole **2** and isoxazole **5** have similar looking shielding mounds, isothiazole **11** appears to be the steepest.

1H-pyrazole **2**



isoxazole **5**



isophosphazole (P-H side) **8**

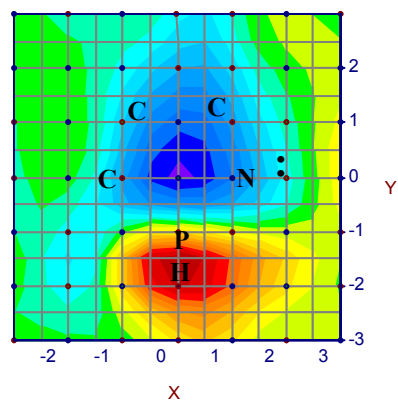
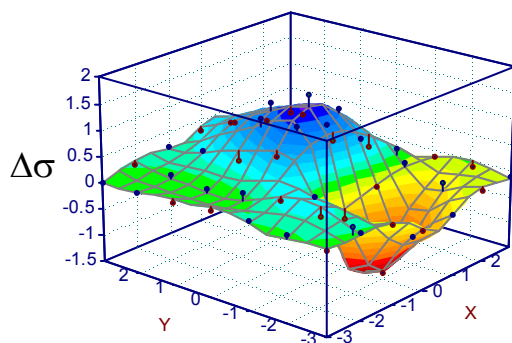
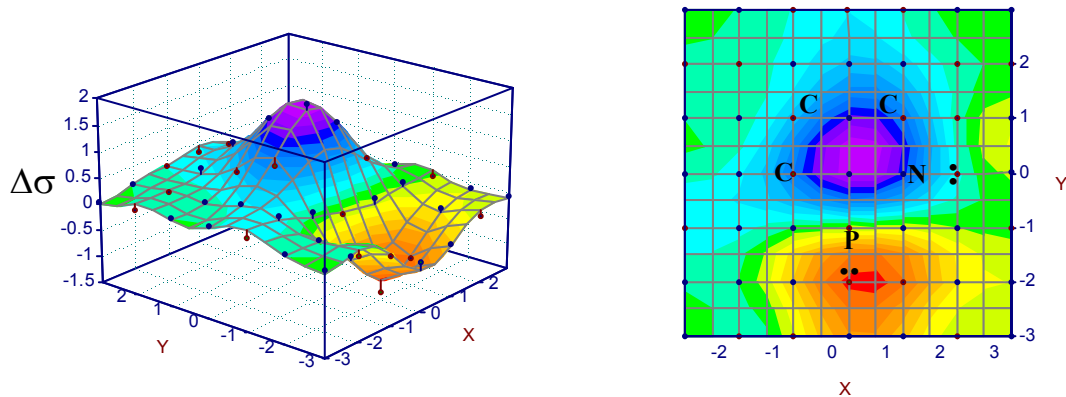


Fig. 17. NMR shielding increment surfaces (in ppm) at the 2.5 Å level for parent five-membered structure derivatives with nitrogen in α position: 1H-pyrazole **2**, isoxazole **5** and isophosphazole (P-H side) **8**.

isophosphazole (lp side) **8**



isothiazole **11**

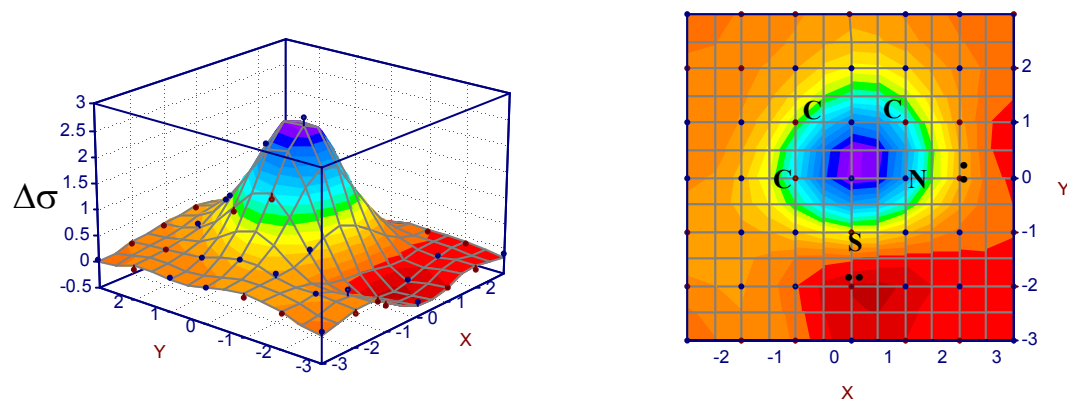
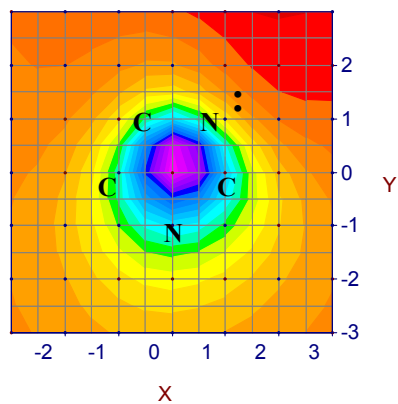
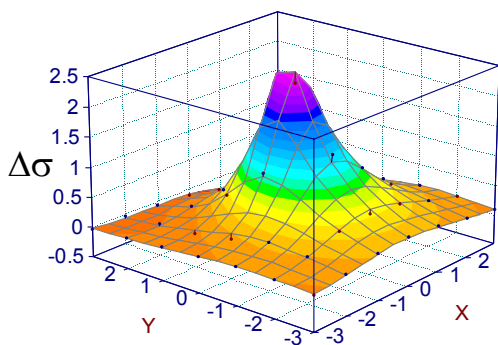


Fig. 18. NMR shielding increment surfaces (in ppm) at the 2.5 Å level for parent five-membered structure derivatives with nitrogen in α position: isophosphazole (lp side) **8** and isothiazole **11**.

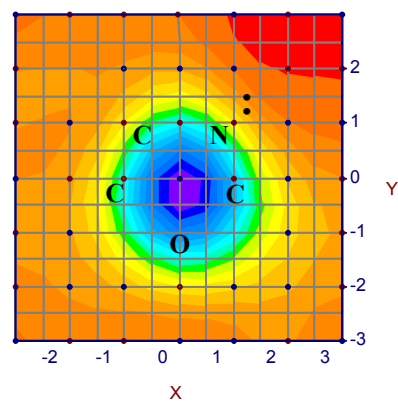
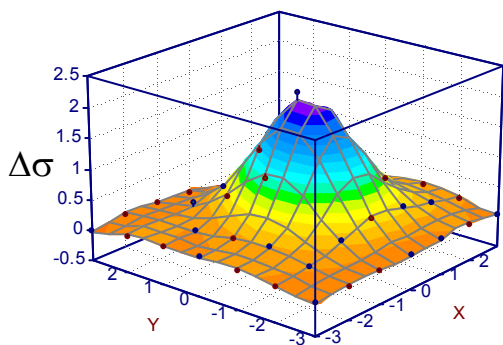
Figures 19 and 20 contain the nitrogen-containing derivatives of the parent five-membered rings with the nitrogen in the β position. Phosphazole **9** and thiazole **12** both have significant deshielding regions. This significant deshielding has already been described. However, all do have a common region of deshielding in the upper right hand corner of their maps which is beyond nitrogen. This deshielding is most likely due to the lone pair of electrons protruding from nitrogen which is now in the β position.

Qualitatively, 1H-imidazole **3** and oxazole **6** have similar looking shielding mounds even though 1H-imidazole **3** is slightly narrower. Phosphazole **9** and thiazole **12**, are more similar to one another than they are to the other two, but differ in that phosphazole **9** seems to have a shielding mound that is similar in magnitude with its significant deshielding region, whereas thiazole **12** has a shielding mound that is more dominant than its deshielding region.

1H-imidazole **3**



oxazole **6**



phosphazole (PH-side) **9**

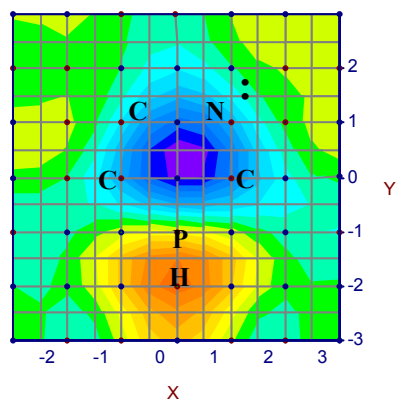
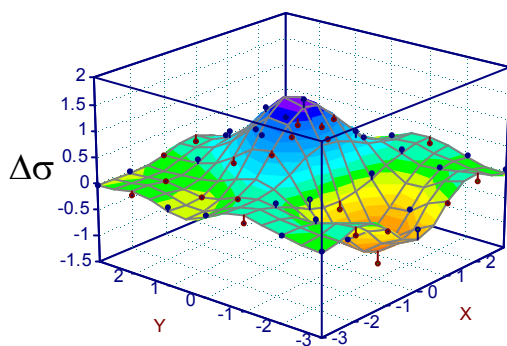
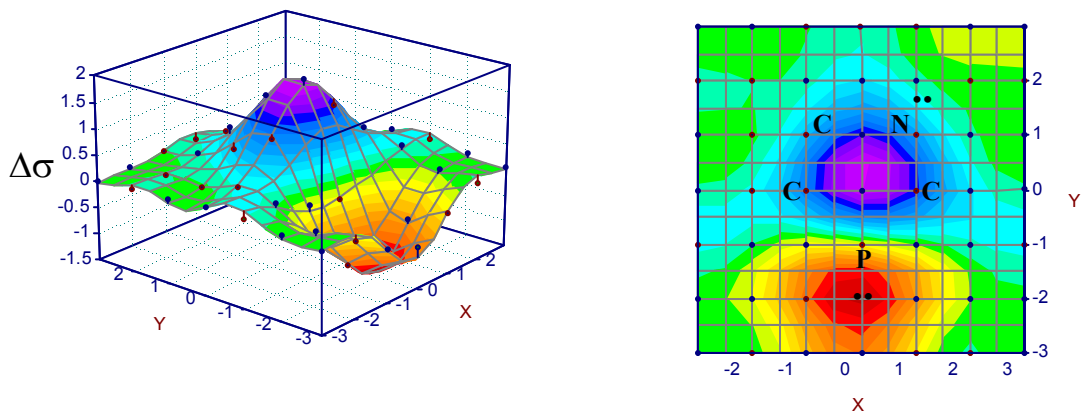


Fig. 19. NMR shielding increment surfaces (in ppm) at the 2.5 Å level for parent five-membered structure derivatives with nitrogen in β position: 1H-imidazole **3**, oxazole **6** and phosphazole (P-H side) **9**.

phosphazole (lp side) **9**



thiazole **12**

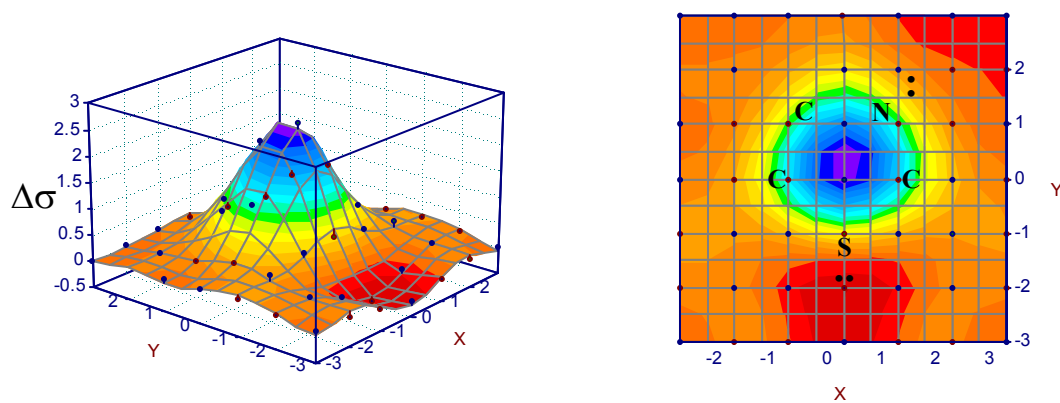


Fig. 20. NMR shielding increment surfaces (in ppm) at the 2.5 Å level for parent five-membered structure derivatives with nitrogen in β position: phosphazole (lp side) **9** and thiazole **12**.

The maximum shielding increment values calculated at 2.5Å ($\Delta\sigma_{\max}$) for a variety of five-membered rings are vastly different. It appears that the structural makeup of these rings influences how large or small the $\Delta\sigma_{\max}$ values may be. Thiophene **12**, which has sulfur as the bottom heteroatom, has the largest $\Delta\sigma_{\max}$ value (2.4 ppm). Pyrrole **1**, which has the nitrogen heteroatom at the bottom of the structure has a maximum $\Delta\sigma$ value of 2.0 ppm. Furan **4**, which has oxygen as its bottom heteroatom, has a maximum $\Delta\sigma$ value of 1.7 ppm. Phosphole **7**, which has phosphorus as its bottom heteroatom, has a maximum $\Delta\sigma$ value of 1.5 ppm.

The $\Delta\sigma_{\max}$ values for the derivatives of each of the parent five-membered rings with nitrogen in the α position seem to follow the same pattern relative to the order of their magnitude. The magnitudes of these maximum shielding increment values increase with the implementation of nitrogen to the α position. These $\Delta\sigma$ value increases are around 0.3 ppm for all except phosphole **7**, which is 0.03 ppm.

The β derivatives of pyrrole **1** (N), furan **4** (O) and thiophene **10** (S) have increases in the magnitudes of their $\Delta\sigma_{\max}$ values in comparison with values from their parent five-membered rings that are comparable to what is seen in the α derivatives. The β derivative of phosphole **7** (P) has a slight decrease in its $\Delta\sigma_{\max}$ value in comparison with its α derivative. Both isophosphazole and phosphazole have $\Delta\sigma_{\max}$ values nearly identical to their parent phosphole.

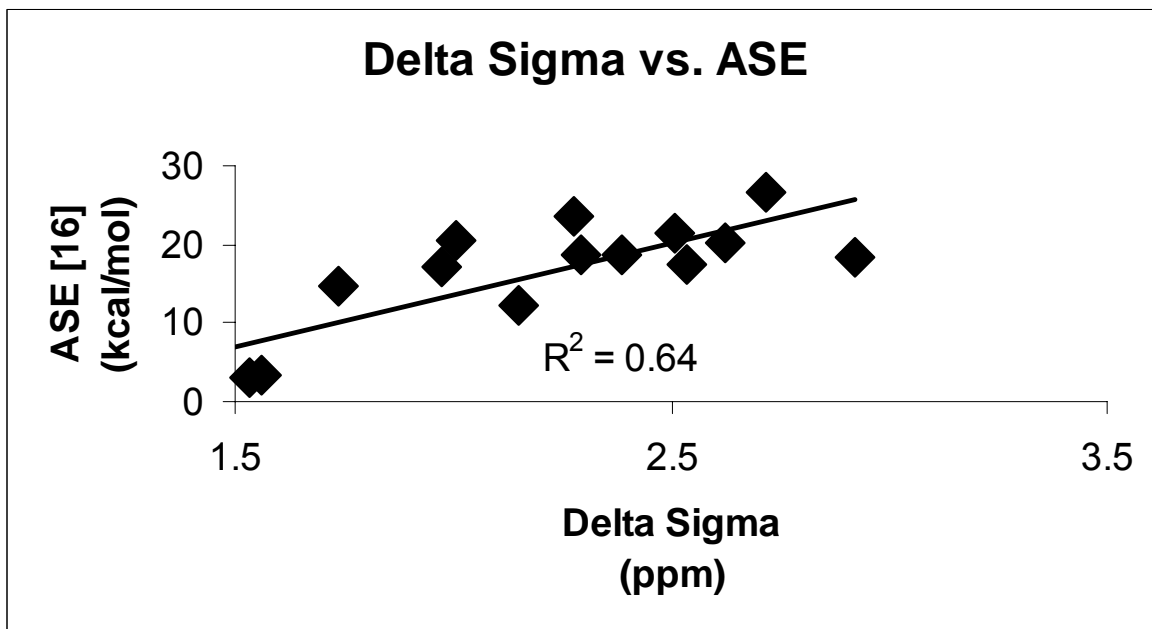
Table 5

This study's $\Delta\sigma$ values calculated at 2.5Å above the geometric center of five-membered rings along with published results [16] corresponding to the same rings

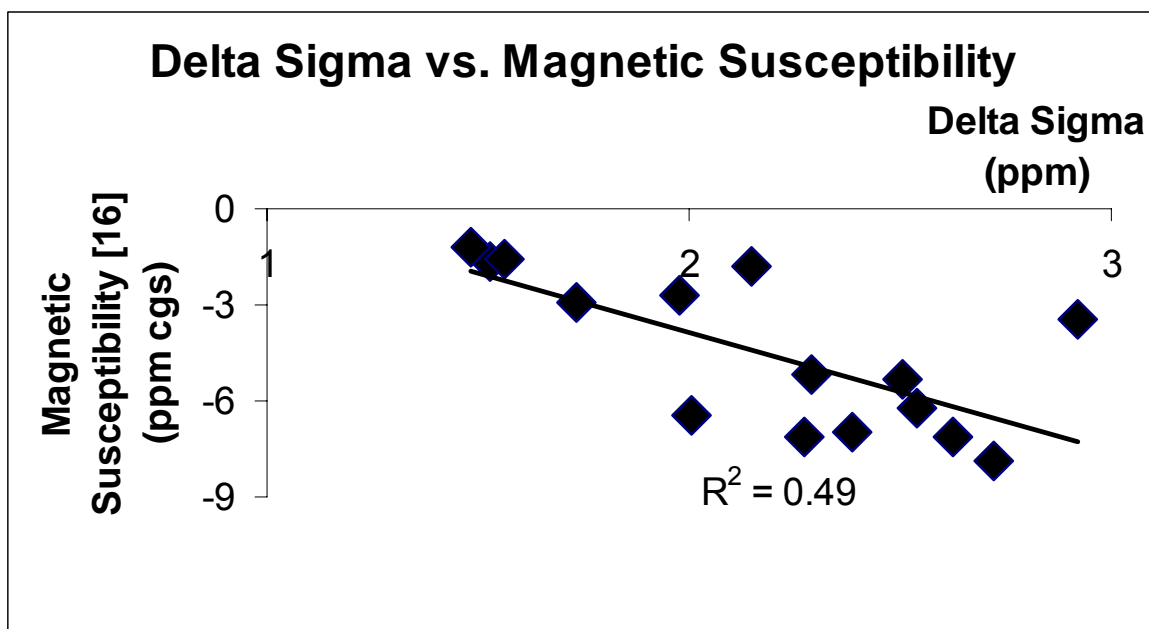
Name	$\Delta\sigma$ (ppm)	NICS(0) (ppm)	NICS(1) (ppm)	HOMA	ASE (kcal/mol)	Λ (ppm cgs)
pyrrole 1	2.0	-14.9	-10.6	0.876	20.6	-6.5
1H-pyrazole 2	2.3	-14.8	-11.9	0.926	23.7	-7.1
1H-imidazole 3	2.3	-13.9	-10.8	0.908	18.8	-5.2
1,2,3-triazole 13	2.7	-14.8	-13.6	0.960	26.7	-7.9
1,2,4-triazole 14	2.5	-13.7	-11.8	0.940	21.3	-5.3
1H-tetrazole 15	2.9	-14.8	-14.1	0.897	18.3	-3.5
furan 4	1.7	-12.3	-9.4	0.298	14.8	-2.9
isoxazole 5	2.0	-12.4	-10.6	0.527	17.3	-2.7
oxazole 6	2.2	-11.3	-9.5	0.332	12.4	-1.8
phosphole 7	1.5	-5.4	-6.0	0.236	3.2	-1.7
Isophosphazole 8	1.6	-5.7	-6.8	N/A	3.3	-1.5
phosphazole 9	1.5	-3.8	-6.3	0.276	3.0	-1.2
thiophene 10	2.4	-13.8	-10.8	0.891	18.6	-7.0
isothiazole 11	2.6	-14.0	-11.7	N/A	20.2	-7.1
thiazole 12	2.5	-13.1	-11.4	0.905	17.4	-6.2

B. Correlation with other Methods

The attempt to correlate the results from this research with results from other sources served as a basis to determine whether or not the method tested in this research can be used as a reliable means for measuring the extent of aromaticity. Fortunately, the results of the five-membered rings tested in this research correlated very well with the results from Cyransky [16]. This study's $\Delta\sigma_{\max}$ versus Cyransky's ASE results [16] correlated well with the R^2 value of 0.64 (Fig. 21A). This project's $\Delta\sigma_{\max}$ correlated weakly with magnetic susceptibility results from Cyransky [16]. Figure 21B shows the data points spread about the trend line yielding a R^2 value of 0.49. This project's $\Delta\sigma_{\max}$ calculations matched up very well with Cyransky's NICS(0) and NICS(1) [16] yielding R^2 values of 0.66 and 0.88 respectively (Figs. 22A and B). The correlation between this study's $\Delta\sigma_{\max}$ and NICS in general, is expected to be high because both methods are based on the same principles as described within the Experimental/ Methods section. This project's $\Delta\sigma_{\max}$ also matched up quite well against Cyransky's HOMA results [16] yielding a R^2 value of 0.69 (Fig 23).

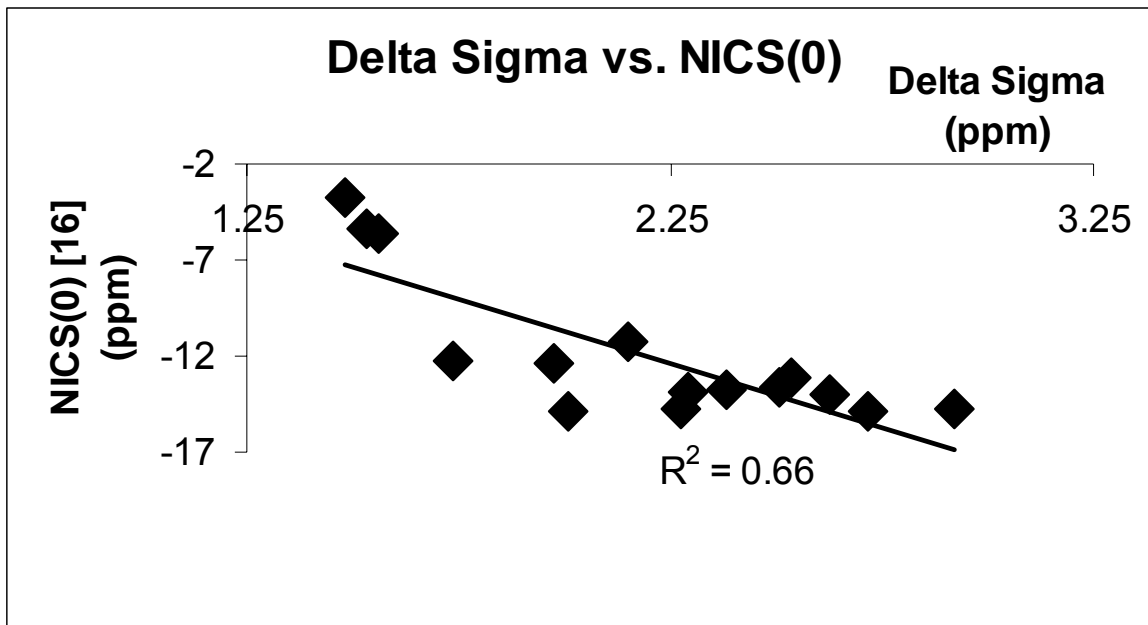


A

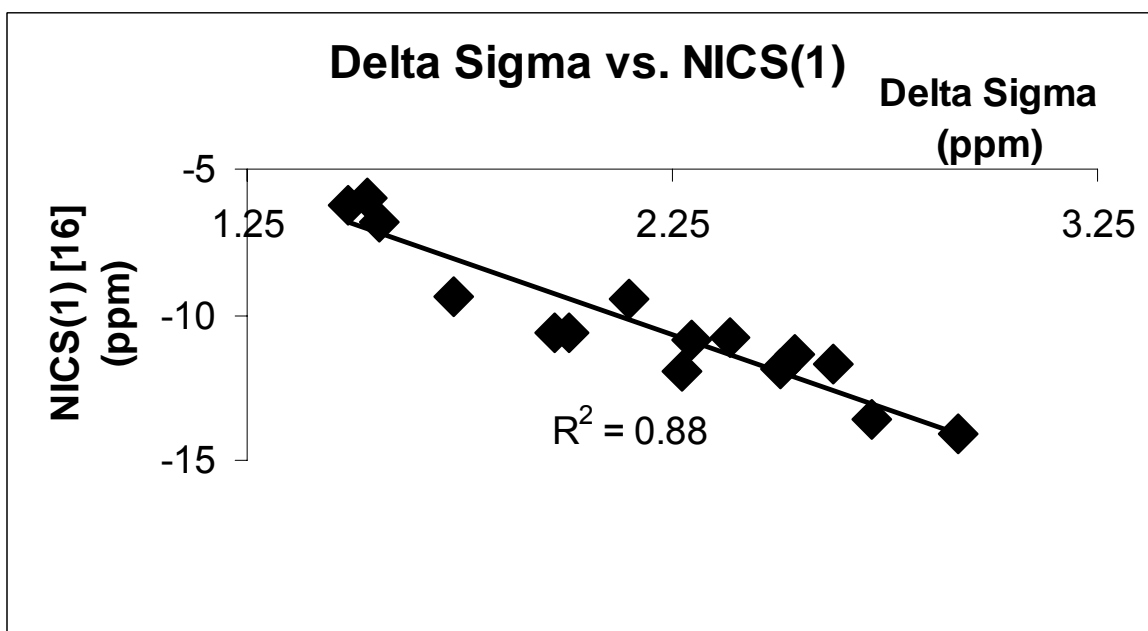


B

Fig. 21. This study's NMR maximum shielding increments ($\Delta\sigma_{\max}$) correlated with (A) Cyraňsky et al's ASE and (B) Magnetic Susceptibility measurements for the five-membered rings.



A



B

Fig. 22. This study's NMR maximum shielding increments ($\Delta\sigma_{\max}$) correlated with (A) Cyraňský et al's NICS(0) and (B) NICS(1) measurements for the five-membered rings.

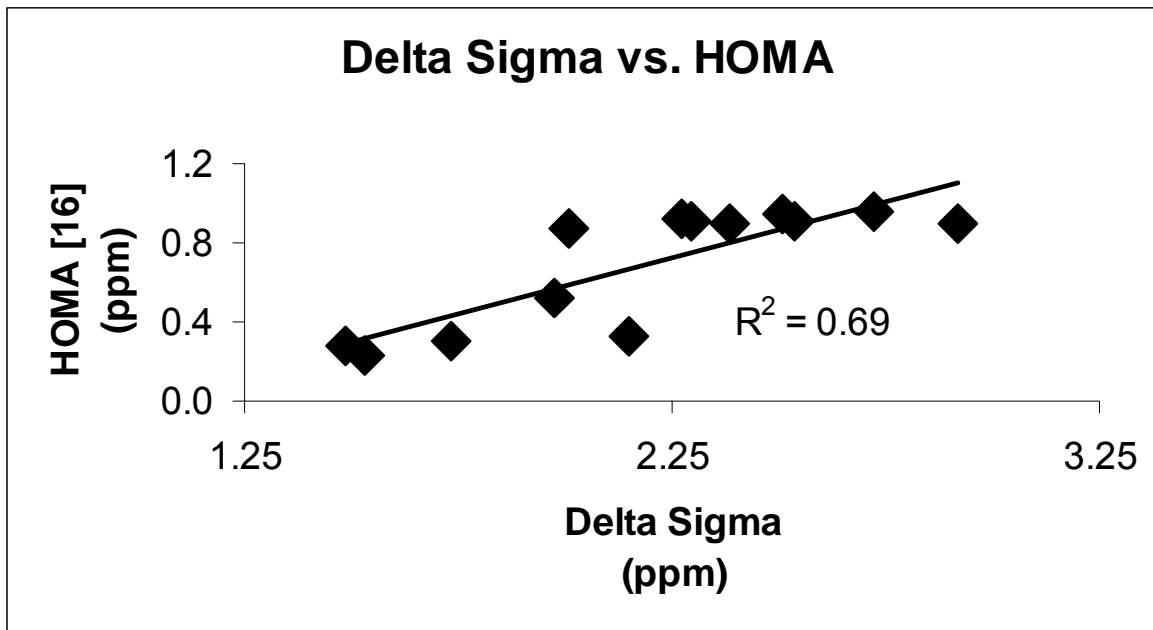
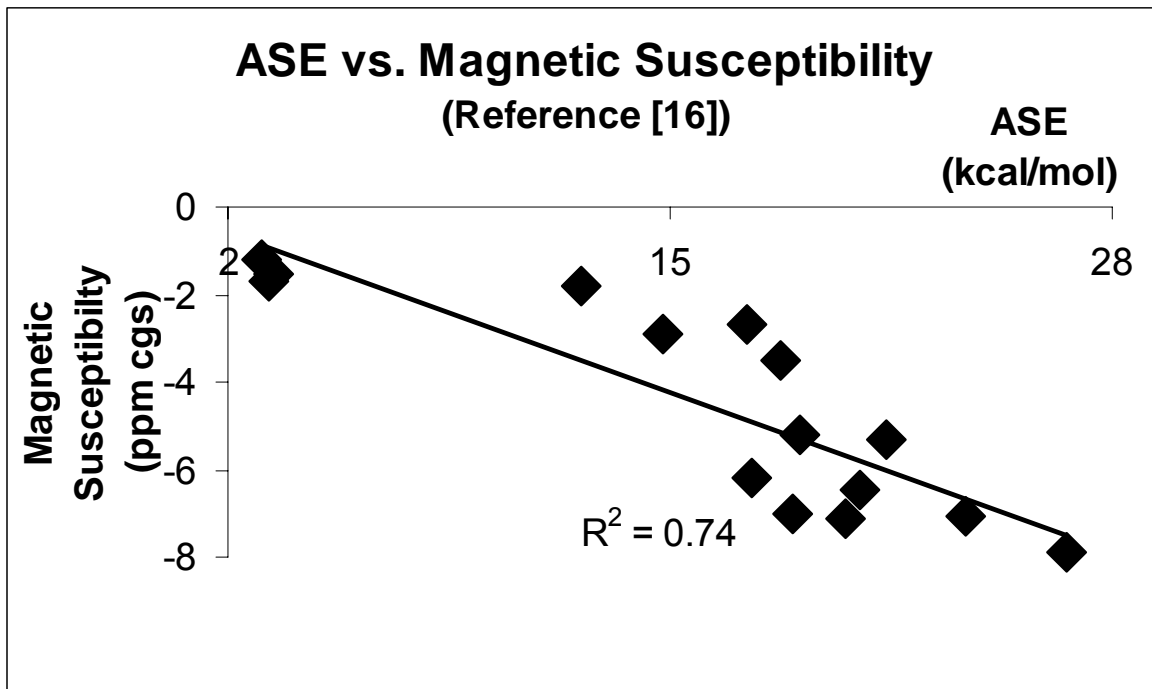


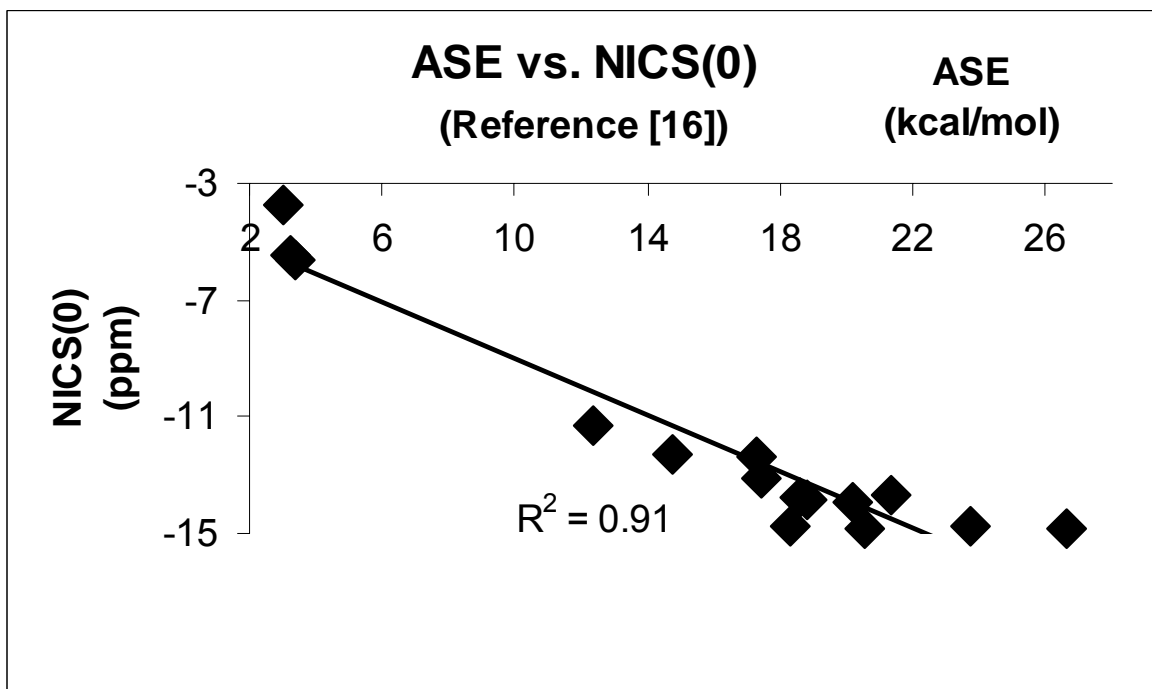
Fig. 23. This study's NMR maximum shielding increments ($\Delta\sigma_{\max}$) correlated with Cyraňsky et al's HOMA measurements for the five-membered rings.

C. Other Methods Correlated with each other

This project's $\Delta\sigma_{\max}$ results generally correlated well against the various methods from Cyransky [16]. In order to check the reliability of Cyransky's data, the results from the various methods that he reported were correlated with one another (Figs. 24-28). The ASE vs. magnetic susceptibility results correlated well yielding a R^2 value of 0.74 (Fig. 24A). Figure 24A reflects that this correlation would have been almost perfect had it not been for the first two data points. Cyransky's ASE and NICS(0) correlated very well yielding a R^2 of 0.91 (Fig. 24B). That same ASE data did almost as well with Cyransky's NICS(1) yielding a R^2 of 0.85 (Fig. 25A). These ASE results against Cyransky's HOMA results yielded a R^2 value of 0.73 (Fig. 25B). Cyransky's magnetic susceptibility against NICS(0), NICS(1) and HOMA results yielded R^2 values of 0.61, 0.53 and 0.78 respectively (Figs. 26A and B; 27A). This illustrates that Cyransky's magnetic susceptibility results match up well with the HOMA results and fairly well with NICS(0) and NICS(1). The HOMA results correlated with NICS(0) and NICS(1) results to yield R^2 values of 0.65 and 0.70 respectively (Figs. 27B and 28A).

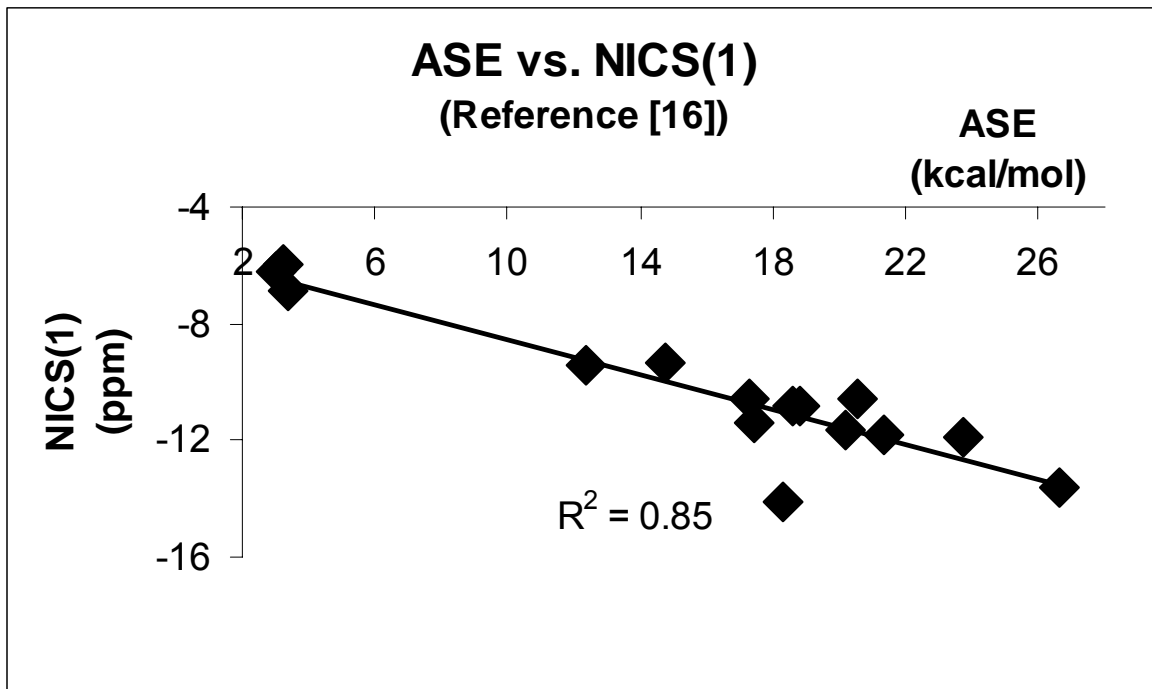


A

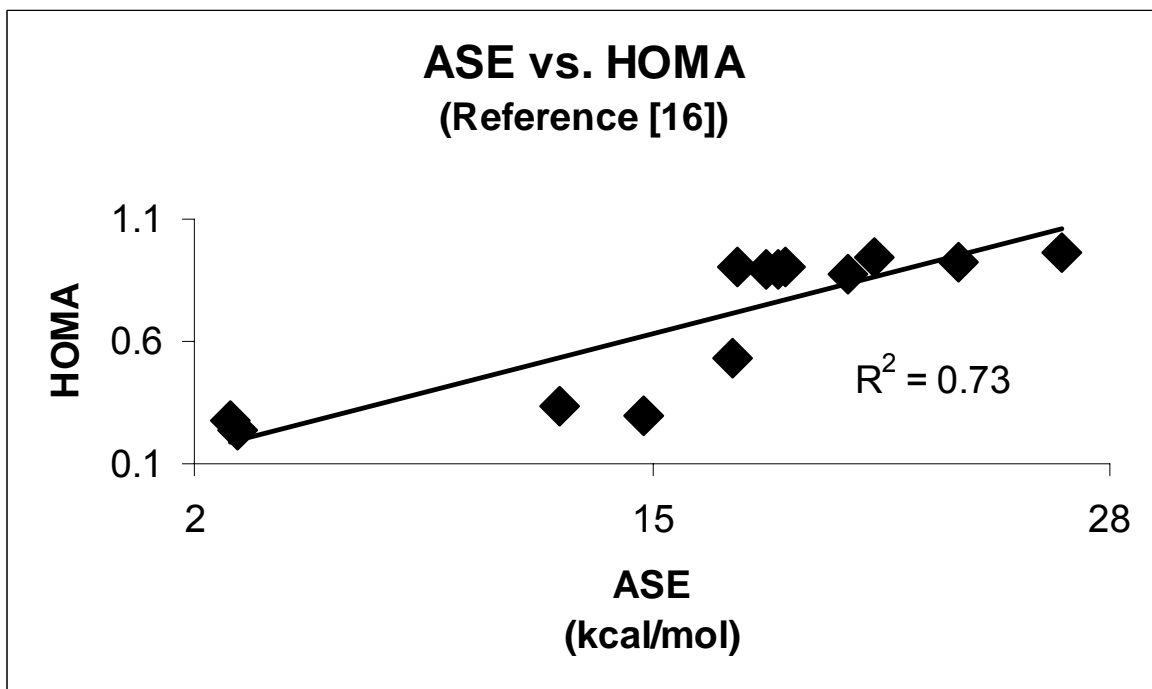


B

Fig. 24. Correlations of Cyraňsky et al's ASE with their magnetic susceptibility (A) and their ASE with their HOMA (B) for the five-membered rings

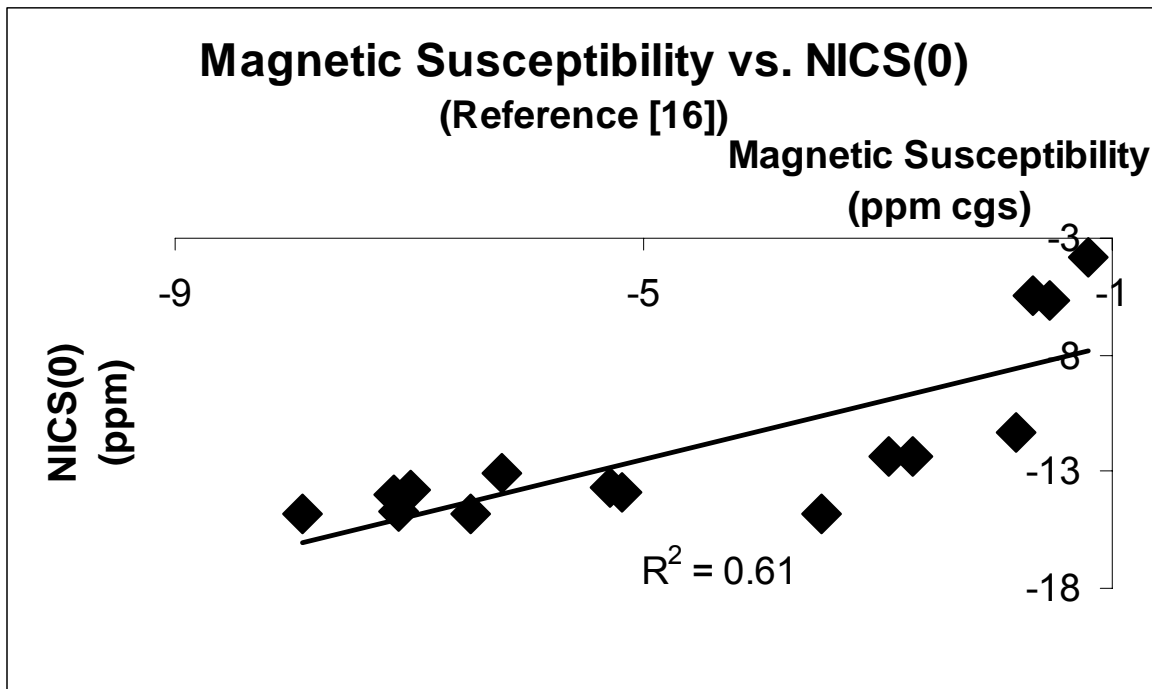


A

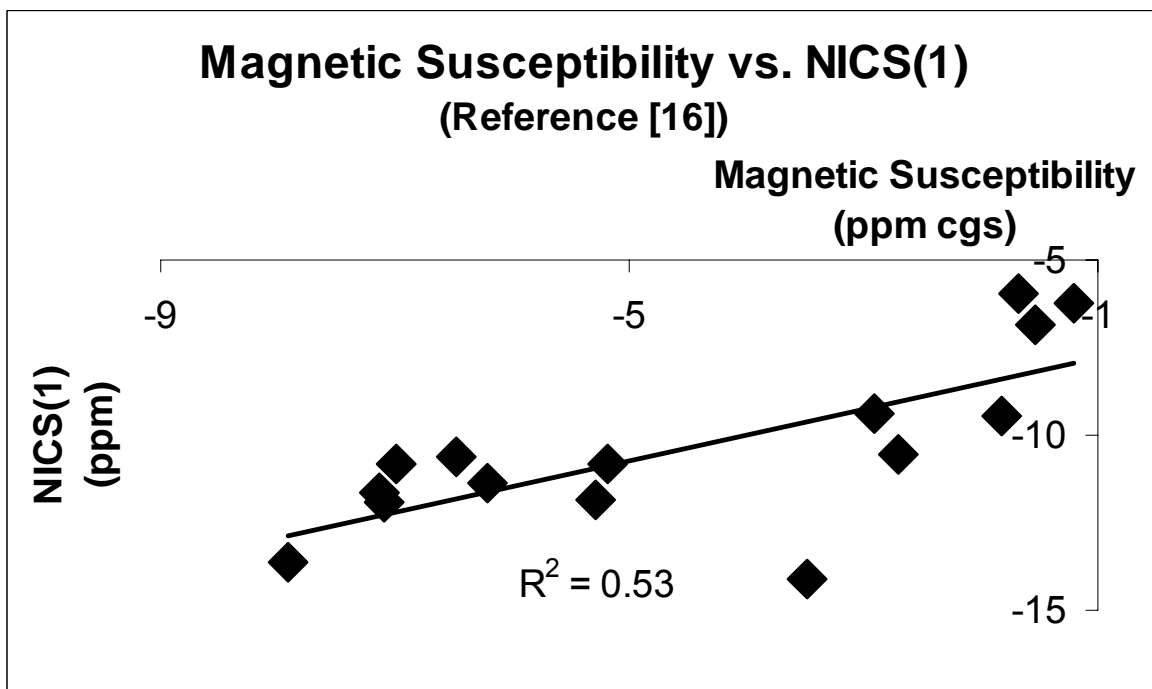


B

Fig. 25. Correlations of (A) Cyrañsky et al's ASE with their NICS(1) and (B) their ASE with their HOMA for the five-membered rings.

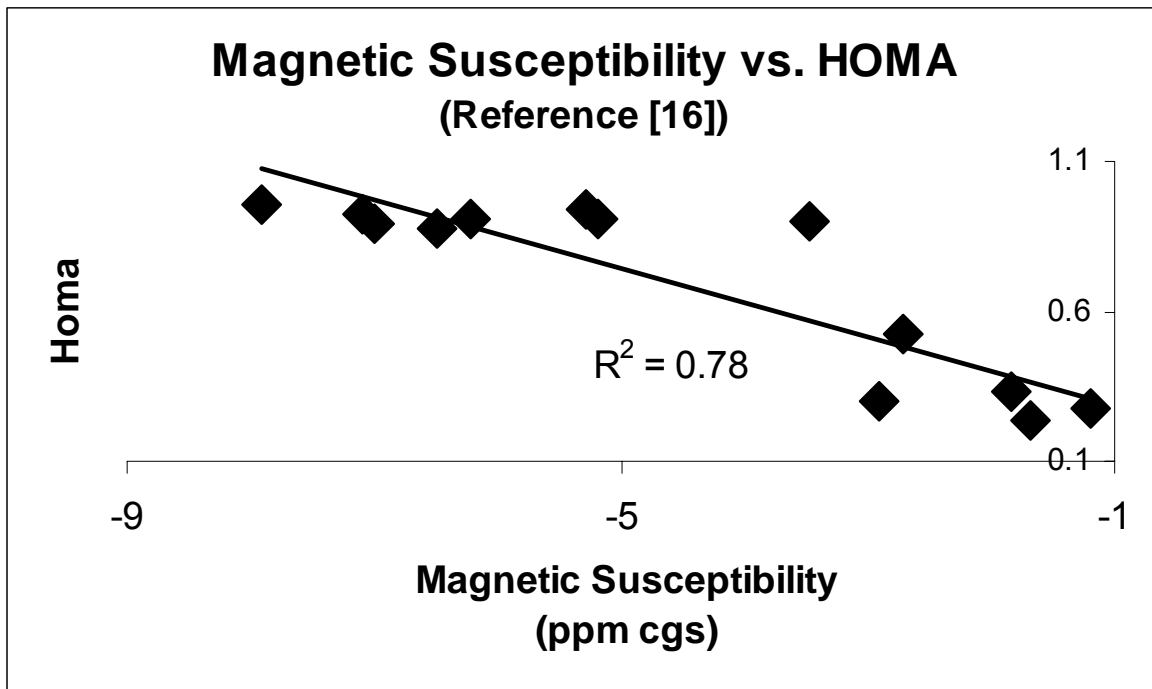


A

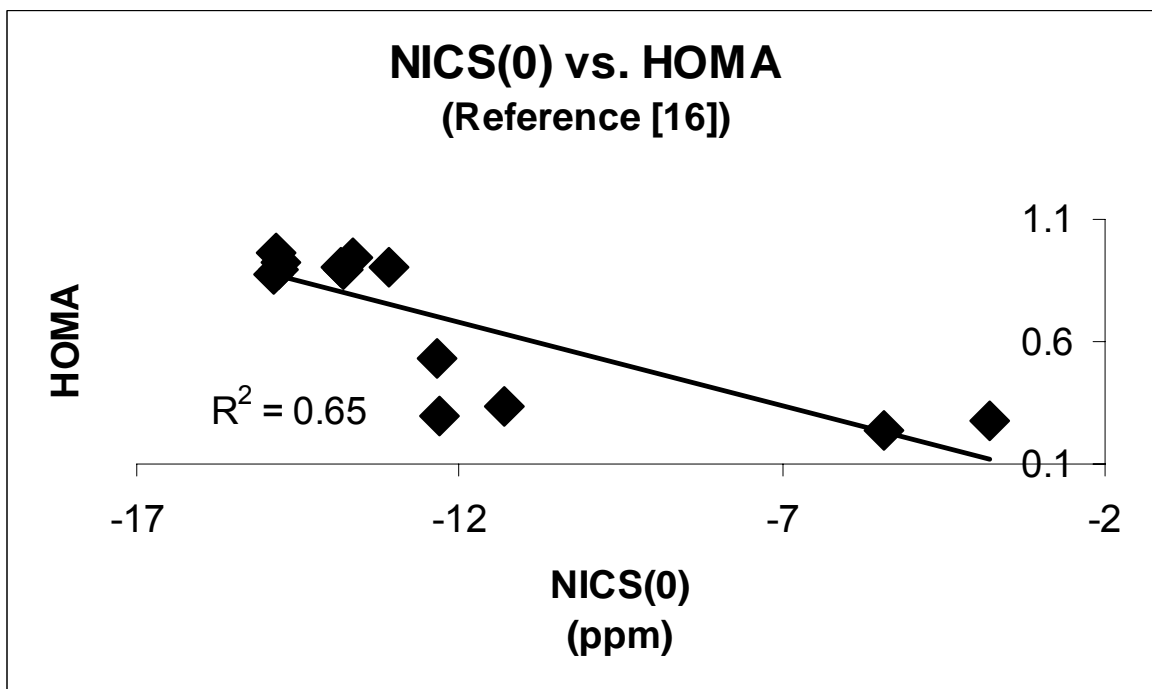


B

Fig. 26. Correlations of Cyraňsky et al's magnetic susceptibility with their NICS(0) (A) and their magnetic susceptibility with their NICS(1) (B) for the five-membered rings.

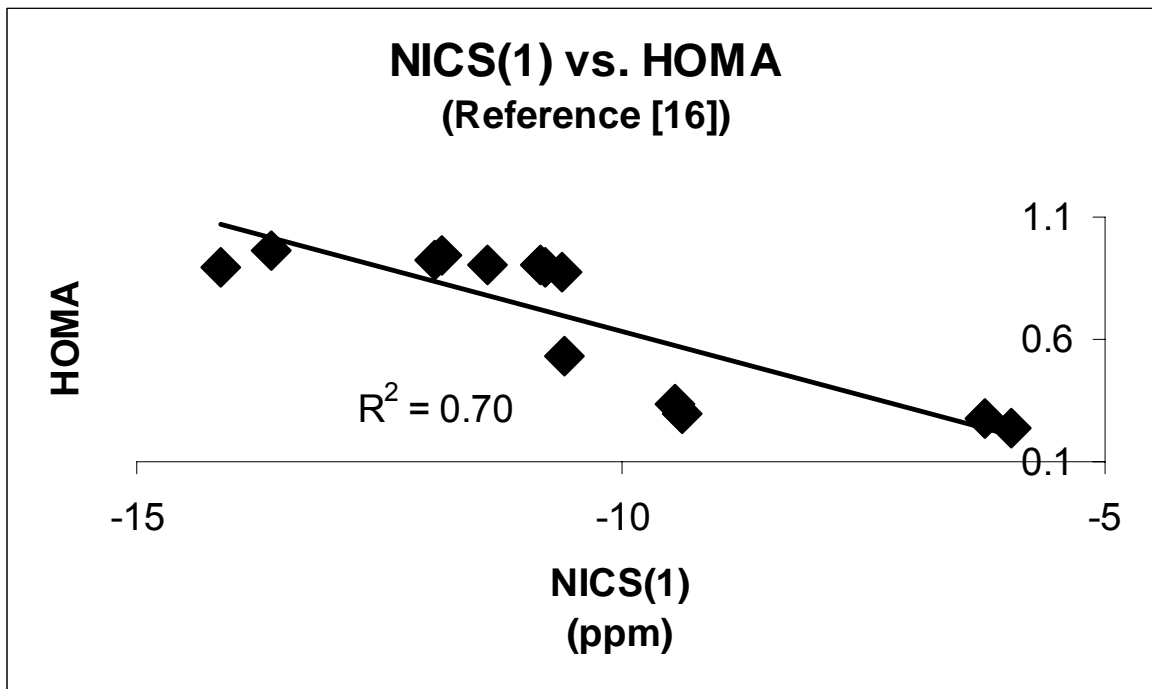


A

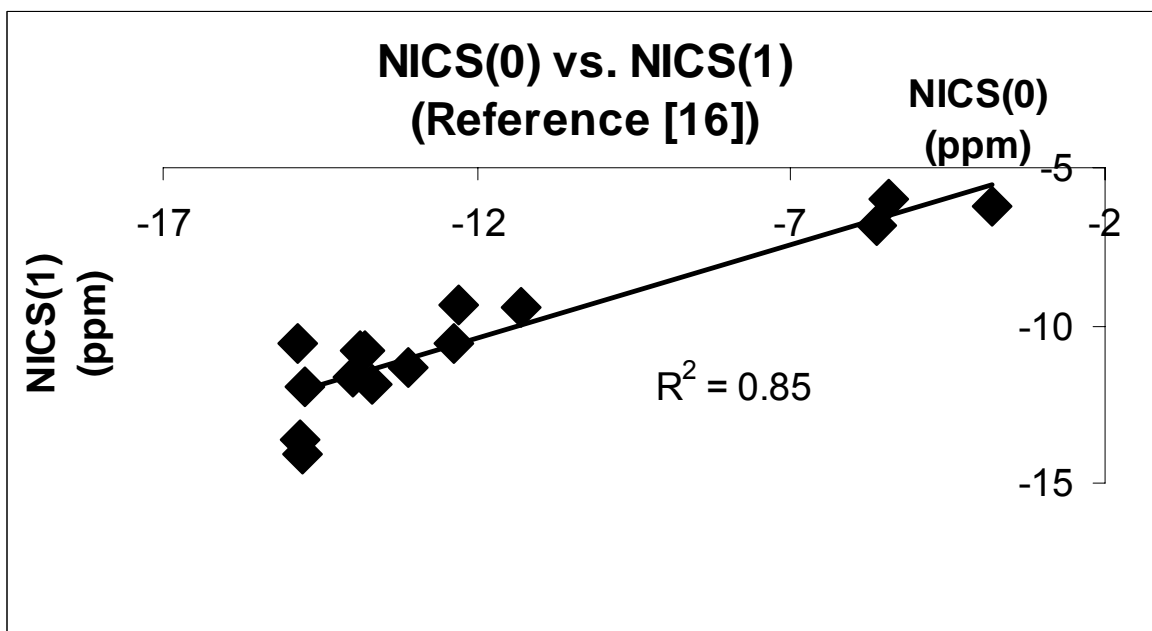


B

Fig. 27. Correlations of Cyraňsky et al's magnetic susceptibility with their HOMA (A) and their NICS(0) with their HOMA (B) for the five-membered rings.



A



B

Fig. 28. Correlations of Cyraňsky et al's NICS(1) with their HOMA (A) and their NICS(0) vs. NICS(1) (B) for the five-membered rings.

D. Benzo-Fused Unsaturated-Five-Membered Heterocyclic Ring Compounds

The benzo-analogs of the parent five-membered rings (Figs. 36 and 37) displayed the same trends that the parent five-membered rings displayed within Figs. 36 and 37. The major difference between the benzo-analog and parent five-membered ring shielding maps is that the shielding mounds for the benzo-analogs are much fuller which is indicative of greater $\Delta\sigma$ shielding increments. The major deshielding regions for phosphole **7** and thiophene **10** seem to be minimally affected with the addition of benzene to each of these to yield their benzo-analogs.

The benzo-analogs of the parent nitrogen five-membered ring and its derivatives (Fig. 29) showed similar trends as the parent nitrogen five-membered ring derivatives (Fig. 8). Likewise here, the only significant difference is that the benzo-analogs' shielding mounds in Fig. 29 are fuller due to the expected enhanced $\Delta\sigma$ shielding increments as result of a benzene ring being fused to the five-membered rings.

The benzo-analogs of the oxygen parent five-membered ring and its derivatives (Figs. 30 and 31) showed the same trends as their parents (Figs. 10 and 11). Also here, the shielding surfaces of the benzo-analogs (Figs. 29 and 30) are much fuller than those of their parents (Figs. 10 and 11).

The benzo-analog of five-membered rings with phosphorus as its bottom heteroatom (Figs. 31 and 32) showed similar trends (the sequential additions of nitrogen to the α and β positions) between the benzo-analogs and their parents. However, these benzo-analogs appear to have a smaller shielding mound than their five-membered ring counterparts which is different from prior benzo-analog to five-membered ring

comparisons. The deshielding region is also diminished in these benzo-analogs. A more quantitative analysis of this will be made later in this section.

The shielding surfaces for the benzo-analogs of the five-membered rings with sulfur as its bottom heteroatom (Figs 32 and 33) look as anticipated. The fuller looking shielding mounds within these benzo-analogs are very similar to the benzo-analogs of the oxygen and nitrogen containing five-membered rings. The chemical trends with the addition of nitrogen to the α and β positions of these benzo-analogs for the sulfur parent five-membered rings is similar to the trends seen with nitrogen- and oxygen-containing five-membered rings.

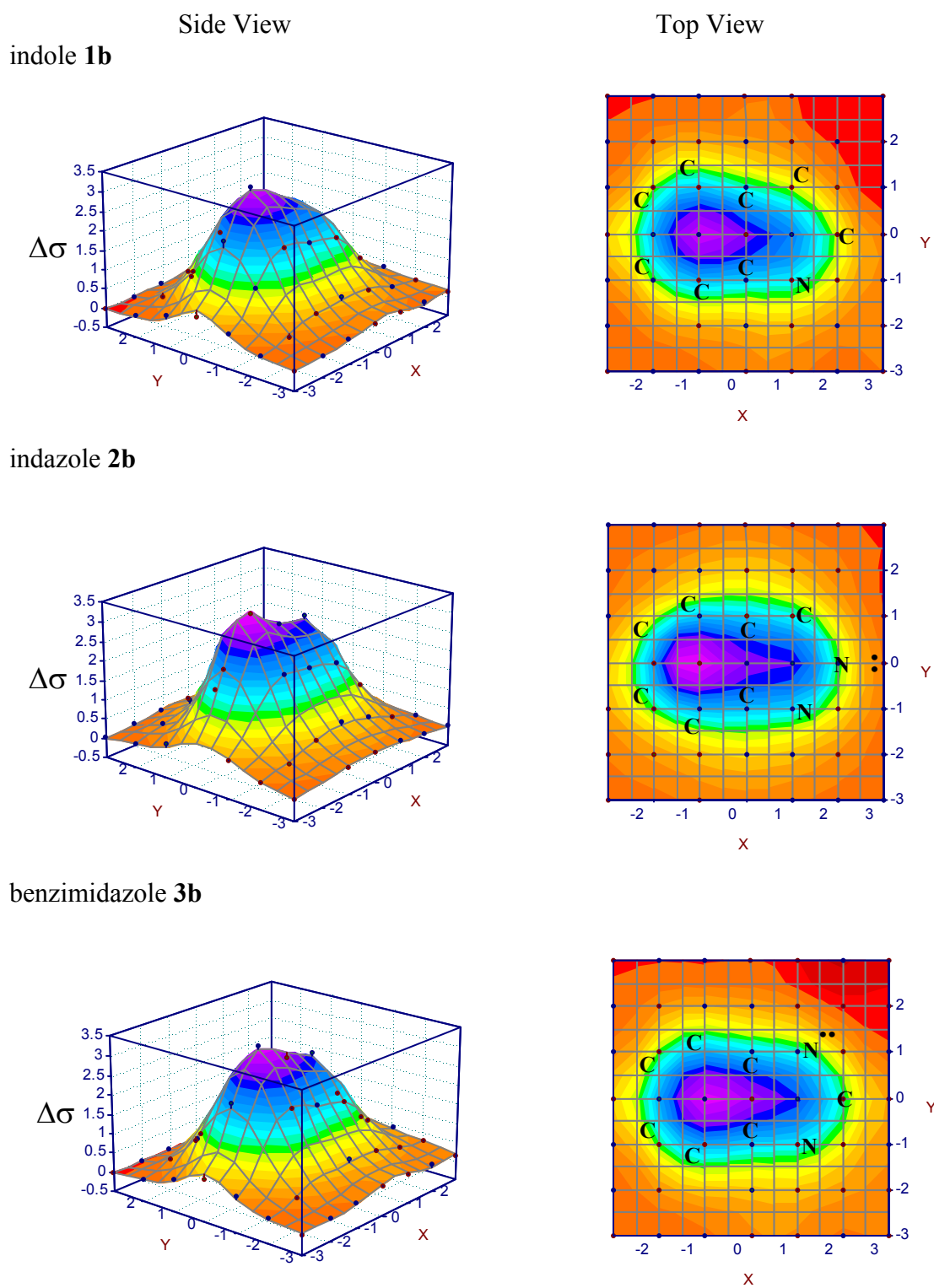
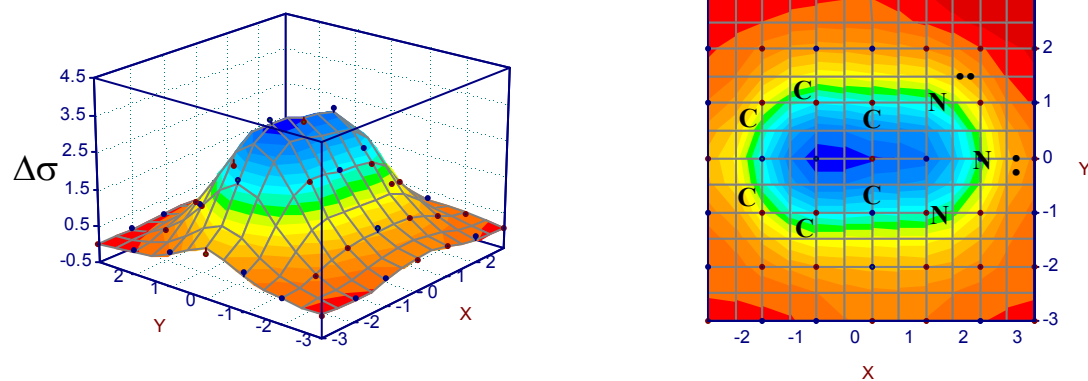
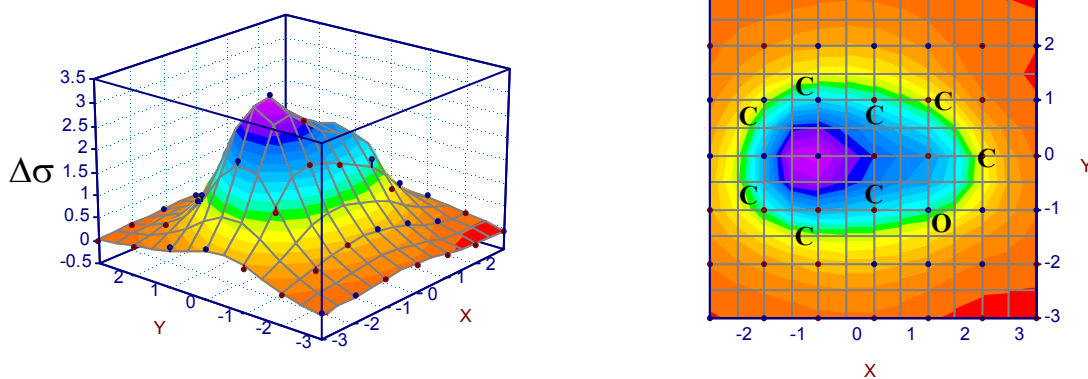


Fig. 29. NMR shielding increment surfaces (in ppm) at the 2.5 Å level for benzo-analogs: indole **1b**, indazole **2b** and benzimidazole **3b**.

1H-benzotriazole **13c**



benzofuran **4b**



1,2-benzisoxazole **5b**

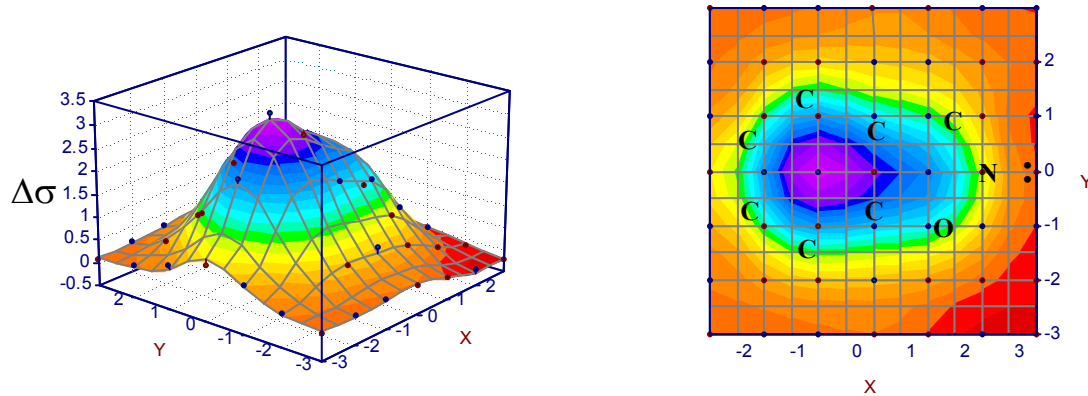
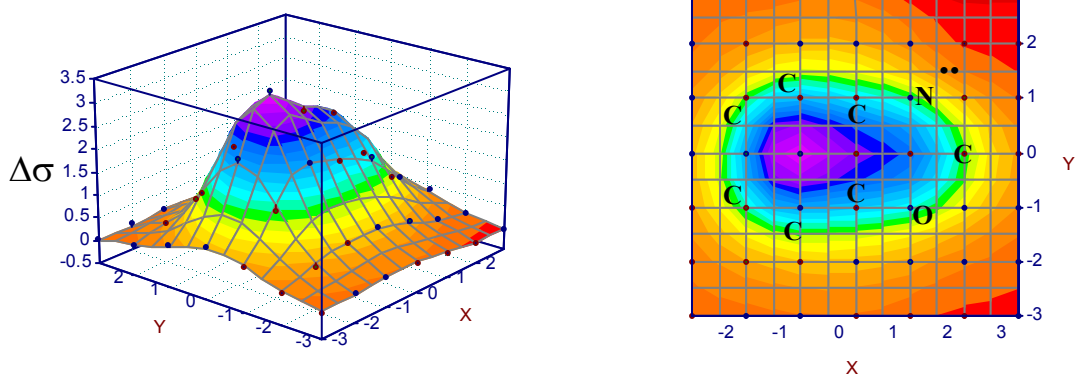
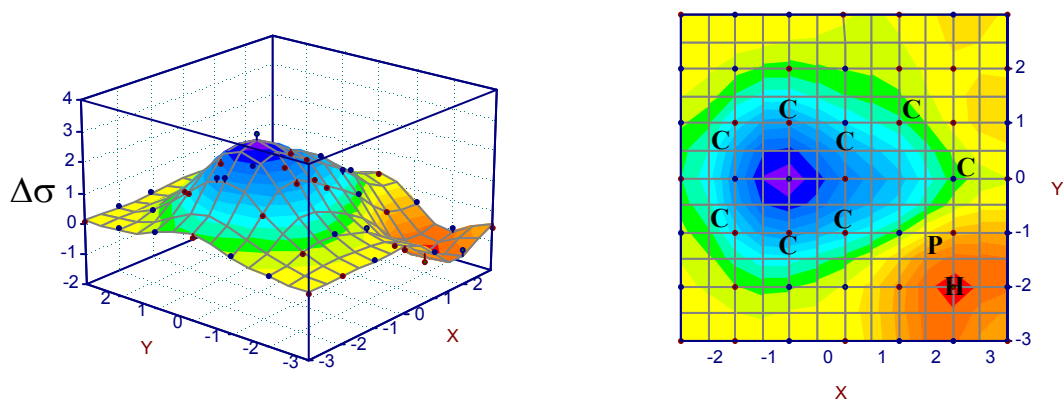


Fig. 30. NMR shielding increment surfaces (in ppm) at the 2.5 Å level for benzo-analogs: 1H-benzotriazole **13c**, benzofuran **4b** and 1,2-benzisoxazole **5b**.

1,3-benzoxazole **6b**



benz[b]phosphole **7b**



1,2-benzisophosphazole **8b**

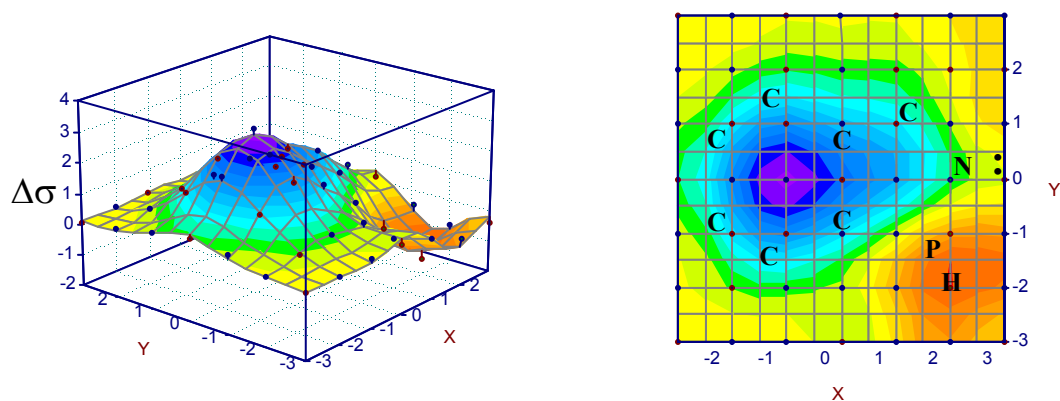
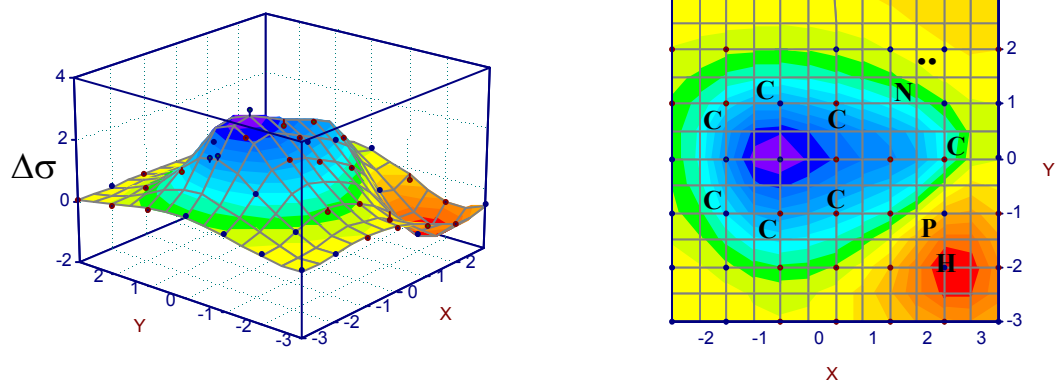
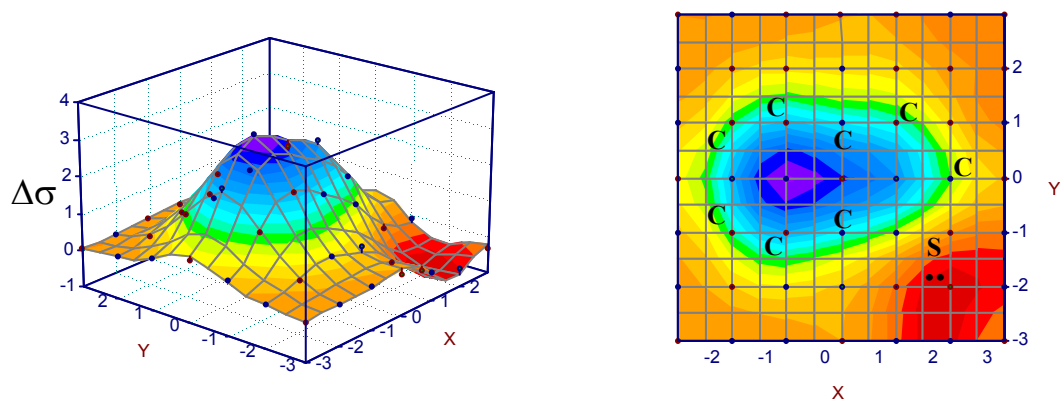


Fig. 31. NMR shielding increment surfaces (in ppm) at the 2.5 Å level for benzo-analogs: 1,3-benzoxazole **6b**, benz[b]phosphole **7b** and 1,2-benzisophosphazole **8b**.

1,3-benzphosphazole **9b**



benzo[b]thiophene **10b**



1,2-benzisothiazole **11b**

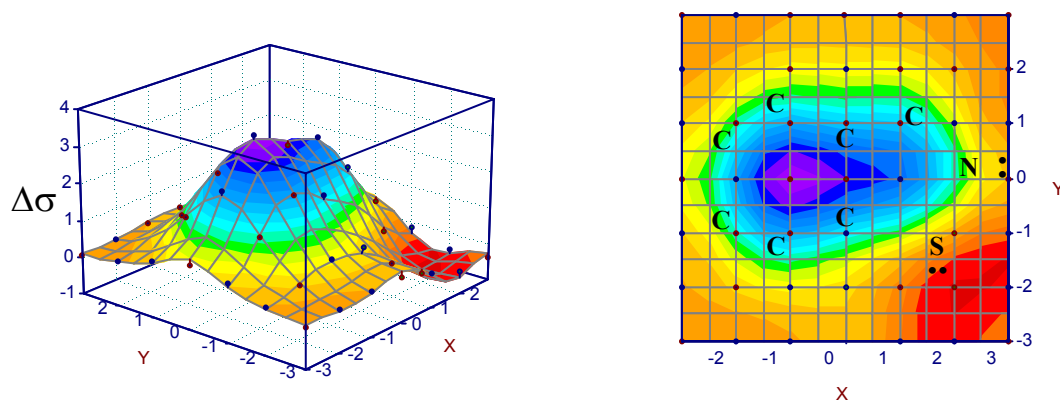
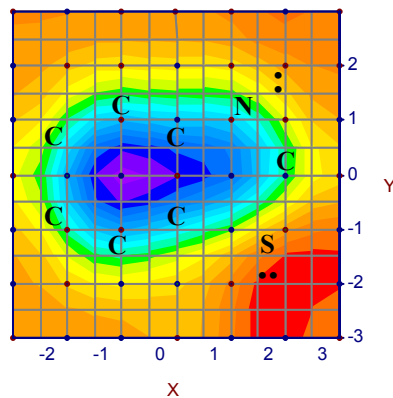
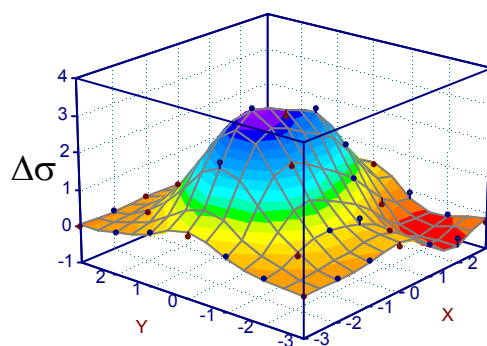
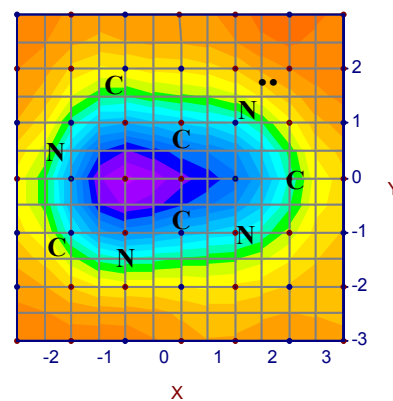
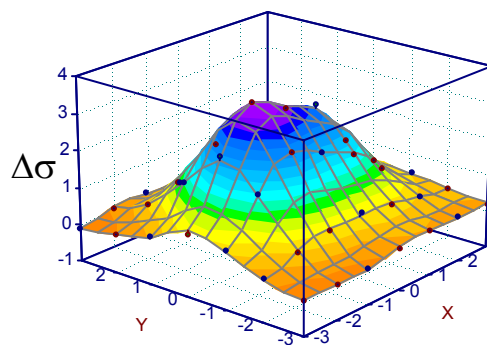


Fig. 32. NMR shielding increment surfaces (in ppm) at the 2.5 Å level for benzo-analogs: 1,3-benzphosphazole **9b**, benzo[b]thiophene **10b** and 1,2-benzisothiazole **11b**.

1,2-benzothiazole **12b**



purine **17**



carbazole **18**

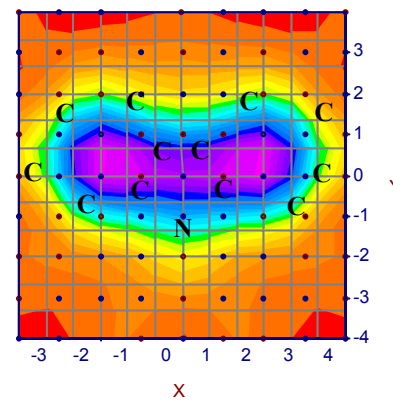
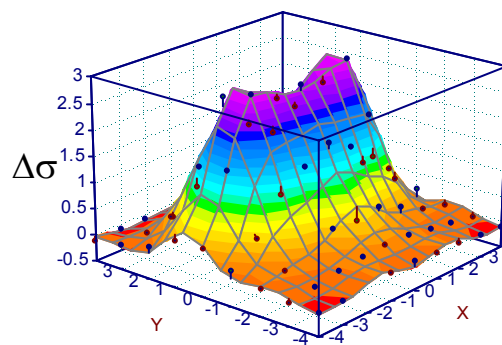
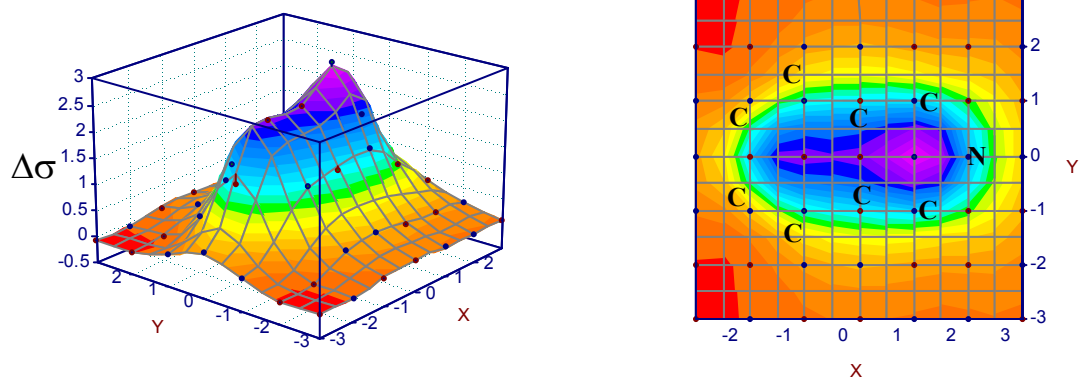
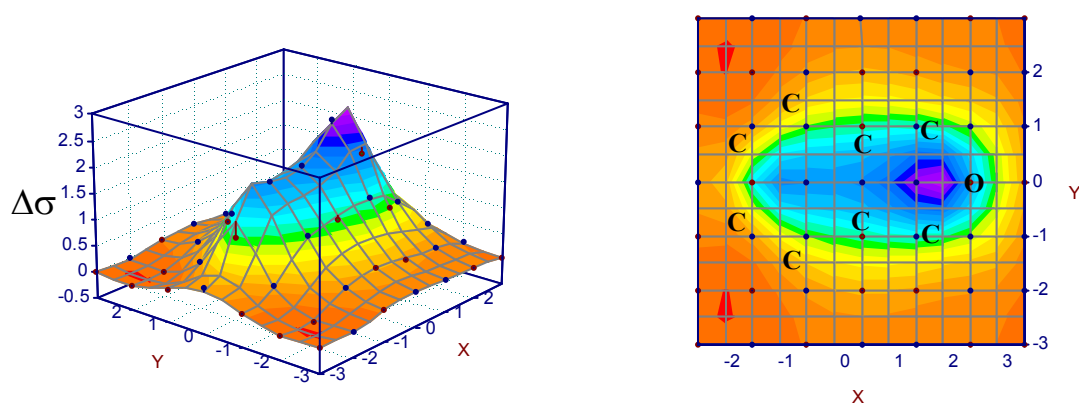


Fig. 33. NMR shielding increment surfaces (in ppm) at the 2.5 Å level for benzo-analogs: 1,2-benzothiazole **12b**, purine **17** and carbazole **18**.

isoindole **1c**



isobenzofuran **4c**



benzo[c]thiophene **10c**

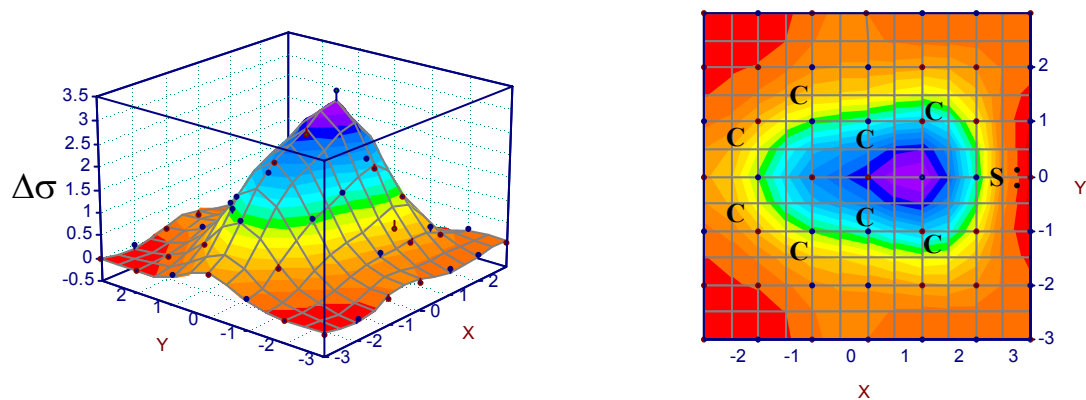
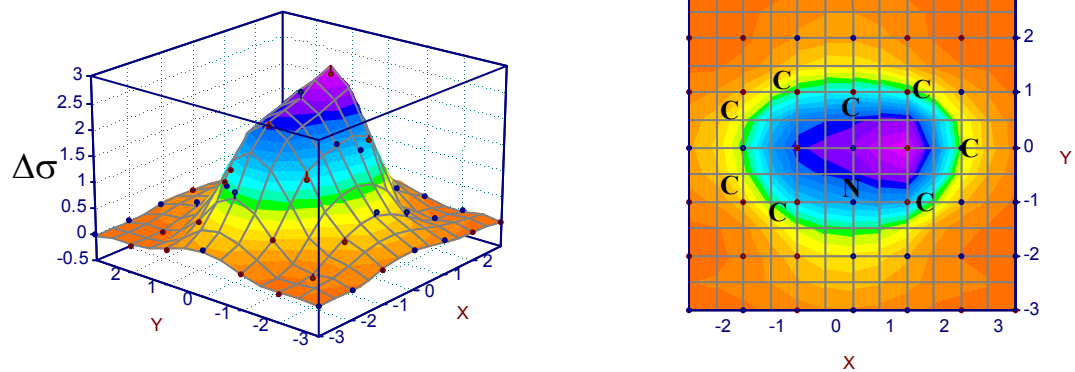


Fig. 34. NMR shielding increment surfaces (in ppm) at the 2.5 Å level for benzo-analogs: isoindole **1c**, isobenzofuran **4c** and benzo[c]thiophene **10c**.

indazoline **19**



cycl[3,2,2]azine **20**

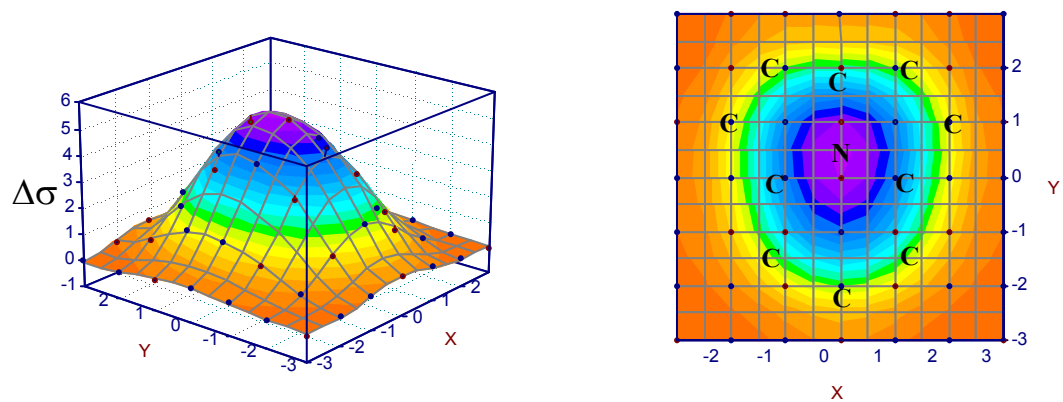
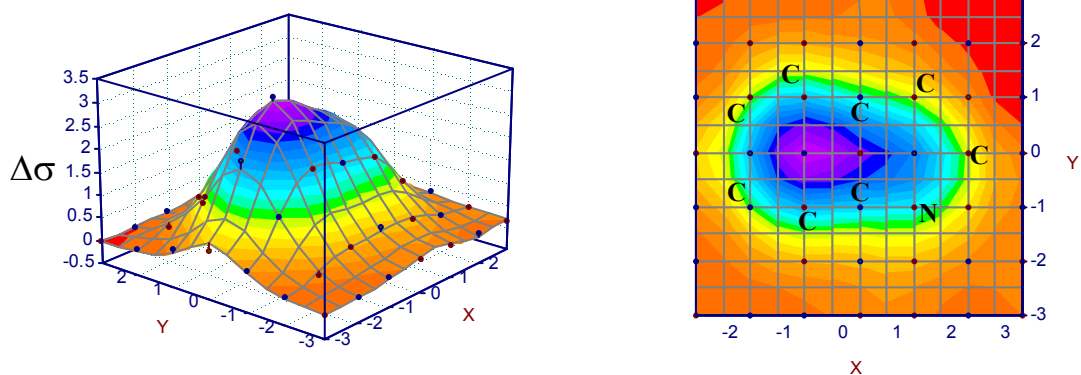
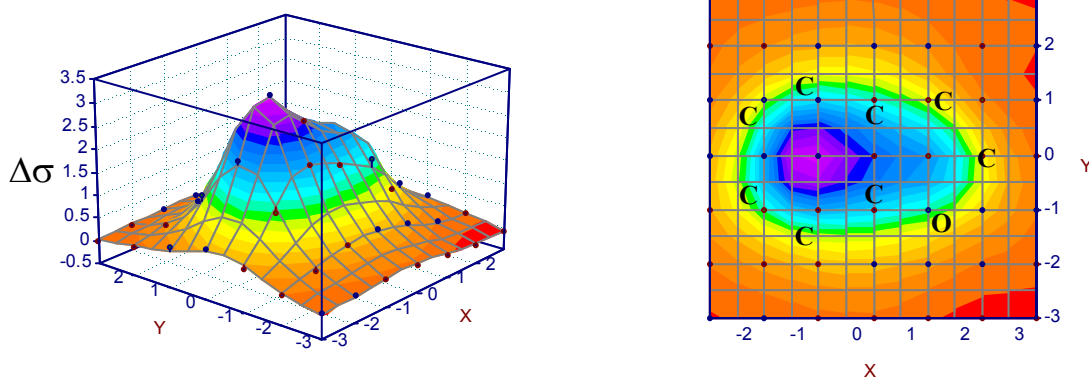


Fig. 35. NMR shielding increment surfaces (in ppm) at the 2.5 Å level for benzo-analogs: indazoline **19** and cycl[3,2,2]azine **20**.

indole **1b**



benzofuran **4b**



benz[b]phosphole **7b**

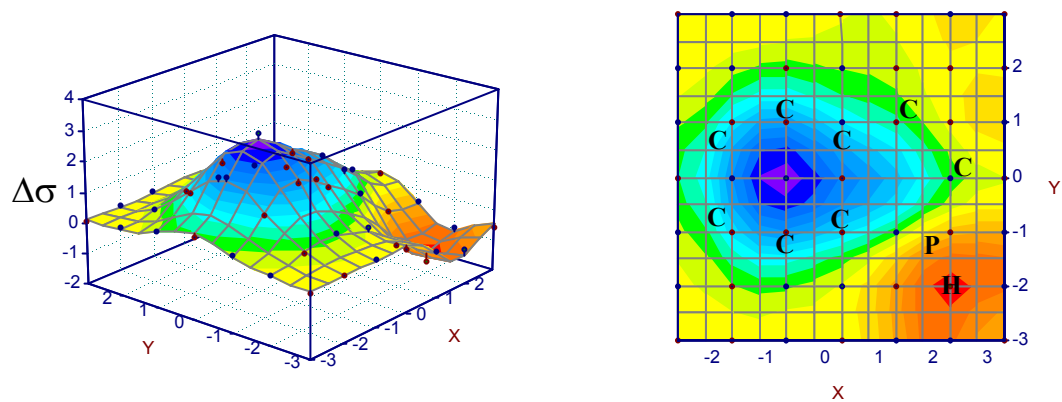


Fig. 36. NMR shielding increment surfaces (in ppm) at the 2.5 Å level for benzo-analogs of parent five-membered rings: indole **1b**, benzofuran **4b** and benz[b]phosphole **7b**.

benzo[b]thiophene **10b**

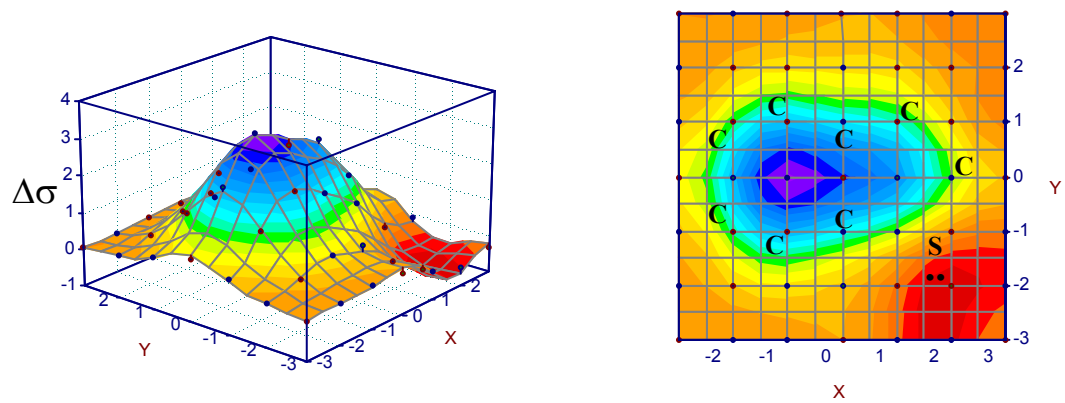
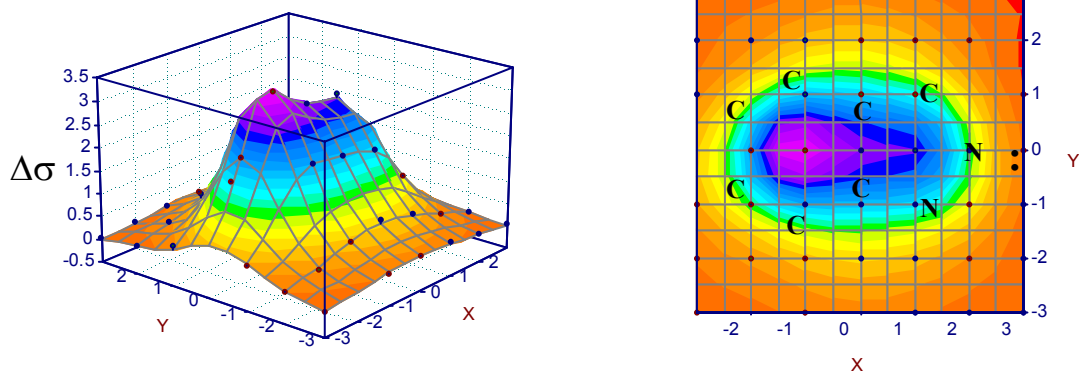


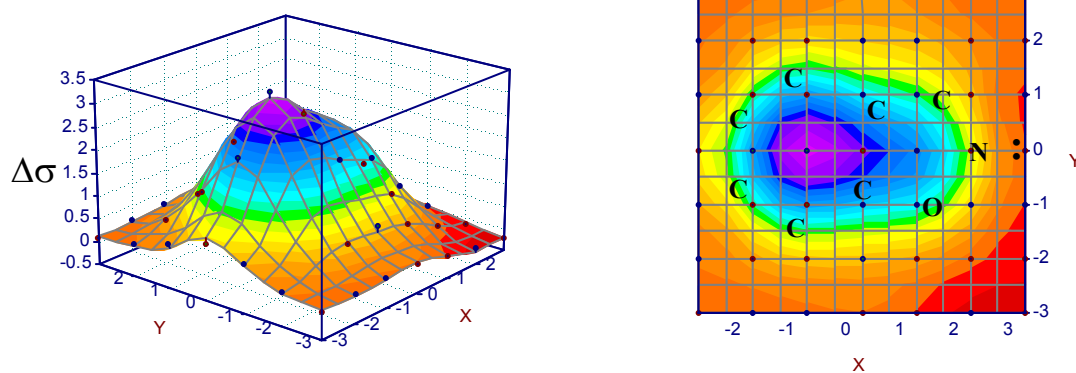
Fig. 37. NMR shielding increment surfaces (in ppm) at the 2.5 Å level for the benzo-analog of parent five-membered ring: benzo[b]thiophene **10b**.

The shielding surfaces of benzo-analogs of α derivatives of different parent five-membered rings (Figs. 38 and 39) appear very similar to those of their parents. However, all shielding mounds benzo-analogs, except for 1,2-benzisophosphazole **8b**, appear fuller. Also, as the exception from what was just mentioned, 1,2-benzisophosphazole **8b**, has a diminished deshielding region in comparison with its parent.

indazole **2b**



1,2-benzisoxazole **5b**



1,2-benzisophosphazole **8b**

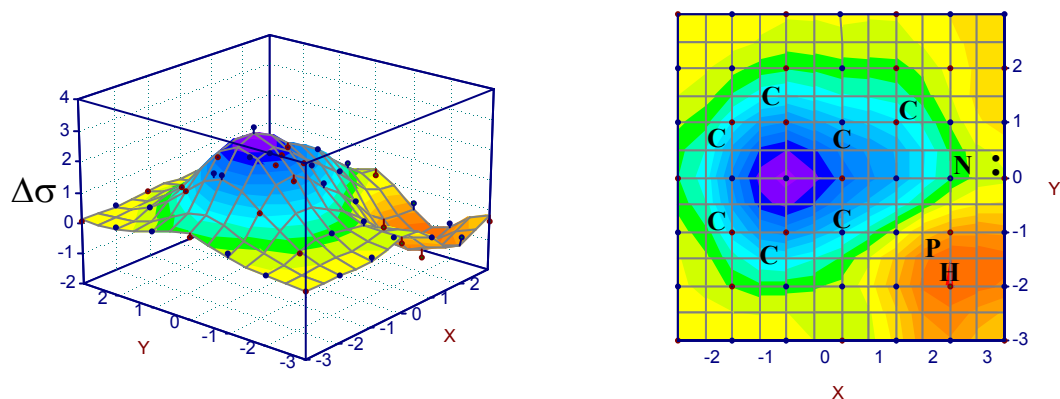


Fig. 38. NMR shielding increment surfaces (in ppm) at the 2.5 Å level for benzo-analogs of parent five-membered structure derivatives with nitrogen in α position: indazole **2b**, 1,2-benzisoxazole **5b** and 1,2-benzisophosphazole **8b**.

1,2-benzisothiazole **11b**

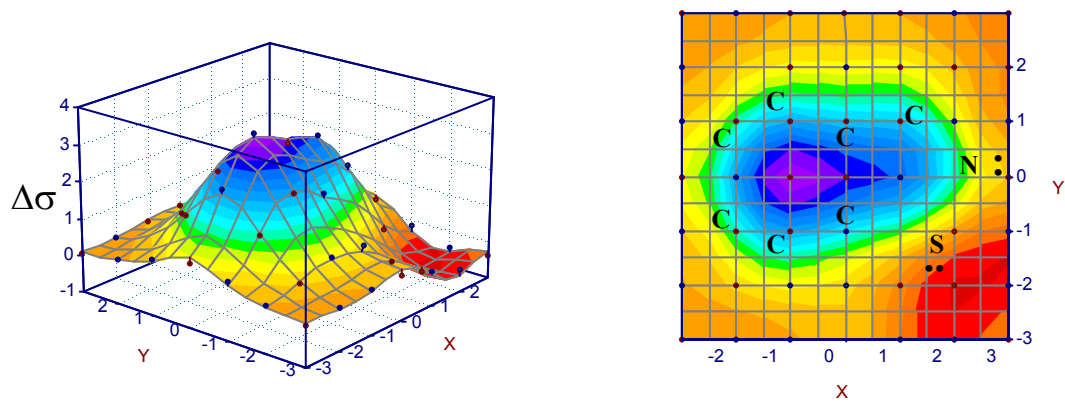
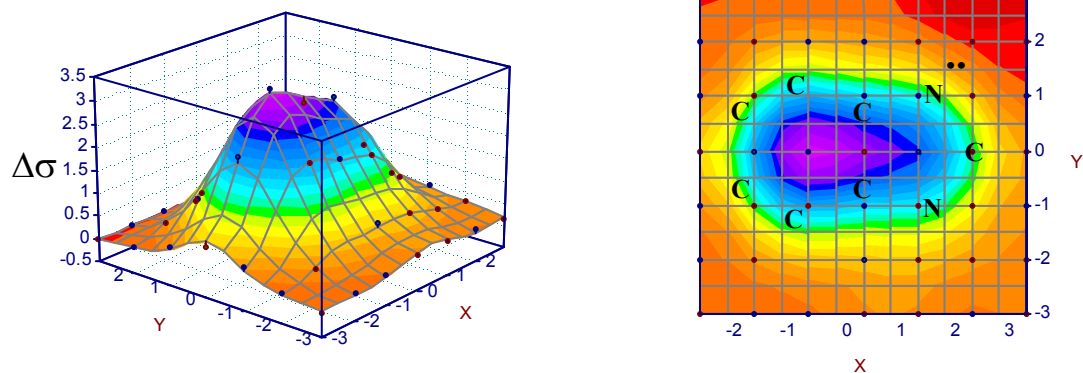


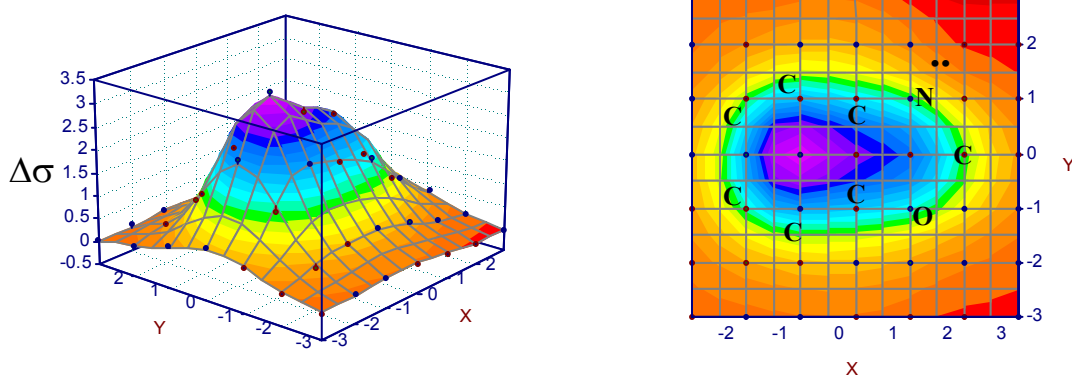
Fig. 39. NMR shielding increment surfaces (in ppm) at the 2.5 Å level for benzo-analog of parent five-membered structure derivative with nitrogen in α position: 1,2-benzisothiazole **11b**.

The shielding surfaces of benzo-analogs of different five-membered rings with nitrogen in β position (Figures 40 and 41) substantiate what has been seen with their five-membered ring parents. The only difference, except for 1,3-benzphosphazole **9b**, is that the benzo-analogs exhibit more fuller shielding mounds than their five-membered ring parents. Also, 1,3-benzphosphazole **9b** appears to have a more diminished deshielding region compared with its parent.

benzimidazole **3b**



1,3-benzoxazole **6b**



1,3-benzphosphazole **9b**

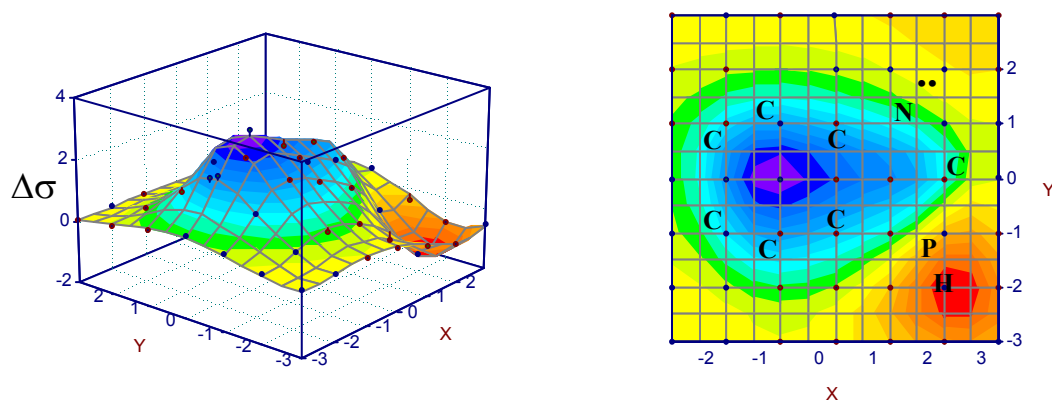


Fig. 40. NMR shielding increment surfaces (in ppm) at the 2.5 Å level for the benzo-analog of the parent five-membered structure derivative with nitrogen in β position: benzimidazole **3b**, 1,3-benzoxazole **6b** and 1,3-benzphosphazole **9b**.

1,2-benzothiazole **12b**

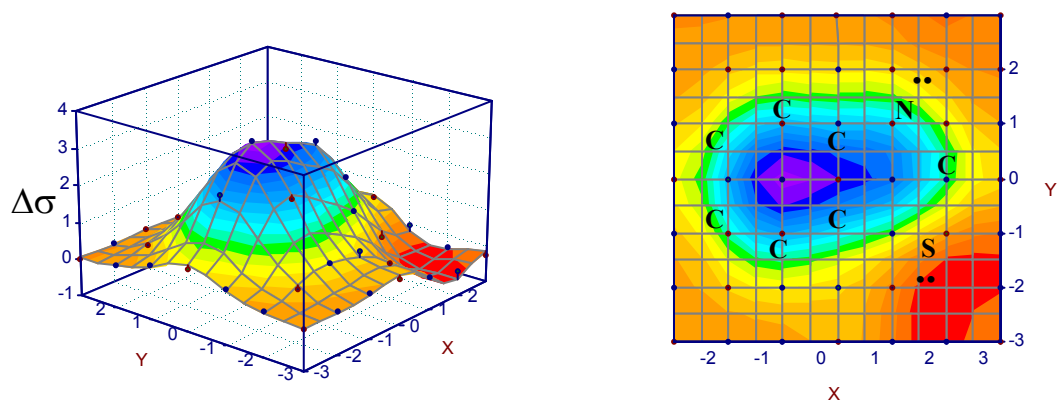
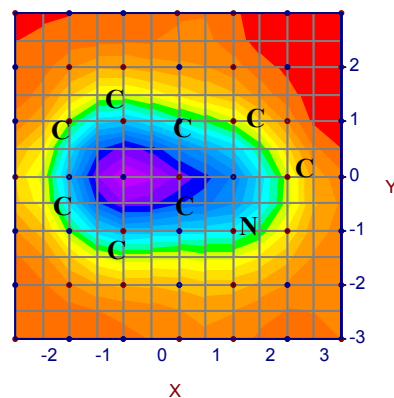
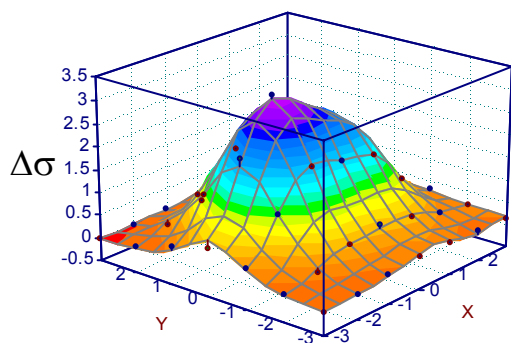


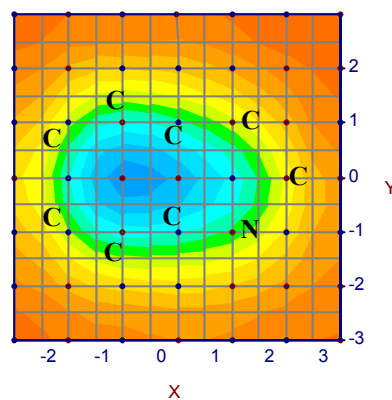
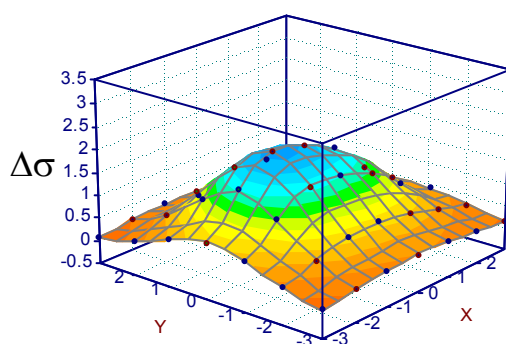
Fig. 41. NMR shielding increment surfaces (in ppm) at the 2.5 Å level for benzo-analog of parent five-membered structure derivative with nitrogen in β position: 1,2-benzothiazole **12b**.

Fig. 42 exemplifies a similar concept conveyed earlier with Fig. 5 in that the greater the distance of the diatomic probe from the plane of the structure, the less featured the shielding mound is.

indole **1b** (2.5Å)



indole **1b** (3.0Å)



indole **1b** (4.0Å)

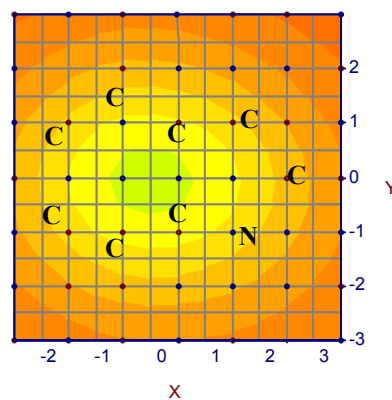
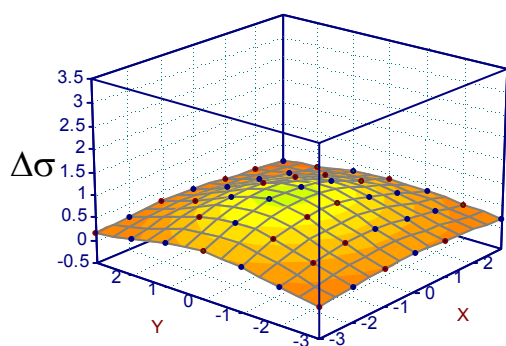


Fig. 42. NMR shielding increment surfaces (in ppm) at the 2.5, 3.0 & 4.0 Å levels for indole **1b**.

E. Correlation with other Methods

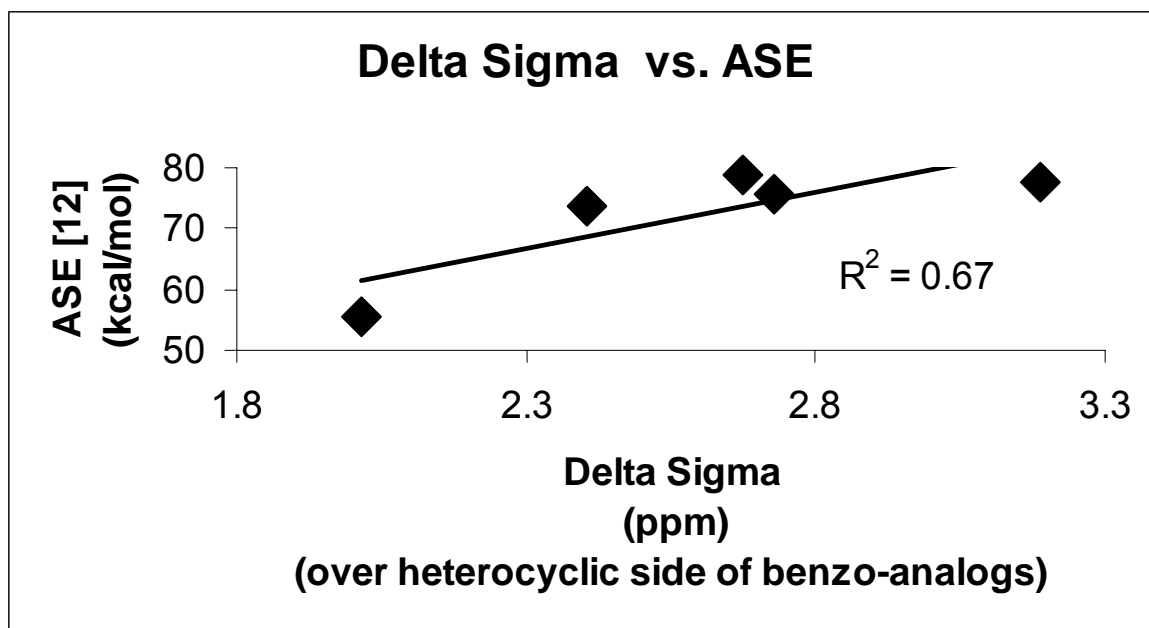
Table 6

This study's maximum isotropic shielding increment values (ppm) at 2.5 Å joined with this study's NICS(0), NICS(1) and NICS(2.5) values calculated over the heterocyclic side of benzo-analogs. All compared with published results from Bird's (ASE) [12] for five of the same structures

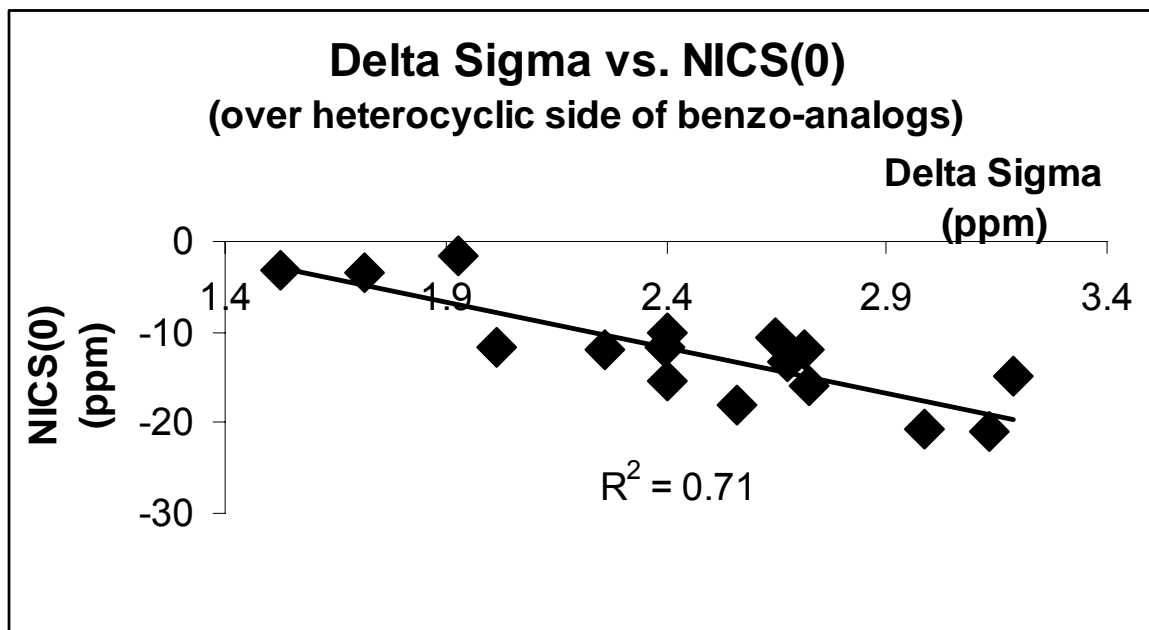
Name	$\Delta\sigma$	NICS(0) (ppm)	NICS(1) (ppm)	NICS(2.5) (ppm)	ASE[12] (kcal/mol)
indole 1b	2.4	-15.4	-11.8	-2.8	73.8
indazole 2b	2.7	-15.9	-13.0	-3.0	75.7
benzimidazole 3b	2.7	-13.2	-11.0	-2.8	78.9
1H-benzotriazole 13c	3.2	-14.9	-14.2	-3.3	77.6
benzofuran 4b	2.0	-11.8	-9.5	-2.3	55.4
1,2-benzisoxazole 5b	2.3	-12.0	-10.3	-2.5	N/A
1,3-benzoxazole 6b	2.4	-10.1	-9.1	-2.4	N/A
benz[b]phosphole 7b	1.5	-3.1	-3.8	-1.7	N/A
1,2-benzisophosphazole 8b	1.7	-3.5	-4.1	-1.8	N/A
1,3-benzphosphazole 9b	1.9	-1.6	-4.1	-1.9	N/A
benzo[b]thiophene 10b	2.4	-11.7	-9.0	-2.6	N/A
1,2-benzisothiazole 11b	2.7	-12.1	-9.5	-2.7	N/A
1,2-benzothiazole 12b	2.7	-10.7	-9.3	-2.7	N/A
purine 17	2.8	-12.8	-10.7	-2.7	N/A
carbazole 18	N/A	N/A	N/A	N/A	N/A
isoindole 1c	3.0	-20.7	-15.1	-3.3	N/A
Isobenzofuran 4c	2.6	-18.0	-13.0	-2.8	N/A
benzo[c]thiophene 10c	3.1	-21.1	-14.1	-3.3	N/A
indazoline 19	2.7	-20.5	-15.9	-3.1	N/A
cycl(3,2,2)azine 20	N/A	N/A	N/A	N/A	N/A

F. Correlations with other Methods; Probe over Heterocyclic Ring

These correlations involve measurements acquired with the diatomic H₂ probe being above the center of the heterocyclic ring portion of the benzo-analogs. Only one suitable outside source [12] was found to correlate with these shielding increment and NICS calculations. Data from Bird provided ASE values for only five of this study's benzo-analogs (indole, indazole, benzimidazole, 1H-benzotriazole and benzofuran) that could be correlated with data calculated over the heterocyclic side, the benzene side and the center bond of the benzo-analogs. The results from the probe doing calculations over the benzene side and center bond will be discussed later separately. As seen in Fig. 43A, the correlation between this study's shielding increment data and Bird's ASE data yielded an R² value of 0.67. Since outside sources were limited for these benzo-analogs, NICS(0), NICS(1) and NICS(2.5) calculations were done to further substantiate the $\Delta\sigma$ calculations indirectly. The $\Delta\sigma$ vs. NICS(0) correlation yielded a R² value of 0.71. The same $\Delta\sigma$ values vs. NICS(1) correlation yielded a R² value of 0.80 and 0.95 vs. NICS(2.5).

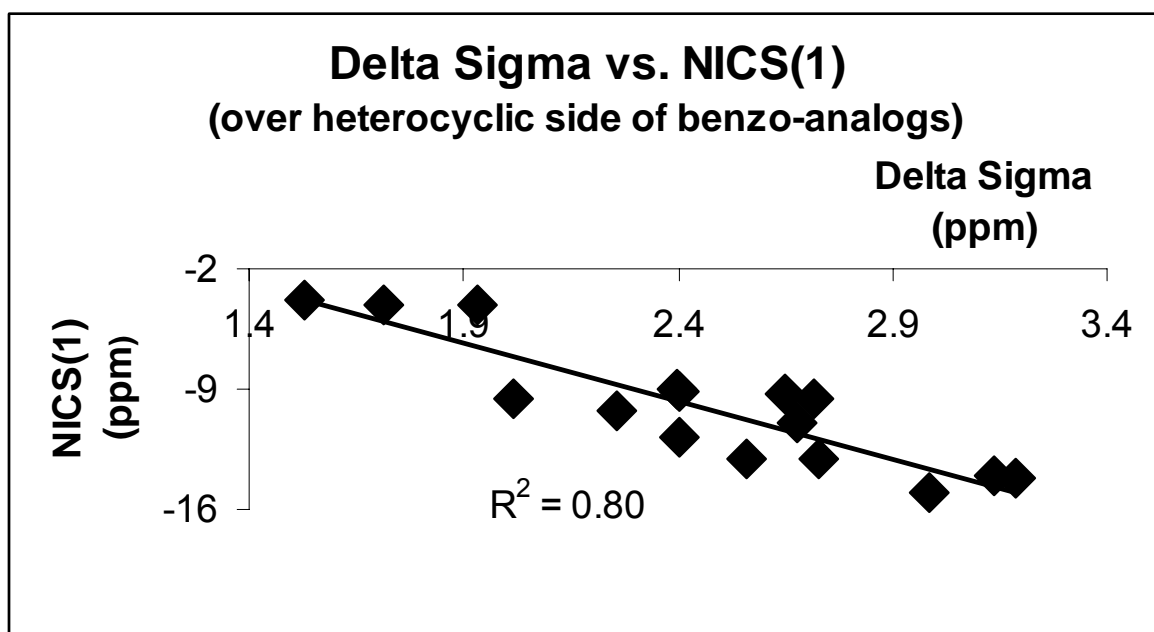


A

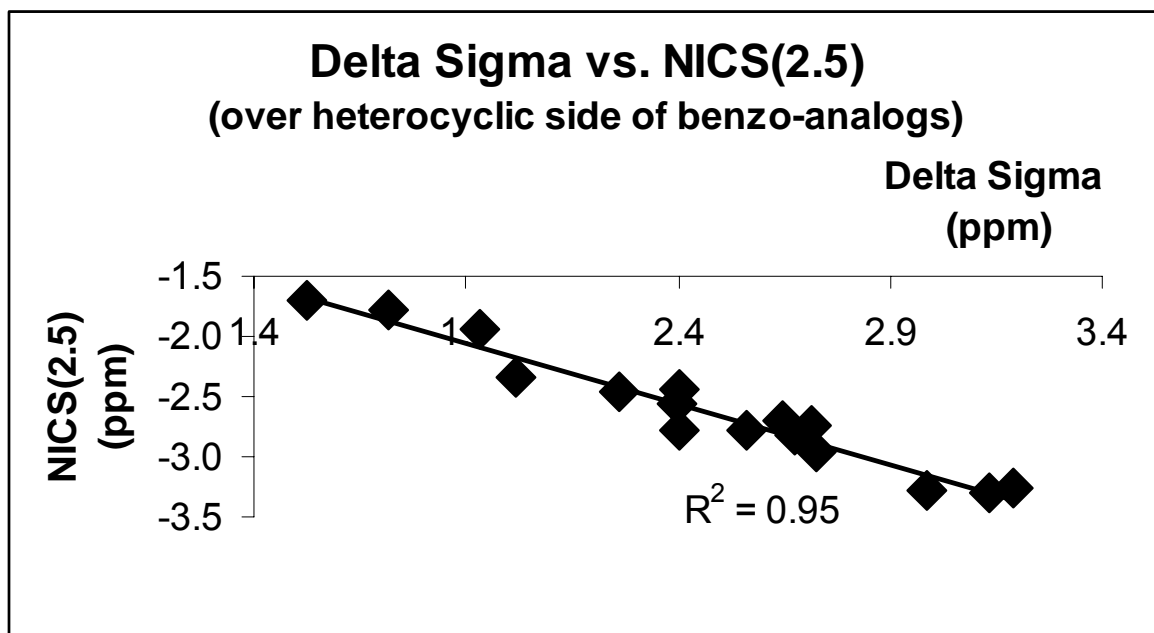


B

Fig. 43. This study's NMR maximum shielding increments ($\Delta\sigma_{\max}$) over the heterocyclic side correlated with ASE [12] (A) and this study's NICS(0) (B) measurements for the benzo-analogs.



A

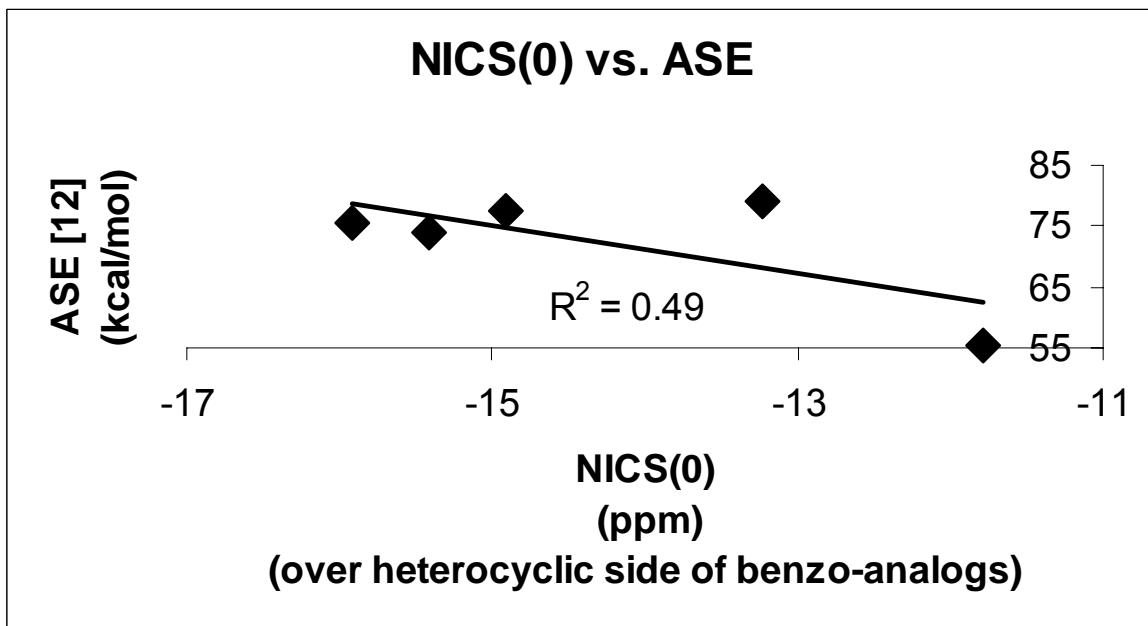


B

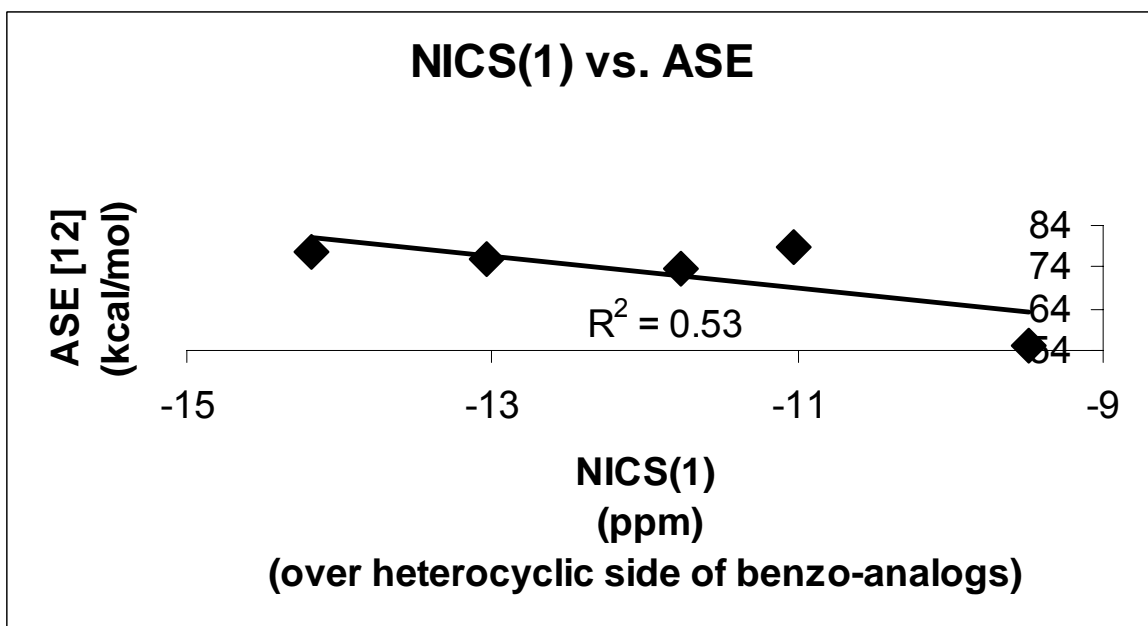
Fig. 44. This study's NMR maximum shielding increments ($\Delta\sigma_{\max}$) over the heterocyclic side correlated with this study's NICS(1) (A) and this study's NICS(2.5) (B) for the benzo-analogs.

G. Other Methods Correlated with each other; Probe over Heterocyclic Ring

The NICS(0) correlated with ASE [12] yielded a R^2 value of 0.43. The NICS(1) results correlated with ASE [12] results to yield a R^2 value of 0.80. The NICS(2.5) results correlated with ASE [12] results to yield a R^2 value of 0.95. Even with NICS calculations being in house, a near perfect correlation of NICS(2.5) with ASE [12] indirectly helps to substantiate this study's shielding increment calculations.

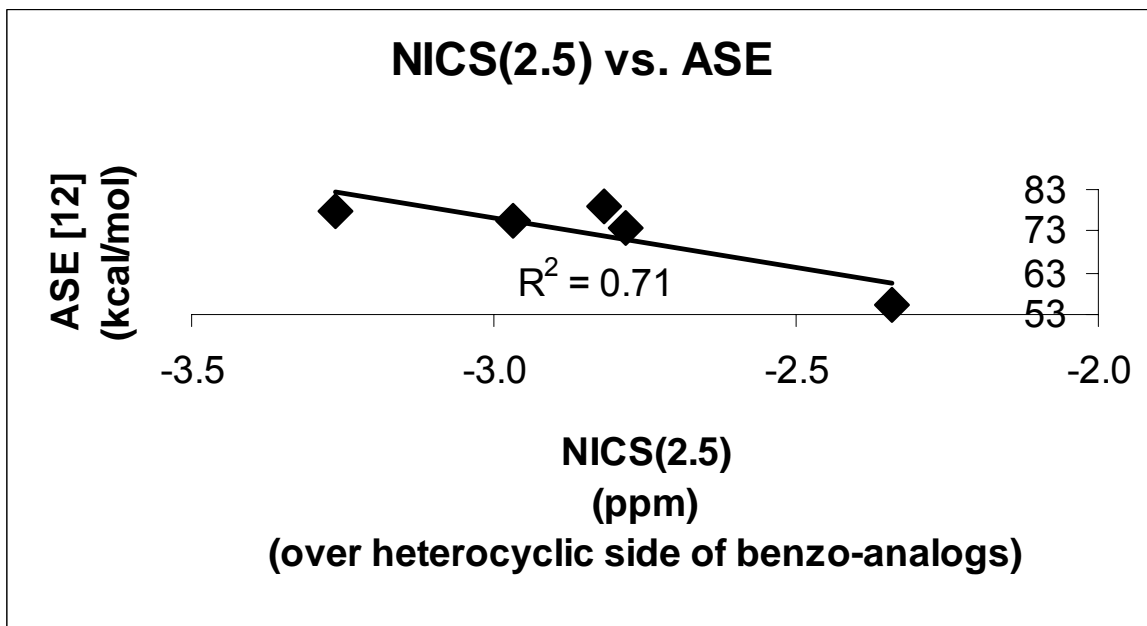


A

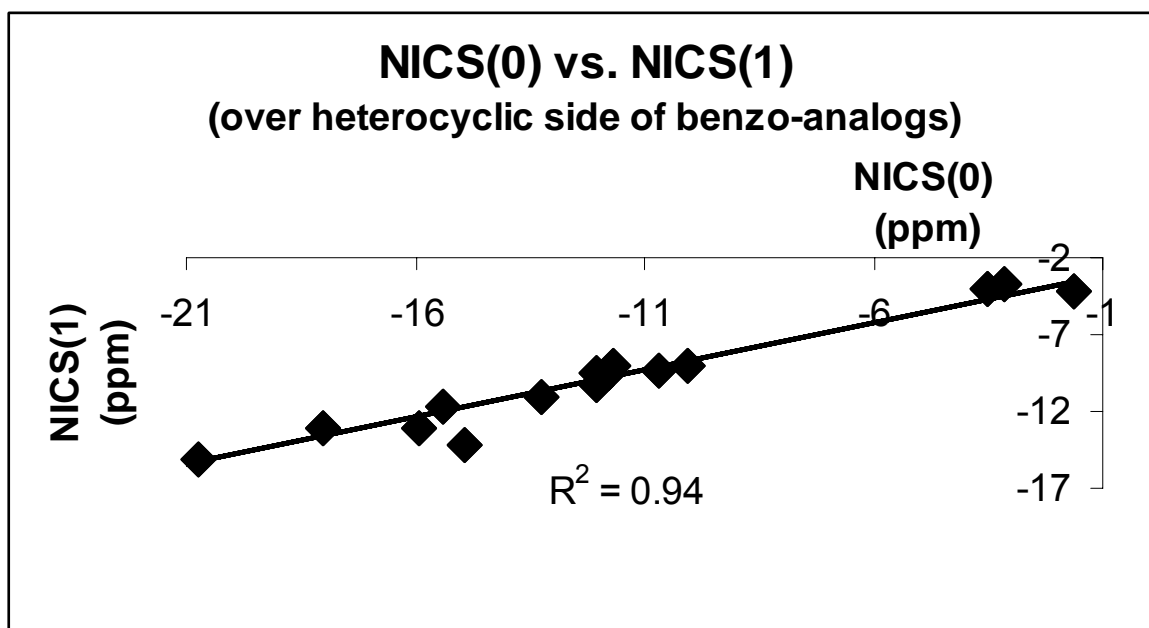


B

Fig. 45. ASE [12] correlated with both this study's NICS(0) over the heterocyclic side (A) and NICS(1) over the heterocyclic side (B), both for the benzo-analogs.

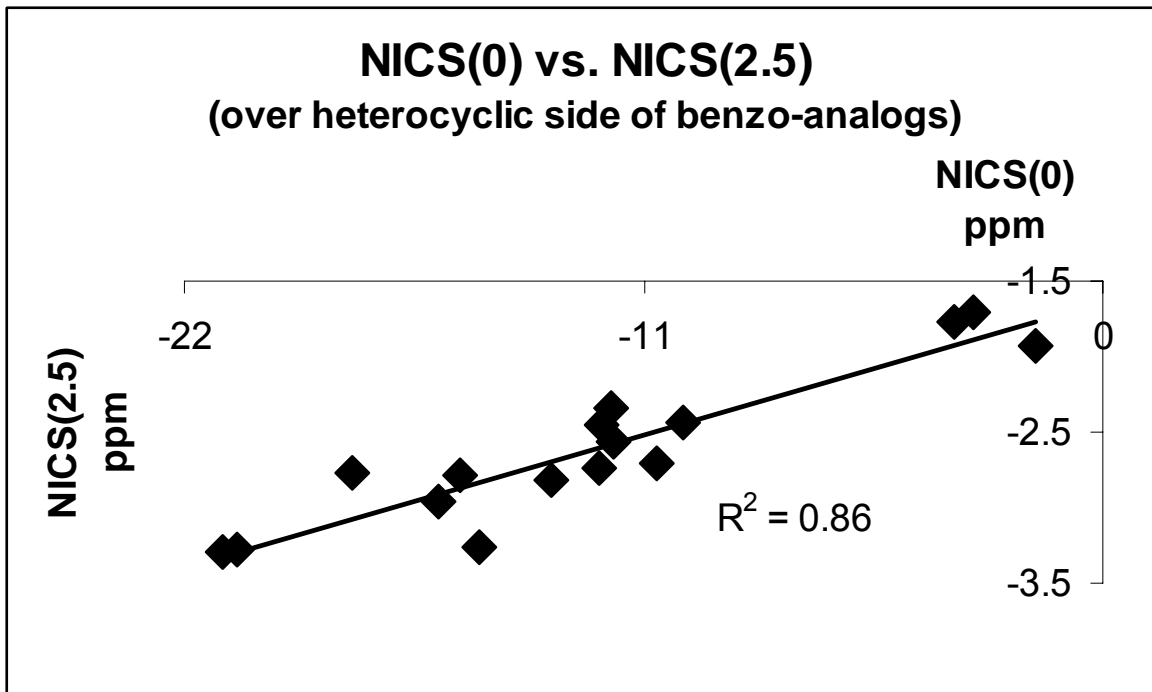


A

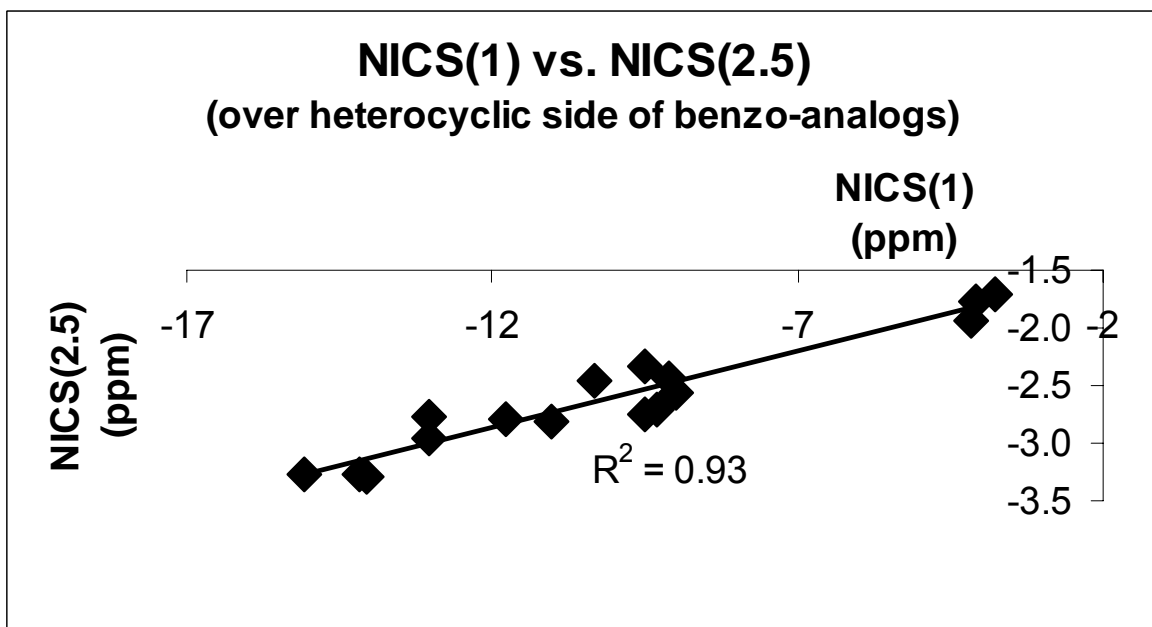


B

Fig. 46. This study's NICS(2.5) over the heterocyclic side correlated with ASE [12] (A) and this study's NICS(0) and NICS(1) both over the heterocyclic side correlated with each other (B) for the benzo-analogs.



A



B

Fig. 47. This study's NICS(0) and NICS(2.5), both over the heterocyclic side, correlated with each other (A) and this study's NICS(1) and NICS(2.5), both over the heterocyclic side, with each other (B) for the benzo-analogs.

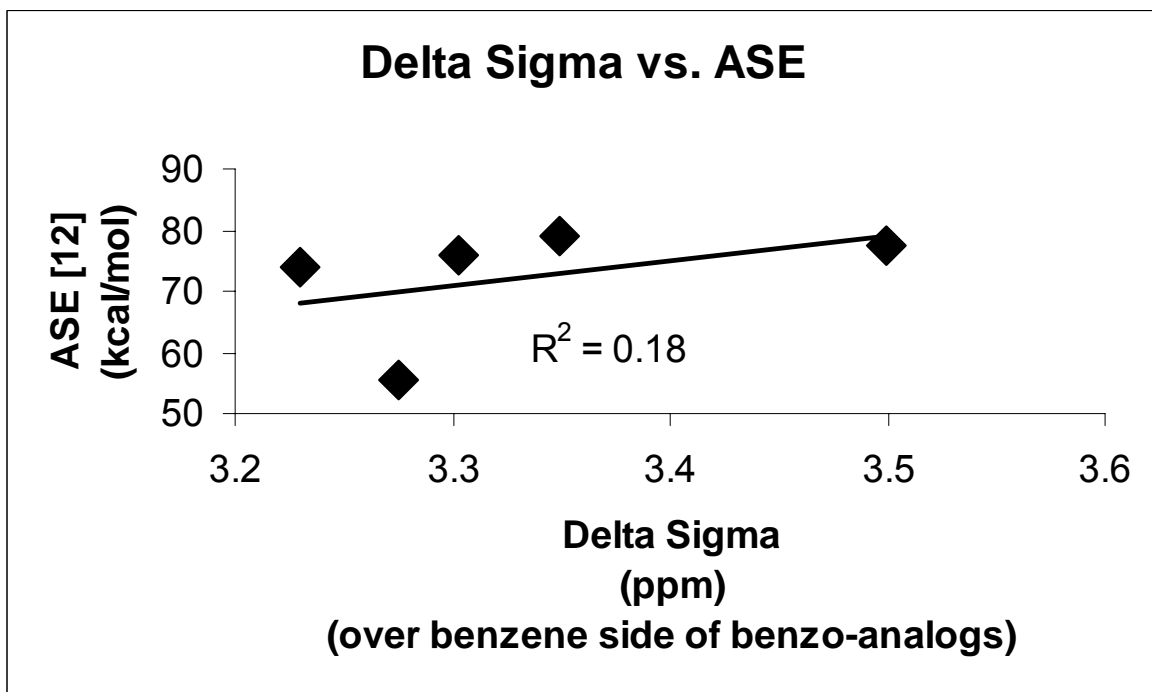
H. Correlations with other Methods; Probe over Benzene side

Table 7

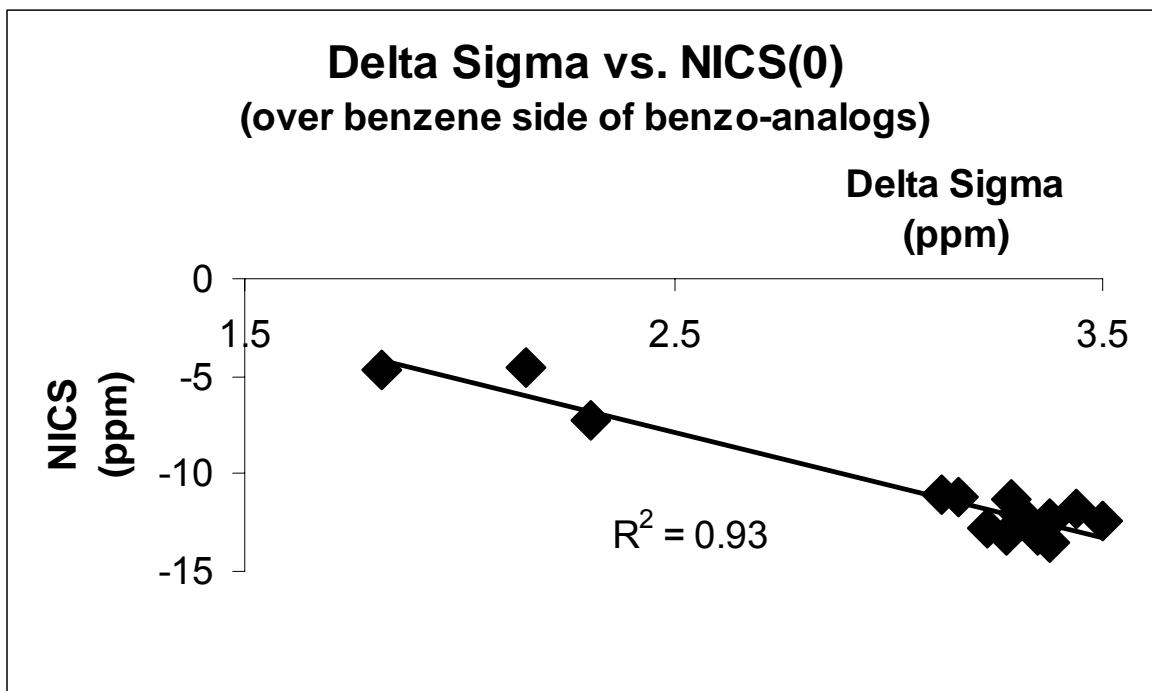
This study's maximum isotropic shielding increment values (ppm) at 2.5 Å joined with this study's NICS(0), NICS(1) and NICS(2.5) values calculated over the benzene side of benzo-analogs. All compared with published results from Bird's (ASE) [12] for five of the same structures

Name	$\Delta\sigma$ (ppm)	NICS(0) (ppm)	NICS(1) (ppm)	NICS(2.5) (ppm)	ASE[12] (kcal/ mol)
indole 1b	3.2	-12.8	-13.3	-3.6	73.8
indazole 2b	3.3	-12.1	-12.8	-3.6	75.7
benzimidazole 3b	3.4	-13.2	-13.5	-3.7	78.9
1H-benzotriazole 13c	3.5	-12.4	-13.1	-3.7	77.6
benzofuran 4b	3.3	-13.1	-13.5	-3.6	55.4
1,2-benzisoxazole 5b	3.4	-12.4	-13.1	-3.6	N/A
1,3-benzoxazole 6b	3.4	-13.5	-13.6	-3.6	N/A
benz[b]phosphole 7b	3.1	-11.0	-12.8	-3.4	N/A
1,2-benzisophosphazole 8b	3.3	-11.3	-12.9	-3.5	N/A
1,3-benzphosphazole 9b	3.2	-11.2	-12.7	-3.4	N/A
benzo[b]thiophene 10b	3.3	-12.1	-13.1	-3.6	N/A
1,2-benzisothiazole 11b	3.4	-11.8	-13.0	-3.6	N/A
1,2-benzothiazole 12b	3.4	-12.4	-13.1	-3.6	N/A
purine 17	3.4	-9.7	-12.3	-3.5	N/A
carbazole 18	N/A	N/A	N/A	N/A	N/A
isoindole 1c	2.3	-7.3	-8.8	-2.8	N/A
isobenzofuran 4c	1.8	-4.7	-6.5	-2.2	N/A
benzo[c]thiophene 10c	2.2	-4.5	-7.2	-2.5	N/A
indazoline 19	2.1	-6.1	-7.2	-2.4	N/A
cycl(3,2,2)azine 4bb	N/A	N/A	N/A	N/A	N/A

These correlations involve measurements acquired with the diatomic H₂ probe being above the center of the benzene side of the benzo-analogs. The $\Delta\sigma$ values correlated with ASE [12] to yield R² value of 0.18. The $\Delta\sigma$ values correlated with NICS(0), (1.0) and (2.5) to yield R² values of 0.93, 0.96 and 0.98 respectively

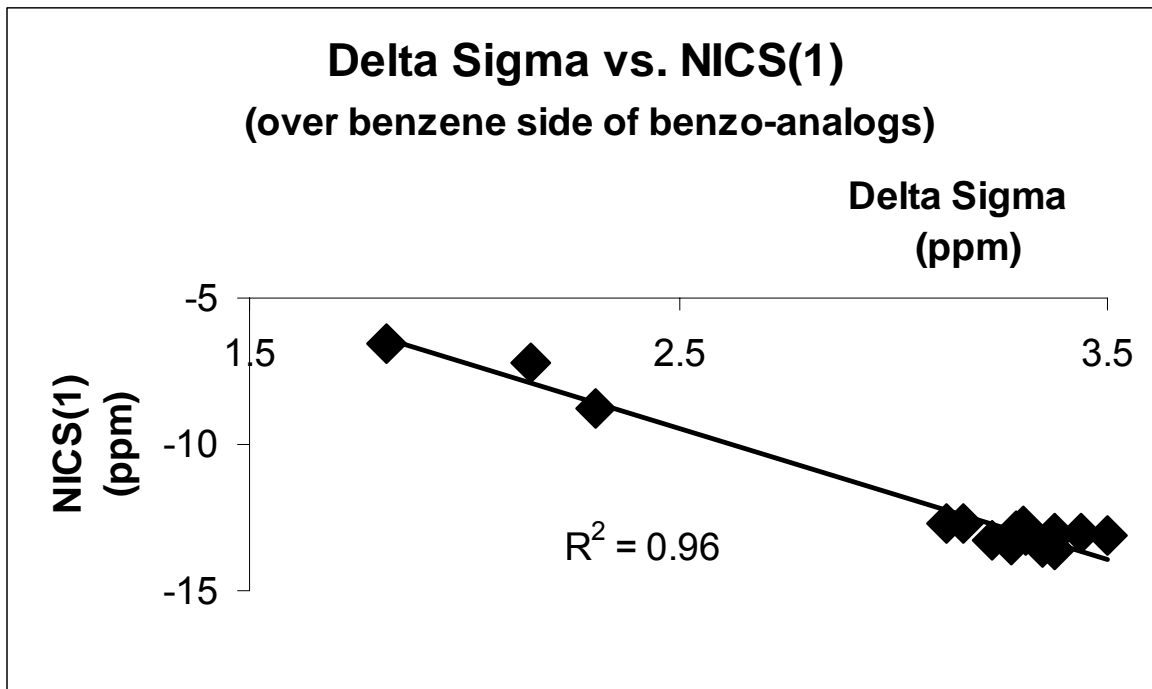


A

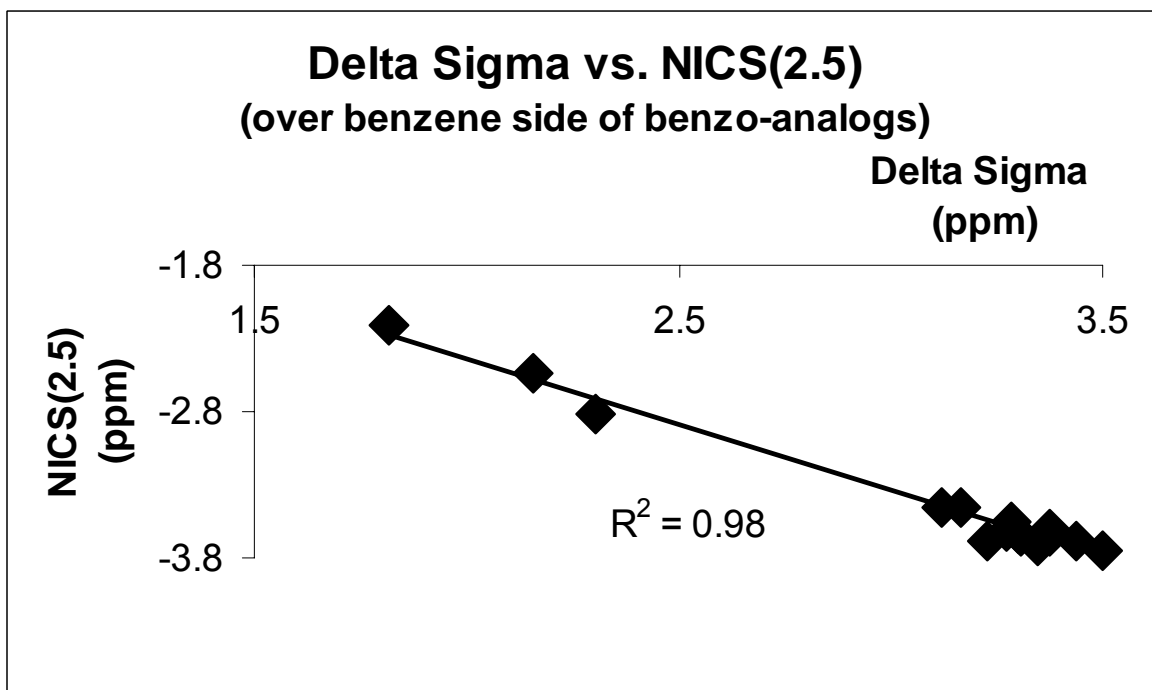


B

Fig. 48. This study's NMR maximum shielding increments ($\Delta\sigma_{\max}$) over benzene correlated with both ASE [12] (A) and this study's NICS(0) over benzene (B) for the benzo-analogs.



A

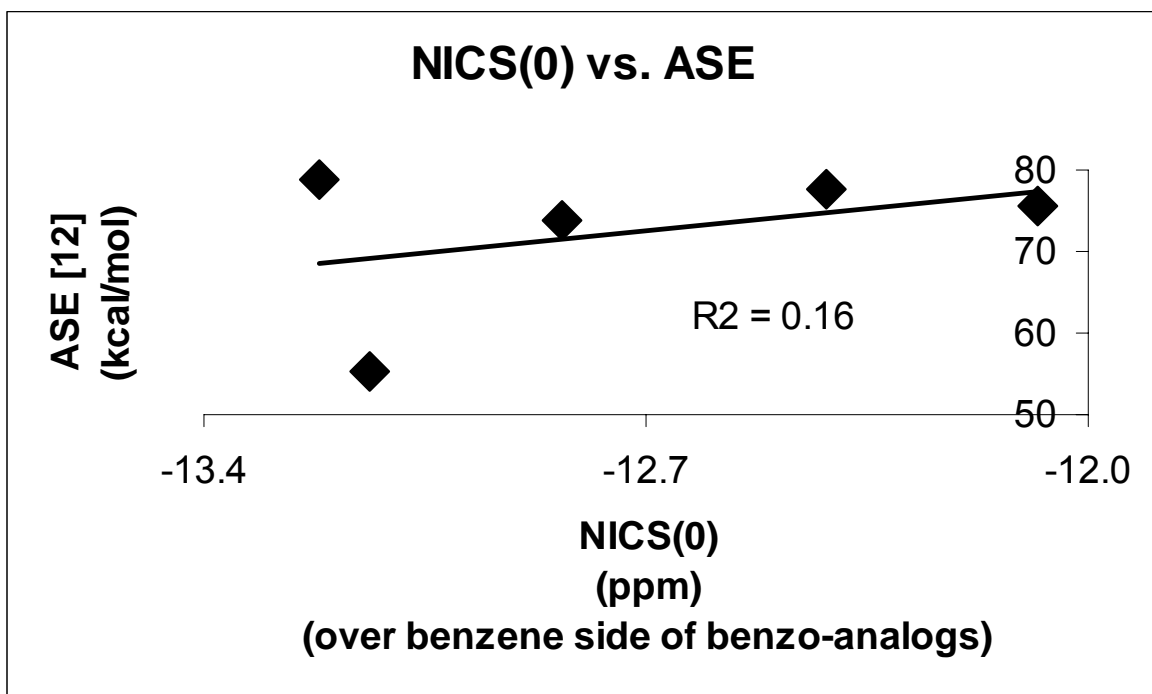


B

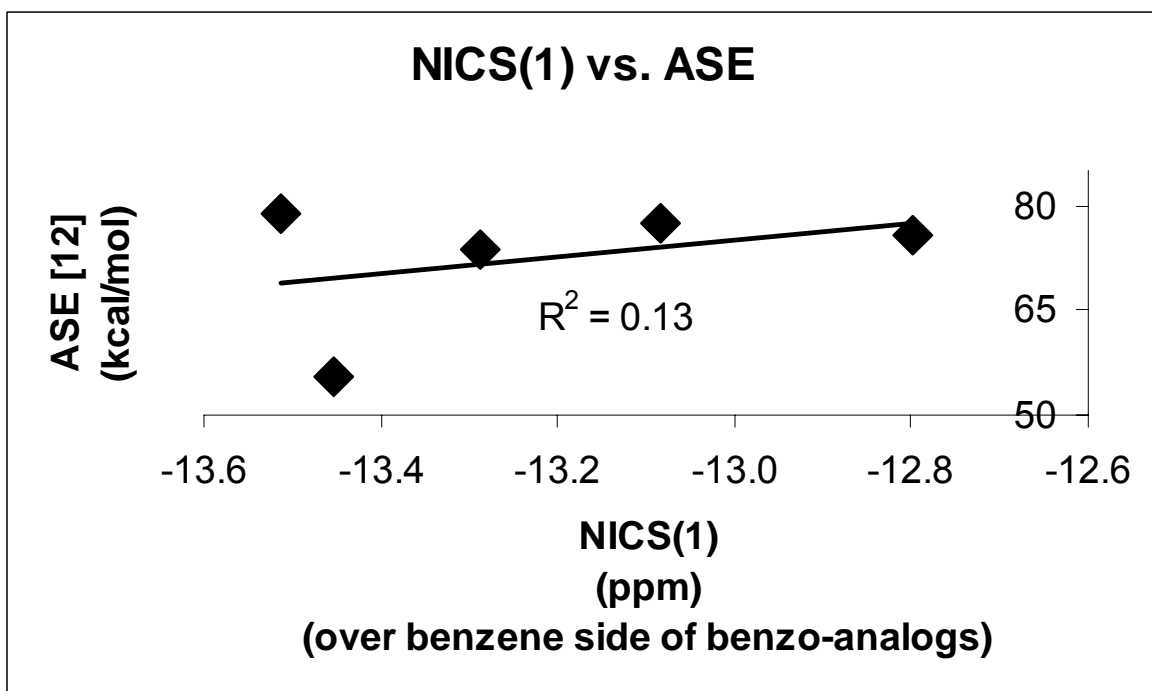
Fig. 49. This study's NMR maximum shielding increments ($\Delta\sigma_{\max}$) over benzene correlated with both this study's NICS(1) over benzene (A) and this study's NICS(2.5) over benzene (B) for the benzo-analogs.

I. Other Methods Correlated with each other; Probe over Benzene side

Methods other than shielding increment values were correlated with each other. NICS(0) correlated with ASE [12] yielded a R^2 value of 0.16. NICS(1) correlated with ASE[12] yielded a R^2 value of 0.13. NICS(2.5) correlated with ASE [12] yielded a R^2 value of 0.53. NICS(0) correlated with NICS(1) yielded a R^2 value of 0.97. NICS(0) correlated with NICS(2.5) yielded a R^2 value of 0.95 and NICS(1) with NICS(2.5) yielded a R^2 value of 0.98.

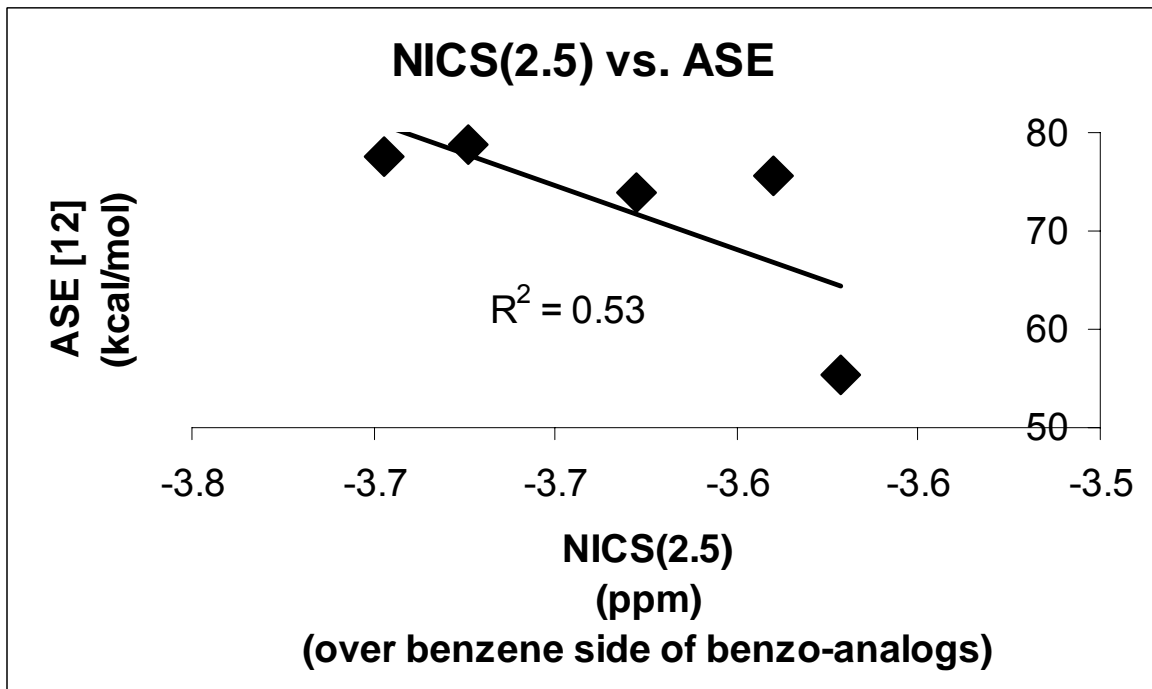


A

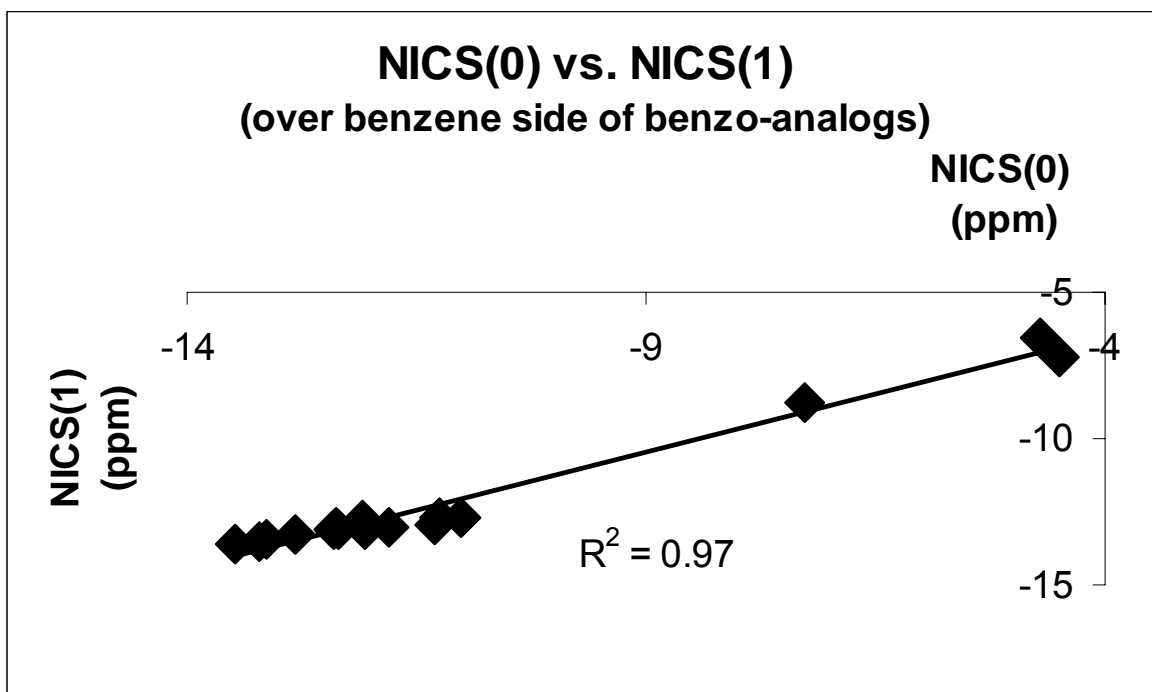


B

Fig. 50. ASE [12] correlated with both this study's NICS(0) over benzene side of benzo-analogs (A) and NICS(1) over benzene side of benzo-analogs(B).



A



B

Fig. 51. This study's NICS(2.5) over benzene side of benzo-analogs correlated with ASE [12] (A). This study's NICS(0) and NICS(1) both over benzene side of benzo-analogs correlated with each other (B).

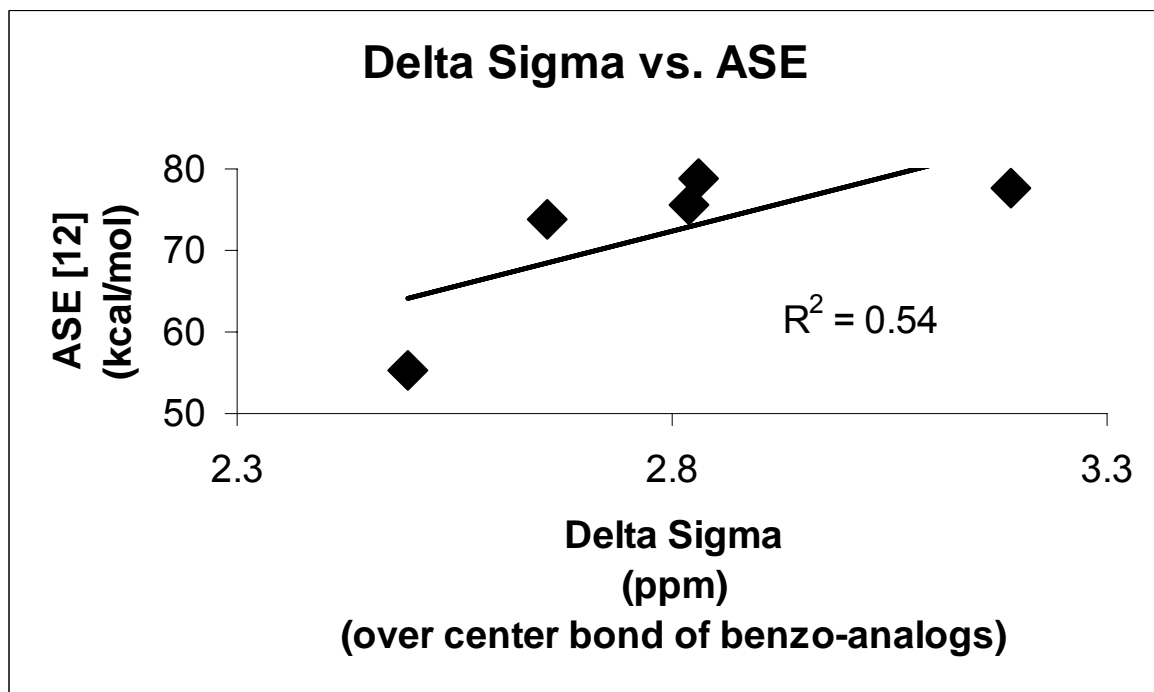
J. Correlations with other Methods; Probe over Center bond

Table 8

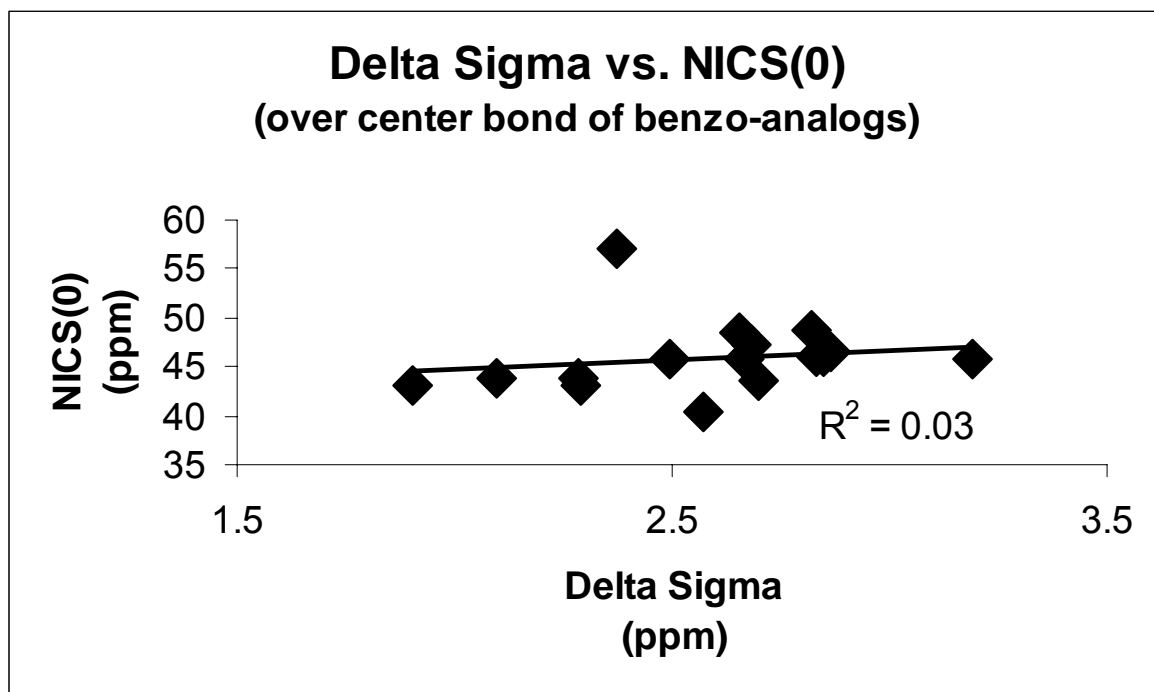
This study's maximum isotropic shielding increment values (ppm) at 2.5 Å joined with this study's NICS(0), NICS(1) and NICS(2.5) values calculated over the center bond of benzo-analogs. All compared with published results from Bird's (ASE) [12] for five of the same structures

Name	$\Delta\sigma$ (ppm)	NICS(0) (ppm)	NICS(1) (ppm)	NICS(2.5) (ppm)	ASE[12] (kcal/mol)
indole 1b	2.7	-48.4	-19.3	-3.4	73.8
indazole 2b	2.8	-48.7	-19.5	-3.4	75.7
benzimidazole 3b	2.8	-46.0	-18.8	-3.4	78.9
1H-benzotriazole 13c	3.2	-45.9	-19.7	-3.6	77.6
benzofuran 4b	2.5	-45.7	-18.1	-3.1	55.4
1,2-benzisoxazole 5b	2.7	-45.9	-18.5	-3.1	N/A
1,3-benzoxazole 6b	2.7	-43.7	-17.7	-3.1	N/A
benz[b]phosphole 7b	2.1	-43.8	-16.9	-2.7	N/A
1,2-benzisophosphazole 8b	2.3	-43.7	-18.0	-2.8	N/A
1,3-benzphosphazole 9b	2.3	-43.2	-16.7	-2.8	N/A
benzo[b]thiophene 10b	2.7	-47.3	-18.7	-3.2	N/A
1,2-benzisothiazole 11b	2.9	-46.4	-19.0	-3.3	N/A
1,2-benzothiazole 12b	2.9	-46.0	-18.4	-3.3	N/A
purine 17	2.4	-57.2	-17.2	-1.8	N/A
carbazole 18	1.9	-43.1	-15.4	-2.6	N/A
isoindole 1c	2.6	-40.4	-16.6	-3.1	N/A
isobenzofuran 4c	N/A	N/A	N/A	N/A	N/A
benzo[c]thiophene 10c	N/A	N/A	N/A	N/A	N/A
indazoline 19	N/A	N/A	N/A	N/A	N/A
cycl(3,2,2)azine 4bb	N/A	N/A	N/A	N/A	N/A

These correlations involve measurements acquired with the diatomic H₂ probe being above the center bond of the benzo-analogs. The research's $\Delta\sigma$ results correlated with ASE [12] to yield a R² value of 0.54. The same $\Delta\sigma$ results correlated with NICS(0), NICS(1) and NICS(2.5) yielded R² values of 0.028, 0.72 and 0.94.

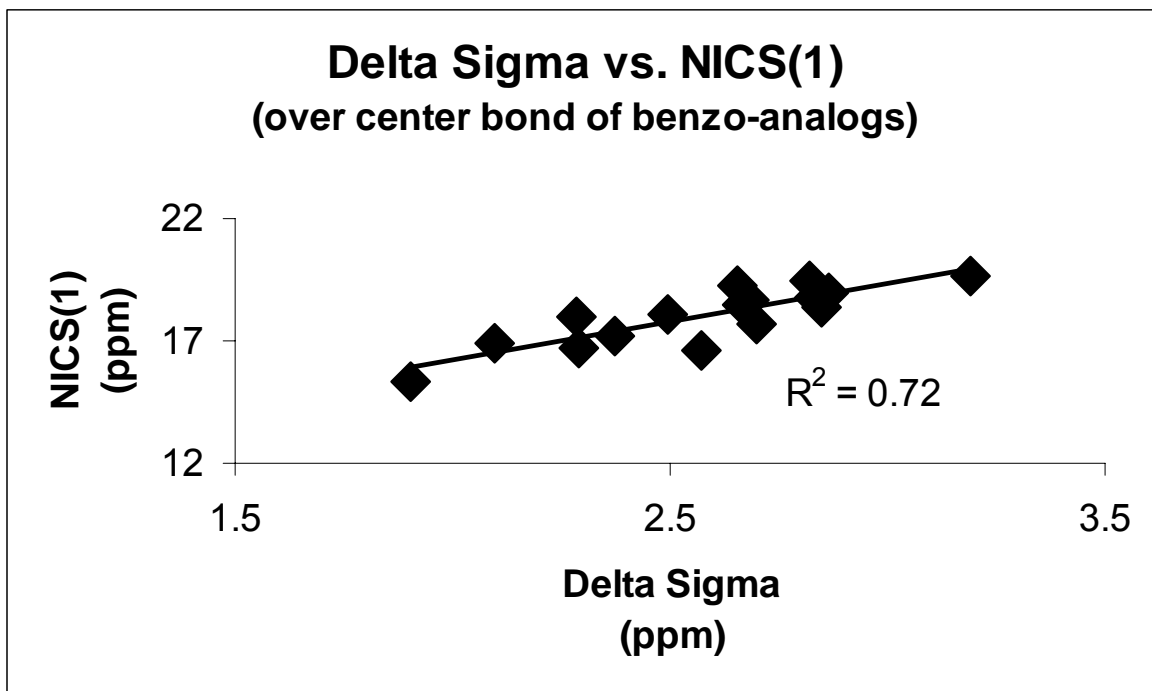


A

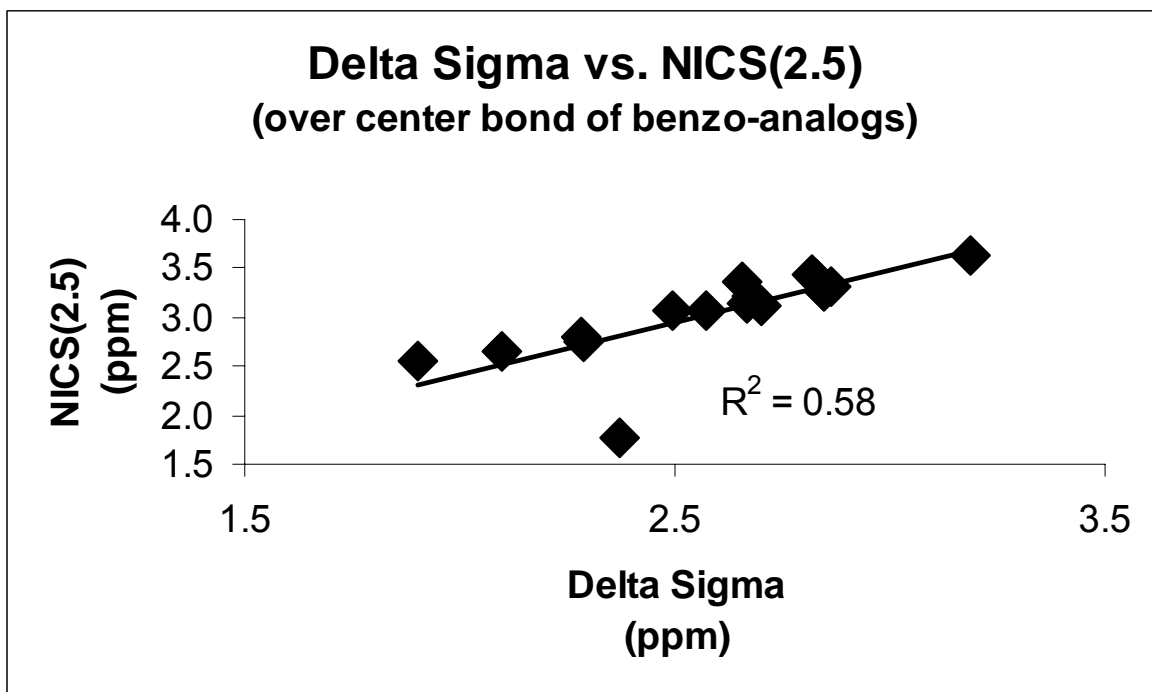


B

Fig. 53. This study's NMR maximum shielding increments ($\Delta\sigma_{\max}$) over the center bond correlated with both ASE [12] (A) and this study's NICS(0) over the center bond (B) for the benzo-analogs.



A

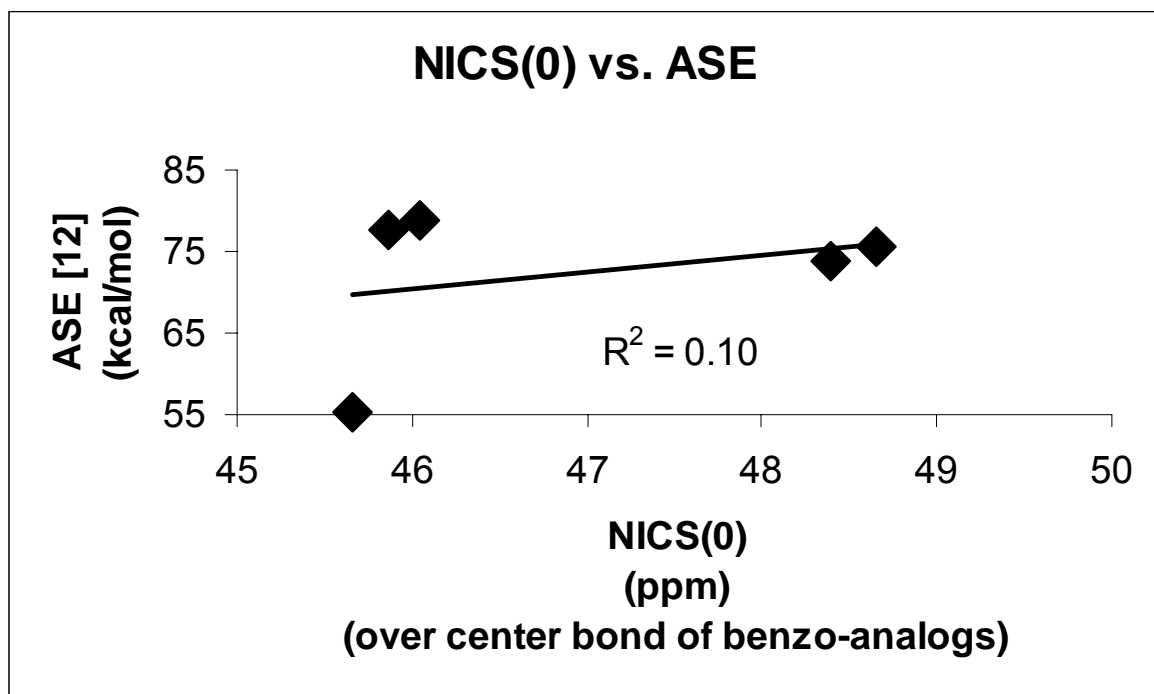


B

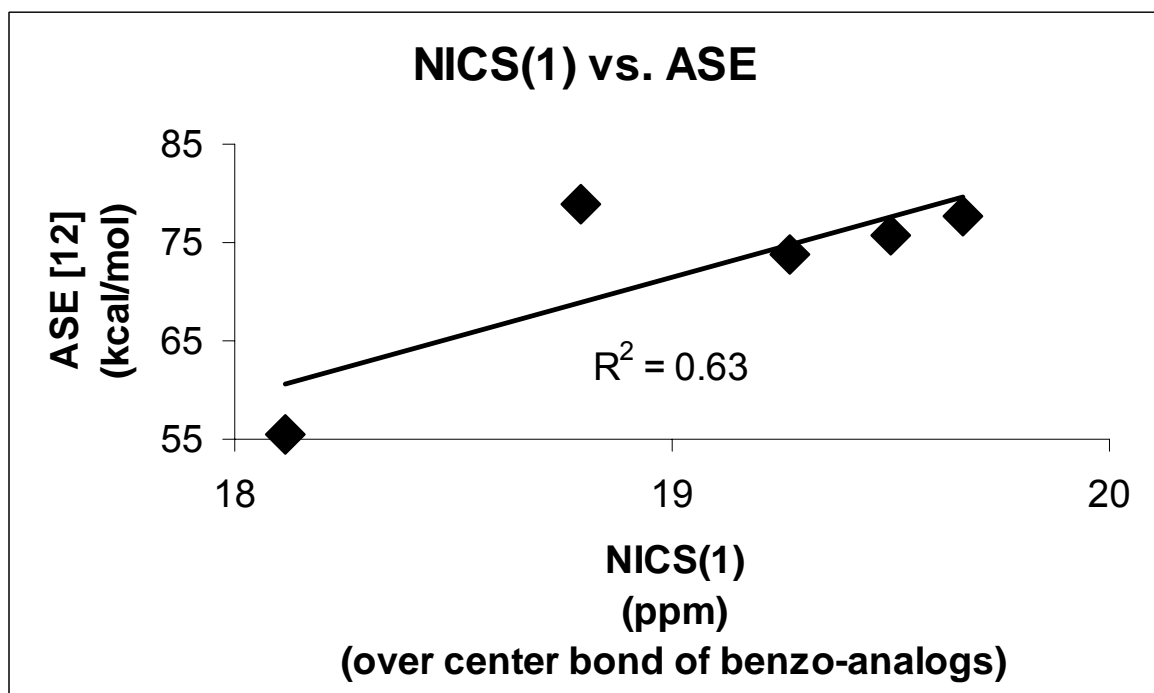
Fig. 54. This study's NMR maximum shielding increments ($\Delta\sigma_{\max}$) over the center bond correlated with both this study's NICS(1) over the center bond (A) and this study's NICS(2.5) over the center bond (B) for the benzo-analogs.

K. Other Methods Correlated with each other; Probe over Center bond

NICS measurements for calculations over the center bond were correlated with each other and with Bird's ASE values [12]. ASE correlated with NICS(0), NICS(1) and NICS(2.5) to yield R^2 values of 0.10, 0.63 and 0.74 respectively. NICS(0) correlated with NICS(1) and NICS(2.5) to yield R^2 values of 0.10 and 0.13. Finally, NICS(1) correlated with NICS(2.5) to yield R^2 values of 0.52.

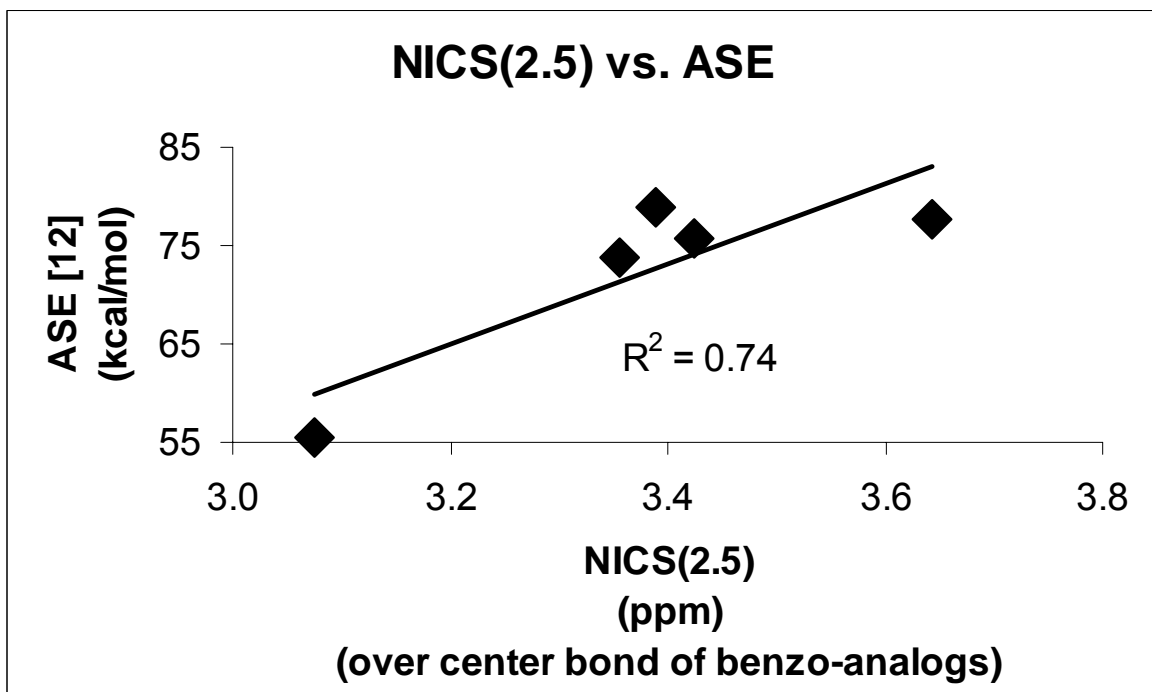


A

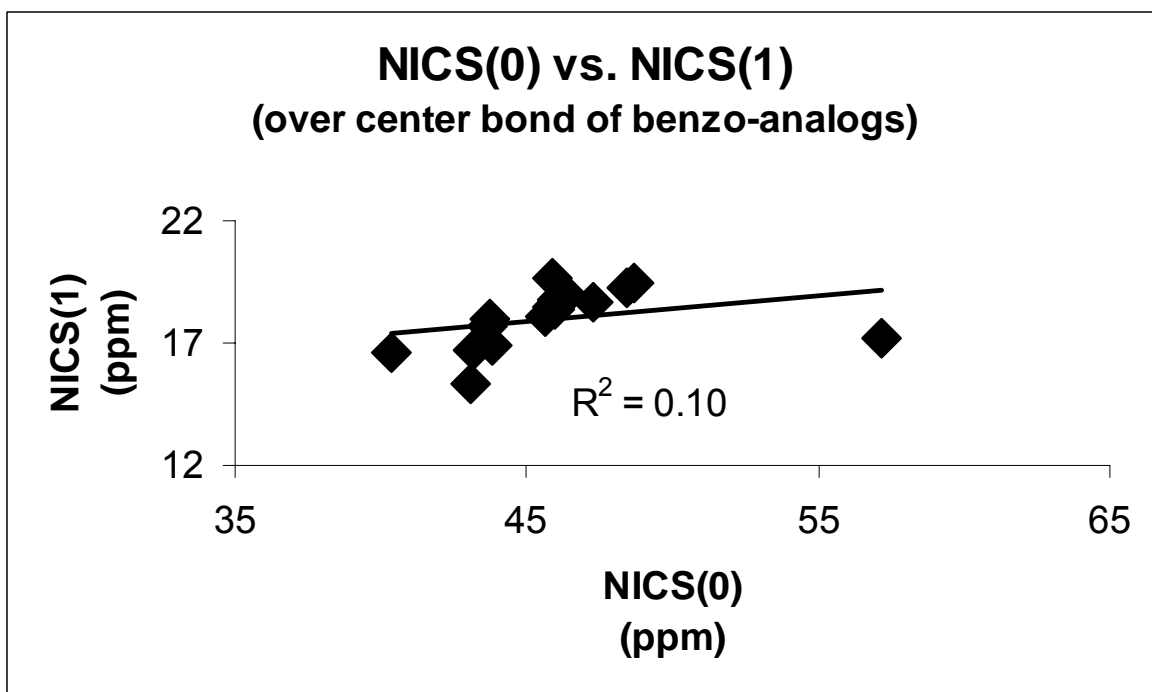


B

Fig. 55. ASE [12] correlated with this study's NICS(0) (A) and NICS(1) (B) both over the center bond of the benzo-analogs.

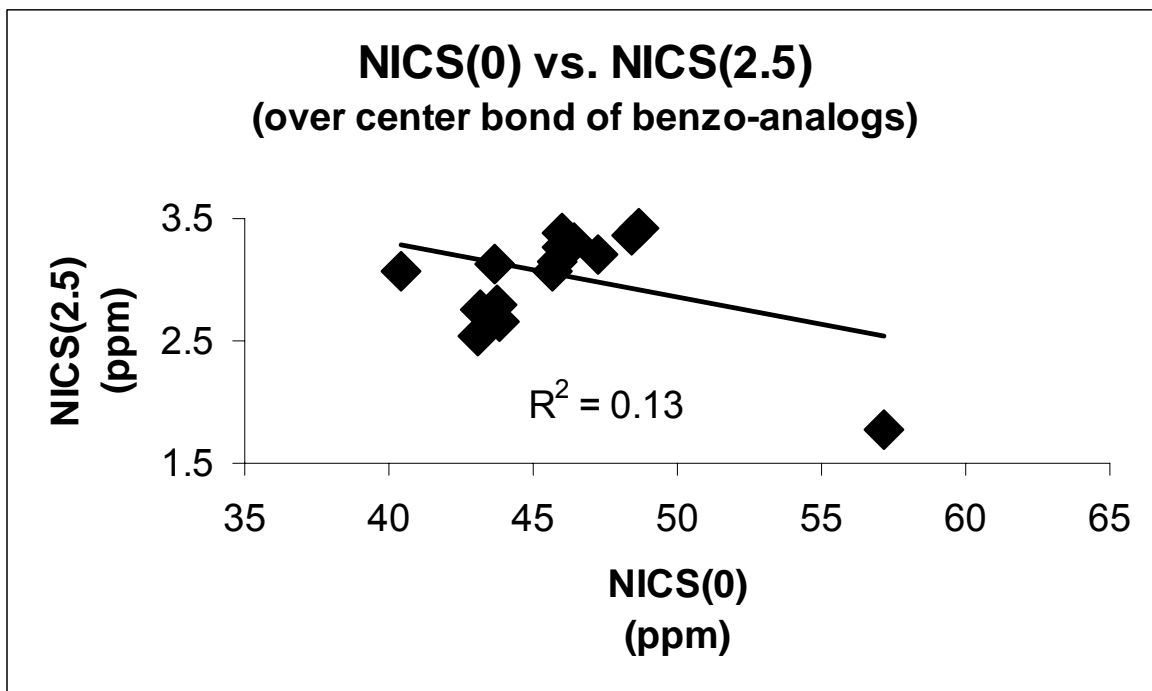


A

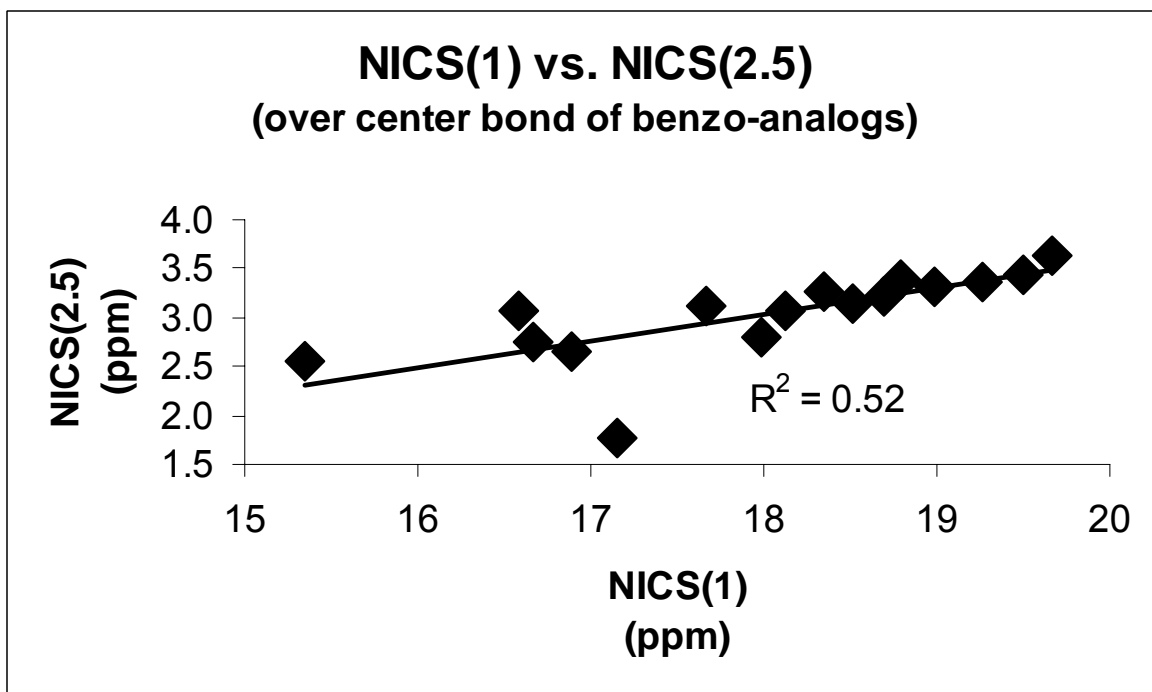


B

Fig. 56. This study's NICS(2.5) over the center bond of benzo-analogs correlated with ASE [12] (A). This study's NICS(0) and NICS(1) both over the center bond of benzo-analogs correlated with each other (B).



A



B

Fig. 57. This study's NICS(0) and NICS(2.5), both over the center bond of benzo-analogs, correlated with each other (A). This study's NICS(1) and NICS(2.5), both over the center bond of benzo-analogs, correlated with each other (B).

L. Summary Tables of most important Data related to this Study

Table 9: Summary of $\Delta\sigma$ values of five-membered rings and their benzo-analogs

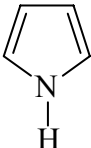
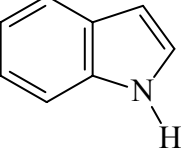
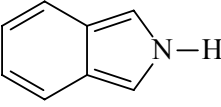
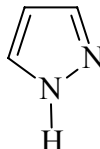
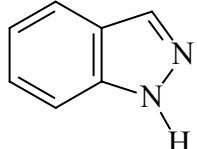
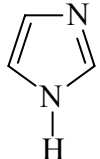
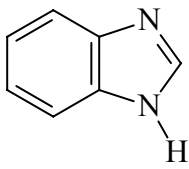
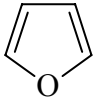
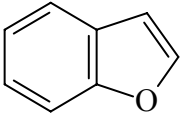
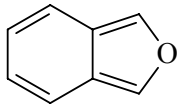
Structure Name 5-membered rings	$\Delta\sigma$ (ppm)	Structure Name benzo-analogs	$\Delta\sigma$ over heterocyclic side (ppm)	$\Delta\sigma$ over benzene side (ppm)	$\Delta\sigma$ over bond between rings (ppm)
 pyrrole 1	2.0	 indole 1b	2.4	3.2	2.7
		 isoindole 1c	3.0	2.3	2.4
 1H-pyrazole 2	2.3	 indazole 2b	2.7	3.3	2.8
 1H-imidazole 3	2.3	 benzimidazole 3b	2.7	3.3	2.8
 furan 4	1.7	 benzofuran 4b	2.0	3.3	2.5
		 isobenzofuran 4c	2.6	1.8	1.9

Table 9 continued: Summary of shielding increments ($\Delta\sigma$) of five-membered rings and their benzo-analogs

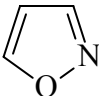
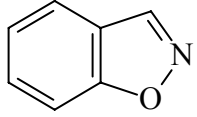
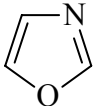
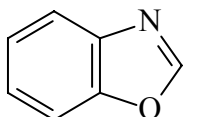
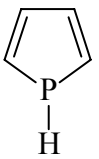
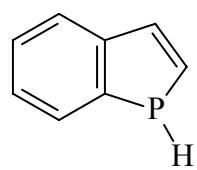
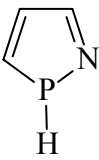
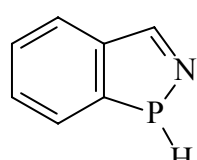
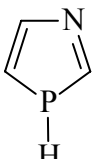
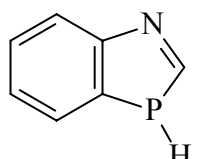
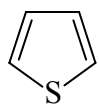
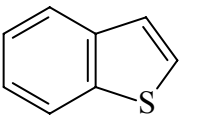
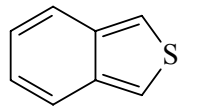
	2.0		2.3	3.4	2.7
isoxazole 5		1,2benzisoxazole 5b			
	2.2		2.4	.43	2.7
oxazole 6		1,3benzoxazole 6b			
	1.5		1.5	3.1	2.1
phosphole 7		benz[b]phosphole 7b			
	1.6		1.7	3.3	2.3
isophosphazole 8		1,2benzisophosphazole 8b			
	1.5		1.9	3.2	2.3
phosphazole 9		1,3-benzphosphazole 9b			
	2.4		2.4	3.3	2.7
thiophene 10		benzo[b]thiophene 10b			
			3.1	2.2	2.6
		benzo[c]thiophene 10c			

Table 9 continued: Summary of shielding increments ($\Delta\sigma$) of five-membered rings and their benzo-analogs

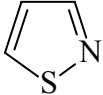
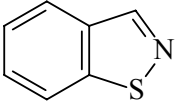
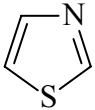
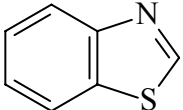
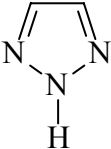
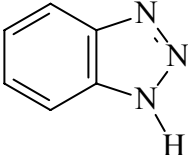
	2.6		2.7	3.4	2.9
isothiazole 11		1,2-benzisothiazole 11b			
	2.5		2.7	3.4	2.9
thiazole 12		1,2-benzothiazole 12b			
	2.7		3.2	3.5	3.2
1,2,3-triazole 13		1H-benzotriazole 13c			

Table 9 continued: Summary of shielding increments ($\Delta\sigma$) of miscellaneous single and multi-ring structures

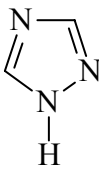
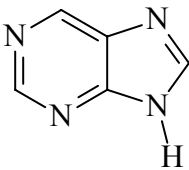
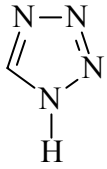
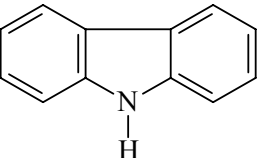
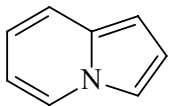
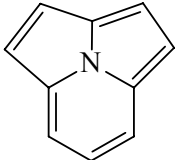
miscellaneous 5-membered rings	$\Delta\sigma$	miscellaneous multi-ring structures	$\Delta\sigma$ over heterocyclic side	$\Delta\sigma$ over benzene side	$\Delta\sigma$ over bond between rings
 1,2,4-triazole 14	2.5	 purine 17	2.8	3.4	
 1H-tetrazole 15	2.9	 carbazole 18			2.8
		 indazoline 19	2.7	2.1	2.6
		 cycl(3,2,2)azine 20			5.1

Table 10

Correlation (R^2) values involving this study's $\Delta\sigma_{\max}$ and other published results [16] relating to the five-membered rings

	ASE	Magnetic Susceptibility	NICS(0)	NICS(1)	HOMA
$\Delta\sigma_{\max}$	0.64	0.49	0.66	0.88	0.69
ASE	N/A	0.74	0.91	0.85	0.73
Λ		N/A	0.61	0.53	0.78
NICS(0)			N/A	0.85	0.65
NICS(1)				N/A	0.70
HOMA					N/A

Table 11

Summary of correlation (R^2) values involving this study's $\Delta\sigma_{\max}$, NICS(0), NICS(1); NICS(2.5) over the heterocyclic side (top), benzene side (middle) and center bond (bottom of the benzo-analogs along with other published results [12] relating to the same benzo-analogs

	NICS(0)	NICS(1)	NICS(2.5)	ASE [12]
$\Delta\sigma_{\max}$	0.71	0.80	0.95	0.67
	0.93	0.96	0.98	0.18
	0.03	0.72	0.58	0.54
NICS(0)	N/A	0.94	0.86	0.49
		0.97	0.95	0.16
		0.10	0.13	0.10
NICS(1)		N/A	0.93	0.53
			0.98	0.93
			0.52	0.63
NICS(2.5)			N/A	0.71
				0.53
				0.74
ASE [12]			N/A	

5. DISCUSSION

A. Unsaturated Five-Membered Heterocyclic Ring Compounds

An analysis of the five-membered rings, qualitatively, was accomplished via the use of shielding increment surface graphs. This resulted in the establishment of trends to be expected with respect to the derivatives incorporating nitrogen in the alpha and/or beta positions. The shielding surface graphs (top views) for nearly all sets of five-membered parents and their derivatives displayed a region of deshielding beyond the nitrogen in either the α or β position. These trends existed with all sets of five-membered parent rings and their derivatives at varying degrees of distinction, depending on the bottom heteroatom. This analogy also runs parallel with certain bottom heteroatoms (sulfur and phosphorus) displaying significant deshielding regions. Along with these significant deshielding regions, came a lesser distinction of the deshielding beyond the nitrogen in either the α or β position with the derivatives. Amongst these two sets of rings with significant deshielding in the phosphorus or sulfur atom area, the set with phosphorus as the bottom heteroatom exhibited so much deshielding that the shielding mounds of phosphole and its derivatives look very much similar to those of their derivatives. This concept led to the study of phosphole et al. more extensively. This was achieved via the construction of 3D models of phosphole and its derivatives within the *Titan* program. These 3D views displayed the pyramidal shape of phosphorus along with the hydrogen bonded to it extending out of the plane of the rest of the structure and the lone pair on phosphorus to extend out on the other side of phosphorus. This pyramidal shape of phosphorus is due to the geometric, torsional and bond angle strain caused by phosphorus being bonded to two different atoms within the ring and a lone hydrogen leaving a lone

pair of electrons on phosphorus as well. Both the lone pair and hydrogen on the phosphorus atom extends out of the plane at an angle (tilted) preventing this lone electron pair orbital from overlapping efficiently with p orbitals from other atoms of the structure. Aromaticity results from electrons in adjacent orbitals overlapping which establishes pi bonds resulting in conjugation. The sulfur atom of thiophene and its derivatives along with their benzo-analogs, on the other hand, has its lone pair of electrons extending straight up enabling orbital overlap with other p orbitals to occur. Notwithstanding that sulfur and phosphorus atoms exhibit chemical properties consistent with the electrons on the proximal hydrogen of the diatomic H₂ probe experiencing repulsion leading to the prominent deshielding regions beyond these respective atoms, phosphorus electrons are not contributing to pi bond overlapping as much as the sulfur atom does, consistent with structures having phosphorus exhibiting more deshielding than those with sulfur. Thus calculations were run with the diatomic hydrogen probe on both sides of the structures with phosphorus as the bottom heteroatom and the results proved to be indistinguishable qualitatively.

This study's $\Delta\sigma_{\max}$ results for the parent five-membered rings which are differentiated with having either nitrogen, oxygen, sulfur or phosphorus as the bottom heteroatom, differed. While pyrrole and furan had similar $\Delta\sigma_{\max}$ values of 2.0 and 1.7 respectively, the significance of a five-membered structure having a larger bottom heteroatom is reflected with thiophene having a $\Delta\sigma_{\max}$ value of 2.4. However, the $\Delta\sigma_{\max}$ value of phosphole is only 1.5 and this is consistent with lone pair on phosphorus being tilted and out of position to participate in p orbital overlapping with other atoms of the ring.

The study of the five-membered rings yielded $\Delta\sigma_{\max}$ results which correlated well against the various methods from Cyransky [16]. This success is realized with the study's results correlated with results of other different methods published by Cyransky to yield R^2 values which feel in the range of (0.50 to 0.88). Cyransky's results from different methods yielded R^2 values which feel in the range of (0.53 to 0.91) which is very similar to the range involving this study's results.

B. Benzo-Fused Unsaturated-Five-Membered Heterocyclic Ring Compounds

A qualitative analysis of the benzo-analogs was also accomplished via the use of shielding increment graphs. The benzo-analogs often displayed fuller shielding mounds than their five-membered ring counterparts. However, that fuller shielding mound difference was less distinct with structures which had sulfur or phosphorus as their bottom heteroatom in comparing the benzo-analogs with their five-membered ring counterparts. These effects are consistent with the significant deshielding regions observed in proximity of these particular heteroatoms (sulfur or phosphorus). Obviously, this significant deshielding diminishes, qualitatively, the effect of the implementing of nitrogen into either the α or β position. The implementation of nitrogen more than likely had an effect on the structures but was less noticeable due to the major deshielding regions in proximity of the bottom heteroatoms, sulfur and phosphorus. More so, the deshielding was so significant with structures having phosphorus as the bottom heteroatom that ignoring the scales of the Z axis, which uses shielding increment values, fuller shielding mounds are hardly noticeable in the benzo-analogs in comparison with their five-membered ring counterparts.

The study of benzo-analogs was analyzed quantitatively via the use of correlation graphs where R^2 values were calculated in order to assess how well this shielding increments correlated with results from other methods. Unfortunately, only Bird's ASE results [12] were found and correlated with only 5 of this study's benzo-analogs. Therefore, NICS(0), NICS(1) and NICS(2.5) were calculated along with the shielding increments within this study to help the situation. Furthermore, doing calculations on these benzo-analogs was not as simple as doing calculations on the five-membered rings with regard to determining what part of each benzo-analog would be best suited for the diatomic hydrogen to be positioned over. Thus, it was determined that calculations (shielding increments, NICS₀, NICS₁ & NICS_{2.5}) would be done with the diatomic H₂ probe being over the heterocyclic side, the benzene side and the center bond of the benzo-analogs (Figure 4) in an effort to see which probe position would give shielding values that correlate best with Bird's ASE data [12].

Bird's ASE results were done experimentally and serve as representations of each molecule as a whole. The shielding increments calculated over the heterocyclic side of the benzo-analogs correlated with Bird's ASE with an R^2 value of 0.67. The study's same shielding increments correlated with this study's NICS(0), NICS(1) and NICS(2.5) with R^2 values of 0.71, 0.80 and 0.95. Since $\Delta\sigma$ and NICS calculations are based on the same theory, they are expected to correlate well with one another. Therefore, the correlation between this study's shielding increments and this study's NICS serves as a calibration check to validate the credibility of the shielding increment calculations. Since Bird's ASE calculations are experimental due to the measuring of resonance energy energies while this study's shielding increments are computational, a correlation R^2 value of 0.67

can be considered respectable. The shielding increments calculated over the benzene side of the benzo-analogs correlated with Bird's ASE results to yield an R^2 value of 0.18 which is not very good. Calculations over the benzene ring don't give a clear representation of the whole structure and is mostly a representation of benzene. Since the shielding increment calculations done over the benzene side of the benzo-analogs are mostly of a reflection of benzene and not the whole benzo-analog structure, they should not correlate very well with values that accurately access the whole structure. These calculations over the benzene side of the benzo-analogs inaccurately yield values which indicate much more aromatic character than these structures possess as a whole. The shielding increment values done with the diatomic probe over the center bond of the benzo-analogs correlated with Bird's ASE results to yield an R^2 value of 0.54. This value is reasonable since this is a correlation between two distinct methods, one involving computational calculations and the other involving experimentally measuring resonance energies. However, this study's same shielding increments correlated with this study's NICS(0), NICS(1) and NICS(2.5) yielded R^2 values of 0.03, 0.72 and 0.58 respectively. Since the NICS(0) is poor and NICS(2.5) is not as good as it should be, the calculations taken over the center bond of the benzo analogs are not reliable. Theory supports this finding because when the probe is situated over the center bond of the benzo analogs, the diatomic hydrogen probe is in the middle of an electron dense area of pi and sigma bonds. The probe being in the middle of this cloud of electron density shifts electrons in the hydrogen of the probe that is in proximity to the aromatic system thereby complicating the calculation process. Thus, the diatomic hydrogen probe measurements taken over the center bond of the benzo-analogs are not reliable.

6. CONCLUSIONS

This method of measuring the extent of aromaticity, $\Delta\sigma_{2,5}$ shielding increments, shows potential as being a reliable method for measuring the degree of aromaticity. This study's shielding increments correlated very well with Cyransky's published results yielding an average R^2 value of 0.67 while Cyransky's results from different methods correlated with each other yielded an average R^2 value of 0.73. Since both averages are approximately the same, that gives credibility to this study's method. This study's calculations taken over the heterocyclic side of the benzo-analogs correlated most closely with Bird's ASE data demonstrating that the area of the benzo-analog over which the probe is positioned makes a difference. However, the study exposed the fact that there is a need for more aromatic measurements, experimental and/or computational, to be done for the benzo-analogs and other multi-ring structures in order to further substantiate this study's shielding increment method.

REFERENCES

- [1] W. Reusch, Aromaticity: Benzene and other Aromatic Compounds, Virtual Textbook of Organic Chemistry, (July 16 2007).
- [2] N.H. Martin, D.M. Loveless, K.L. Main and D.C. Wade, Computational of through-space NMR Shielding effects by small-ring aromatic and antiaromatic hydrocarbons, *Journal of Molecular Graphics and Modeling*. 25 (2006) 389-395.
- [3] P.V. Scheyer; H. Jiao, What is Aromaticity?. *Pure and Applied Chemistry*. 68 (2) (1996) 209-218.
- [4] C.H Suresh, N. Koga, Accurate calculation of aromaticity of benzene and antiaromaticity of cyclobutadiene: new homodesmotic reactions, *J. Org. Chem.* 67 (2002) 1965-1968.
- [5] J. March, *Advanced Organic Chemistry, Reaction, Mechanism and structure*, 4th edition, Plenum, New York (1993).
- [6] F. A. Carey; R.J. Sandberg, *Advanced Organic Chemistry*, 3rd edition, Plenum, New York (1993).
- [7] Minkin, V. I.; Glukhovtsev, M. N.; Simkin, B. Ya. *Aromaticity and Antiaromaticity – Electronic and Structural Aspects*; Wiley: New York, (1994).
- [8] P.J. Garratt, *Aromaticity*, Wiley, Inc. New York (1986).

- [9] E.D. Bergmann, B. Pullman (Eds), Aromaticity, Pseudo-Aromaticity, Anti-aromaticity. Israel Academy of Science and Humanities, Jerusalem Symposium on Quantum Chemistry and Biochemistry, Vol. 3. (1971).
- [10] Katritzky, A. R.; Jug, K.; Oniciu, D. C. Quantitative Measures of Aromaticity for Mono-, Bi-, and Tricyclic Penta- and Hexaatomic Heteroaromatic Ring Systems and Their Interrelationships. 101 (5) (2001) 1421-49.
- [11] Bergmann, E. D.; Pullmann, B. Aromaticity, Pseudo-aromaticity, Anti-aromaticity, Jerusalem Symposia on Quantum Chemistry and Biochemistry; Academic Press: New York, Vol. III. 1971.
- [12] C. W. Bird, The Relationship of Classical and Magnetic Criteria of Aromaticity, Tetrahedron. 52 (29) (1996) 9945-9952.
- [13] C.W. Bird, Heteroaromaticity, 5. A unified Aromaticity Index. Tetrahedron. 48 (2) (1992) 335-340.
- [14] A. Kekulé, Sur la constitution des substances aromatiques, Bull. Soc. Chim. Fr. (Paris) 3 (2) (1865) 98-110.
- [15] Cyrañski, M. K.; Krygowski, T. M.; Bird, C. W. Tetrahedron. 54 (1998) 9711-9720.
- [16] M.K. Cyrañsky, T.M. Krygowski, A.R. Katritzky, P.v.R. Schleyer, To what extent can aromaticity be defined uniquely? J. Org. Chem. 67 (4) (2002) 1333-1338.
- [17] Katritzky, A. R.; Karelson, M.; Sild, S.; Krygowski, T. M.; Jug, K. J. Org. Chem. 63 (1998) 5228-5231.

- [18] a) D.M.G. Lloyd, Carbocyclic Non-Benzenoid Aromatic Compounds, Elsevier, Amsterdam, (1966). b) D.M.G. Lloyd, Nonbenzenoid Conjugated Carbocyclic Compounds, Elsevier, Amsterdam, (1984).
- [19] V.I. Minkin, M.N. Glukhovtsev, B. Ya. Simkin, Aromaticity and Antiaromaticity, Electronic and Structural Aspects, Wiley, New York, (1994).
- [20] (a) L. Pauling, J. Sherman, J. Chem. Phys. 1 (1933) 606. (b) B. Kistiakowski, J. R. Ruhoff, H. A. Smith, W. E. Vaughan, J. Am. Chem. Soc. 58 (1936) 146. (c) M. Cohen, S. W. Benson, Chem. Rev. 93 (1993) 2419.
- [21] G. A. Jeffrey, J.R. Ruble, R. K. McMullan, J.A. Pople, Proc. R. Soc. London, Ser.A (1987) 414, 47.
- [22] P.v.R. Schleyer, C. Maerker, A. Dransfield, H. Jiao, N.J.R. van Eikema Hommes, J. Am. Chem. Soc. (1996) 118, 6317.
- [23] H.J. Dauben, J.L. Laity, Diamagnetic susceptibility exaltation as a criterion of aromaticity, J. Am. Chem. Soc. 91 (8) (1969) 1991-1998.
- [24] C.W. Haigh, R.B. Mallion, Ring current theories in nuclear magnetic resonance, in: J.W. Emsley, J. Feeny, L.H. Sutcliffe (eds.), Progress in Nuclear Magnetic Resonance Spectroscopy, vol.13, Pergamon Press, Oxford, U.K. (1979/1980).
- [25] P.v.R. Schleyer, C. Maerker, A. Dransfield, H. Jiao, N.J.R. van Eikema Hommes, Nucleus-independent chemical shifts: a simple and efficient aromaticity probe, J. Am. Chem. Soc. 118 (1996) 6317-6318.

- [26] T.M. Krygowski, M.K. Cyransky, Aromatic character of carbocyclic Π - electron systems deduced from molecular geometry, in: M. Hargittai, I. Hargittai (Eds.), *Advances in Molecular Structure Research*, vol.3, JAI Press, London, (1997) 227-268.
- [27] W.J. Hehre, R.T. McIver, J.A. Pople, P.v.R. Schleyer, Alkyl substituent effects on stability of protonated benzene, *J. Am. Chem. Soc.* 96 (1974) 7162-7163.
- [28] Breslow, R. *Pure Appl. Chem.* (1971) 28, 111.
- [29] N.H. Martin, N.W. Allen, III, E.K. Minga, S.T. Ingrassia, J.D. Brown, A new proton shielding model for alkenes. In *Proceedings of ACS symposium "Modeling NMR Chemical Shifts: Gaining Insights into Structure and Environment,"* ACS Press, (1999) 207-219.
- [30] N.H. Martin, N.W. Allen, III, J.C. Moore, An algorithm for predicting NMR shielding of protons over substituted benzene rings, *J. Mol. Graphics Mod.* 18 (3) (2000) 242-246.
- [31] N.H. Martin, N.W. Allen, III, K.D. Moore, L. Vo, A proton NMR shielding model for the face of a benzene ring, *J. Mol. Struct. (Theochem)* 454 (1998) 161-166.
- [32] J.A.N.F. Gomes, R.B. Mallion, The concept of ring currents. In *Concepts in Chemistry: A Contemporary Challenge*; D.H. Rouvray, Ed.; Research Studies Press: Taunton, Somerset, U.K., (1997) 205-253.
- [33] Lazzeretti, P. Ring currents. In *Progress in Nuclear Magnetic Resonance Spectroscopy*; Emsley, J. W., Feeny, J., Sutcliffe, L. H., Eds.; Elsevier: Amsterdam, The Netherlands, 36 (2000) 1-88.

- [34] T.M Krygowski, M. K Cyranski, Structural aspects of aromaticity, *Chem. Rev.* 101 (5) (2001) 1385-1419.
- [35] W. H. Flygare, *Chem. Rev.* (1974) 74, 653.
- [36] J. H. Dauben, J. D. Wilson, J.L. Laity, *J. Am. Chem. Soc.* (1968) 90, 811.
- [37] T.M. Krygowski, Crystallographic studies of inter- and intramolecular interactions reflected in aromatic character of p-electron systems, *J.Chem. Inf. Comput. Sci.* 33 (1) (1993) 70-78.
- [38] P. George, M. Trachtman, A.M. Brett, C.W. Bock, Comparison of various isodesmic and homodesmotic reaction heats with values derived from published ab initio molecular orbital calculations, *J. Chem. Soc., Perkin Trans. 2* (1977) 1036-1047.
- [39] C.H. Suresh, N. Koga, Accurate calculation of aromaticity of benzene and antiaromaticity of cyclobutadiene: new homodesmotic reactions, *J. Org. Chem.* 67 (2002) 1965-1968.
- [40] L.J. Schaad, B.A. Hess Jr., Dewar resonance energy, *Chem. Rev.* 101 (5) (2001) 1465-1476.
- [41] J.F. Liebman, S.W. Slayden, The energetics of aromatic hydrocarbons: an experimental thermochemical perspective, *Chem. Rev.* 101 (5) (2001) 1541-1566.
- [42] J. Hoarau, Magnetic properties of conjugated molecules, *Ann. Chim.* 13 (1) (1956) 544-587.
- [43] A. Pacault, Magnetochemical studies A, *Ann. Chim.* 12 (1) (1946) 527-587.

- [44] W.H. Flygare, Magnetic interactions in molecules and an analysis of molecular electronic charge distribution from magnetic parameters, *Chem. Rev.* 74 (1974) 653-687.
- [45] D. V. Simion and T. S. Sorensen* A Theoretical Computation of the Aromaticity of (Benzene)Cr(CO)₃ Compared to Benzene Using the Exaltation of Magnetic Susceptibility Criterion and a Comparison of Calculated and Experimental NMR Chemical Shifts in These Compounds *J. Am. Chem. Soc.* 118 (1996) 7345-7352.
- [46] Dauben, H. J., Jr.; Wilson, J. D.; Laity, J. L. *Nonbenzenoid Aromaticity*. Vol. II (1971) 167..
- [47] Z. Chen, C.S. Wannere, C. Cominboeuf, R. Puchta, P.v.R. Schleyer, Nucleus-independent chemical shifts (NICS) as aromaticity criterion, *Chem. Rev.* 105 (10) (2001) 3842-3888.
- [48] A. Stanger, Nucleus-independent chemical shifts (NICS): distance dependence and revised criteria for aromaticity and antiaromaticity, *J. Org. Chem.* 71 (3) (2006) 883-893.
- [49] Gaussian 03W, Version 6.0 Revision-B.01, Gaussian, Inc. Wallington, CT 1995.
- [50] Titan, version 1.0.1, Wavefunction, Inc./ Schrodinger, Inc., 1999.
- [51] Orient.jar, Dr. Clayton S. Ferner, Allen Randall and Tristan Carland, UNCW Computer Science, 2004.
- [52] TableCurve3D, version 3.00A, AISN Software, San Rafael, CA 1997.
- [53] MS Office Excel 2003, Microsoft Corporation, One Microsoft Way, Redmond, WA, 2003.